

10. SITE 632: EXUMA SOUND¹

Shipboard Scientific Party²

HOLE 632A

Date occupied: 25 February 1985, 1050 EST
Date departed: 26 February 1985, 1250 EST
Time on hole: 1 day, 2 hr
Position: 23°50.44'N, 75°26.13'W
Water depth (sea level; corrected m, echo-sounding): 1996
Water depth (rig floor; corrected m, echo-sounding): 2006
Bottom felt (m, drill pipe): 2006.6
Total depth (m): 2147.6
Penetration (m): 141.0
Number of cores: 16
Total length of cored section (m): 141.0
Total core recovered (m): 83.3
Core recovery (%): 59.1
Oldest sediment cored:
Depth sub-bottom (m): 141.0
Nature: chalky limestone
Age: late Miocene (NN11)
Measured velocity (km/s): 3.00, Hamilton Frame; 2.05, multichannel seismic-interval velocity

HOLE 632B

Date occupied: 26 February 1985, 1250 EST
Date departed: 1 March 1985, 0120 EST
Time on hole: 2 days, 12 hr, 30 min
Position: 23°50.44'N, 75°26.13'W
Water depth (sea level; corrected m, echo-sounding): 1996
Water depth (rig floor; corrected m, echo-sounding): 2006
Bottom felt (m, drill pipe): 2006.6
Total depth (m): 2289.9
Penetration (m): 283.3
Number of cores: 17
Total length of cored section (m): 162.6
Total core recovered (m): 34.8
Core recovery (%): 21.4
Oldest sediment cored:
Depth sub-bottom (m): 283.3
Nature: chalky limestone
Age: late Miocene (NN11)
Measured velocity (km/s): 3.00–4.10, Hamilton Frame; 2.05, multichannel seismic-interval velocity

¹ Austin, J. A., Jr., Schlager, W., Palmer, A. A., et al., 1986. *Proc., Init. Repts. (Pt. A), ODP*, 101.

² James A. Austin Jr. (Co-Chief Scientist), Institute for Geophysics, University of Texas at Austin, Austin, TX 78751; Wolfgang Schlager (Co-Chief Scientist), Rosenstiel School of Marine and Atmospheric Sciences, Miami, FL 33149 (current address: Vrije Universiteit, Instituut v. Aardwetenschappen, Postbus 7161, 1007 MC Amsterdam, Netherlands); Amanda A. Palmer, Staff Scientist, Ocean Drilling Program, Texas A&M University, College Station, TX 77843; Paul A. Comet, The University, Newcastle-Upon-Tyne, Newcastle, United Kingdom (current address: Core Labs Singapore, 24A-Lim Teck Boo Rd., Singapore 1953); André Droxler, Rosenstiel School of Marine and Atmospheric Sciences, Miami, FL 33149 (current address: Department of Geology, University of South Carolina, Columbia, SC 29208); Gregor Eberli, Geologisches Institut, ETH-Zentrum, Zürich, Switzerland (current address: Fisher Island Station, University of Miami, Miami, FL 33139); Eric Fourcade, Laboratoire de Stratigraphie, Université Pierre et Marie Curie, 4 Place Jussieu 75230, Paris Cedex 05, France; Raymond Freeman-Lynde, Department of Geology, University of Georgia, Athens, GA 30602; Craig S. Fulthorpe, Department of Geological Sciences, Northwestern University, Evanston, IL 60201; Gill Harwood, Department of Geology, The University, Newcastle-Upon-Tyne, NE1 7RU United Kingdom; Gerhard Kuhn, Geologisches Institut Göttingen, Federal Republic of Germany (current address: Alfred Wegener Institut für Polarforschung, Columbus Center, D-2850 Bremerhaven, West Germany); Dawn LaVoie, NORDA Code 363, Seafloor Geosciences Division, NSTL, MS 39529; Mark Leckie, Woods Hole Oceanographic Institution, Woods Hole, MA 02543 (current address: Department of Geology and Geography, University of Massachusetts, Amherst, MA 01003); Allan J. Melillo, Department of Geological Sciences, Rutgers University, New Brunswick, NJ 08903 (current address: Chevron U.S.A., New Orleans, LA 70114); Arthur Moore, Marathon Oil Company, P.O. Box 269, Littleton, CO 80160; Henry T. Mullins, Department of Geology, Syracuse University, Syracuse, NY 13210; Christian Ravenne, Institut Français du Pétrole, B.P. 311, 92506 Rueil Malmaison Cedex, France; William W. Sager, Department of Oceanography, Texas A&M University, College Station, TX 77843; Peter Swart, Fisher Island Station, University of Miami, Miami, FL 33139 (current address: Marine Geology and Geophysics, Rosenstiel School of Marine and Atmospheric Sciences, Miami, FL 33149); Joost W. Verbeek, Dutch Geological Survey, P.O. Box 157, 2000 A.D. Haarlem, Netherlands; David K. Watkins, Department of Geology, University of Nebraska, Lincoln, NE 68588; Colin Williams, Borehole Research Group, Lamont-Doherty Geological Observatory, Palisades, NY 10964.

Principal results: Site 632 in Exuma Sound was occupied from 25 through 28 February 1985. Two holes were drilled at 23°50.44'N, 75°26.13'W, in 1996 m water depth. Hole 632A penetrated 141.0 m, recovering 59% using the hydraulic-piston-core/extended-core-barrel (HPC/XCB) system. Hole 632B was drilled with a rotary bit to 283 m, recovering being 21% in the cored interval of this hole (120.7–283.3 m sub-bottom).

Site 632 represents the basinward end of the Exuma Sound transect and is located on flat basin floor just above the axial valley of Exuma Sound. The stratigraphic sequence consists of the following units: (1) 0–55 m sub-bottom; periplatform ooze with turbidites of largely platform material, late Pliocene to Holocene; (2) 55–105 m sub-bottom; periplatform ooze and chalk with a few turbidites and a debris flow at least 7 m thick, late Miocene to late Pliocene; and (3) 105–283 m sub-bottom; periplatform chalk and limestone having rhythmic intercalations of turbidites, late Miocene (this unit probably includes great amounts of ooze that were not recovered).

The section at Site 632 represents a typical basin-floor facies having graded turbidites, a lithology conspicuously absent on the bypass slopes in Exuma Sound and north of Little Bahama Bank. Sedimentation rates vary considerably but reach 210 m/m.y. in the Miocene section, a value common in flysch sequences.

Rapid burial diagenesis is indicated by the abundance of limestones below 100 m (Miocene–earliest Pliocene) and by steep gradients in the downhole profiles of density, porosity, and sonic velocity. Despite rapid and extensive lithification, magnesian calcite is present down to 40 m, and aragonite percentages exceed 10% throughout the hole, even in Miocene limestones at the bottom.

The limestones and chinks from 1600 m downward contain traces of asphalt. Small quantities of bitumen and heavy oil were detected in the interval between 265 and 283 m. Hole 632B was abandoned because of these oil shows.

OPERATIONS SUMMARY

The *JOIDES Resolution* left Site 631 for Site 632 (BAH-11-C) at 0230 hr, 25 February 1985. During the 23.5-n.-mi transit, the ship remained in dynamic-positioning mode with thrusters extended, and speed was maintained at 4 kt. A single-channel analog/digital seismic line was collected using two 80-in.³ water guns, along with 3.5/12-kHz records (Fig. 1, Site 631 chapter; "Underway Geophysics" chapter, this volume).

According to radar bearings off the northern tip of Long Island (Fig. 1, Site 631 chapter), the BAH-11-C location at the intersection of site-survey profiles ES-05 and ES-07 was reached at 0733 hr, when a 14.5-kHz beacon was dropped. Two subsequent satellite fixes, however, confirmed that the ship was 0.55 n. mi out of position to the northwest, and the decision was made to move rather than to sacrifice seismic control at this potential deep-penetration site. The maneuver was completed, and a second (16.5-kHz) beacon was dropped at 1050 hr. The final Site 632 position is as follows: 23°50.403–472' N, 75°26.083–182' W (continuous monitoring of SATNAV), about 0.1 n. mi off BAH-11-C. Water depth at Site 632 was 1991 m (uncorr.), 1996 m (corr.).

A successful mud-line hydraulic piston core (HPC) was retrieved from Hole 632A at 1455 hr, and over the next 12 hr 10 more such cores were obtained to a depth of 93.9 m sub-bottom, for a recovery of 73.4%. After switching to the extended-core-barrel (XCB) technique, five XCB cores were collected over the next 9 hr to 141.0 m sub-bottom; recovery was 30.6%. Overall recovery for Hole 630A was 59.1%.

At 141.0 m sub-bottom, lithification in the section was sufficient to reduce recovery with the XCB technique to less than 10%, so the decision was made at 1250 hr, 26 February, to pull out of the hole (POOH) and make up a new bottom-hole assembly (BHA) for rotary coring. The switch of BHAs, along with washing back into Hole 632B to 120.7 m sub-bottom, took 24 hr.

The first rotary core of Hole 632B came on deck at 1210 hr, 27 February. Recovery in the first nine cores never exceeded 16%; running sand contaminated some downhole sections. In Core 632B-4R (149.6–159.2 m sub-bottom), asphalt was discovered in vugs of a limestone fragment. Later, in Core 632B-16R (264.9–274.0 m sub-bottom), blebs of tar were found in unconsolidated sand that had filled the core liner. Geochemical analyses of the tar began immediately. When Core 632B-17R (274.0–283.3 m sub-bottom) brought more tar shows in limestone, the decision was made at 1330 hr, 28 February, to suspend further drilling operations until the substance could be completely analyzed. By 1900 hr, it was confirmed that the shows were heavy oil and bitumen, which could not have been contributed by the drilling equipment, and preparations were begun to abandon Hole 632B.

At 1945 hr, the string was POOH to 141 m sub-bottom, and 150 sacks of cement were slurried into the hole, creating a 100-m plug from 141 to 41 m sub-bottom. This cementing operation was completed by 2200 hr, and the mud line was cleared by 2300 hr. All pipe except the BHA was back on deck by approximately midnight, and the *Resolution* got under way at 0120 hr, 1 March, for Site 633 (BAH-11-B), approximately 15 n. mi away (Fig. 1, Site 631 chapter).

The coring summary for Site 632 appears in Table 1.

Table 1. Coring summary, Site 632.

Core no.	Core type ^a	Date (Feb. 1985)	Time	Sub-bottom depths (m)	Length cored (m)	Length recovered (m)	Percentage recovered
Hole 632A							
1	H	25	1455	0–6.9	6.9	6.92	100
2	H	25	1545	6.9–16.7	9.8	9.32	95
3	H	25	1730	16.7–26.3	9.6	9.18	95
4	H	25	1800	26.3–35.9	9.6	9.08	94
5	H	25	1915	35.9–45.4	9.5	7.94	83
6	H	25	2030	45.4–55.0	9.6	9.70	101
7	H	25	2145	55.0–64.6	9.6	2.18	22
8	H	25	2245	64.6–74.2	9.6	9.44	98
9	H	25	2340	74.2–83.8	9.6	4.02	41
10	H	26	0115	83.8–93.4	9.6	1.06	11
11	H	26	0250	93.4–93.9	0.5	0.11	22
12	X	26	0500	93.9–102.7	8.8	9.63	109
13	X	26	0700	102.7–112.3	9.6	2.17	22
14	X	26	0900	112.3–121.9	9.6	1.36	14
15	X	26	1035	121.9–131.3	9.4	0.55	5
16	X	26	1210	131.3–141.0	9.7	0.63	6
Hole 632B							
1	R	27	1210	120.7–130.3	9.6	0.13	1
2	R	27	1345	130.3–140.0	9.7	0.92	9
3	R	27	1530	140.0–149.6	9.6	1.85	19
4	R	27	1700	149.6–159.2	9.6	1.58	16
5	R	27	1815	159.2–168.9	9.7	0	0
6	R	27	2000	168.9–178.7	9.8	1.57	16
7	R	27	2115	178.7–188.2	9.6	1.43	14
8	R	27	2245	188.2–197.9	9.7	0.95	9
9	R	28	0025	197.9–207.5	9.6	1.67	16
10	R	28	0205	207.5–217.1	9.6	4.50	46
11	R	28	0357	217.1–226.7	9.6	6.19	64
12	R	28	0550	226.7–236.3	9.6	1.95	20
13	R	28	0715	236.3–245.8	9.5	1.15	12
14	R	28	0830	245.8–255.5	9.7	0.12	1
15	R	28	1010	255.5–264.9	9.4	4.64	49
16	R	28	1150	264.9–274.0	9.1	4.26	46
17	R	28	1330	274.0–283.3	9.3	1.90	20

^a H = hydraulic piston; X = extended core barrel; R = rotary.

SEDIMENTOLOGY

Introduction

Two holes were drilled at Site 632. Hole 632A penetrated 141.0 m with 83.3 m (59%) recovery. Hole 632B penetrated 283.2 m. The upper 120.7 m of Hole 632B was washed; recovery in the lower 162.5 m was 34.8 m (21.4%).

Sediments and rocks recovered at Site 632 consist of periplatform ooze, chalk, and limestone, interbedded with turbidites (unlithified and lithified grainstones and packstones), and a 15-m-thick interval of debris flows (unlithified floatstones). Surprisingly, aragonite occurs throughout the entire section, averaging 50%-80% above 105 m sub-bottom and 20%-30% below 105 m sub-bottom (see "Inorganic Geochemistry" section, this chapter).

On the basis of continuous coring in Holes 632A (HPC/XCB) and 632B (rotary), the section penetrated at Site 632 is divided into three lithostratigraphic units (Fig. 1).

Unit I (0-54.7 m sub-bottom; Cores 632A-1H to 632A-6H-7, 28 cm)

Unit I is latest Pliocene to Pleistocene in age (see "Biostratigraphy" section, this chapter). This unit consists of calcareous ooze and minor amounts (< 5%) of chalk interbedded with unlithified grainstone and packstone with minor amounts of rudstone. Ooze is dominantly various shades of white (5Y 8/1, 2.5Y 8/0, 2.5Y 8/2, and 10YR 8/1), minor amounts of very pale brown (10YR 8/3 and 10YR 7/3) being in Core 632A-1H. Grainstones and packstones in this unit are also predominantly

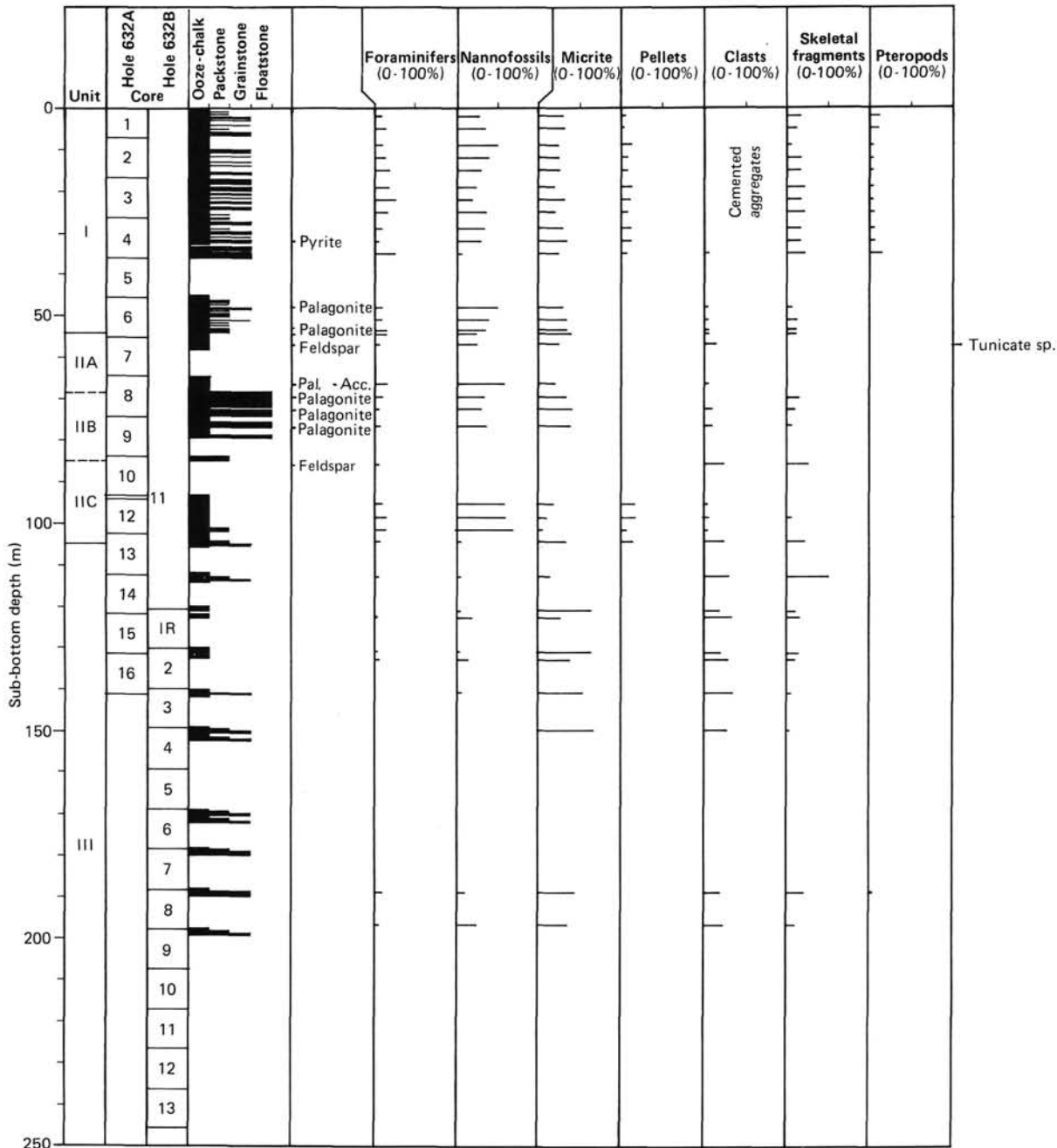


Figure 1. Summary of lithologies and smear slide estimates used to subdivide deposits recovered at Site 632.

white (5Y 8/1, 2.5Y 8/2, 10YR 8/1, and 10YR 8/2), with minor amounts of light gray (5Y 7/1, 2.5Y 7/0, and 10YR 7/1).

The calcareous ooze and chalk are of probable periplatform origin and contain varying proportions (Fig. 1) of platform-derived aragonite (partly as needles) in addition to micrite, nannofossils, and foraminifers (Schlager and James, 1978). Obvious burrowing is slight to moderate and is indicated at many places by gray (7.5YR 4/0 and 2.5Y 7/0) streaks and flecks of pyrite. Lamination is rare.

Unlithified grainstone and packstone layers generally range in thickness from 1 to 20 cm (Fig. 2), although some layers are about 50 cm thick; one grainstone layer in Core 632A-6H is

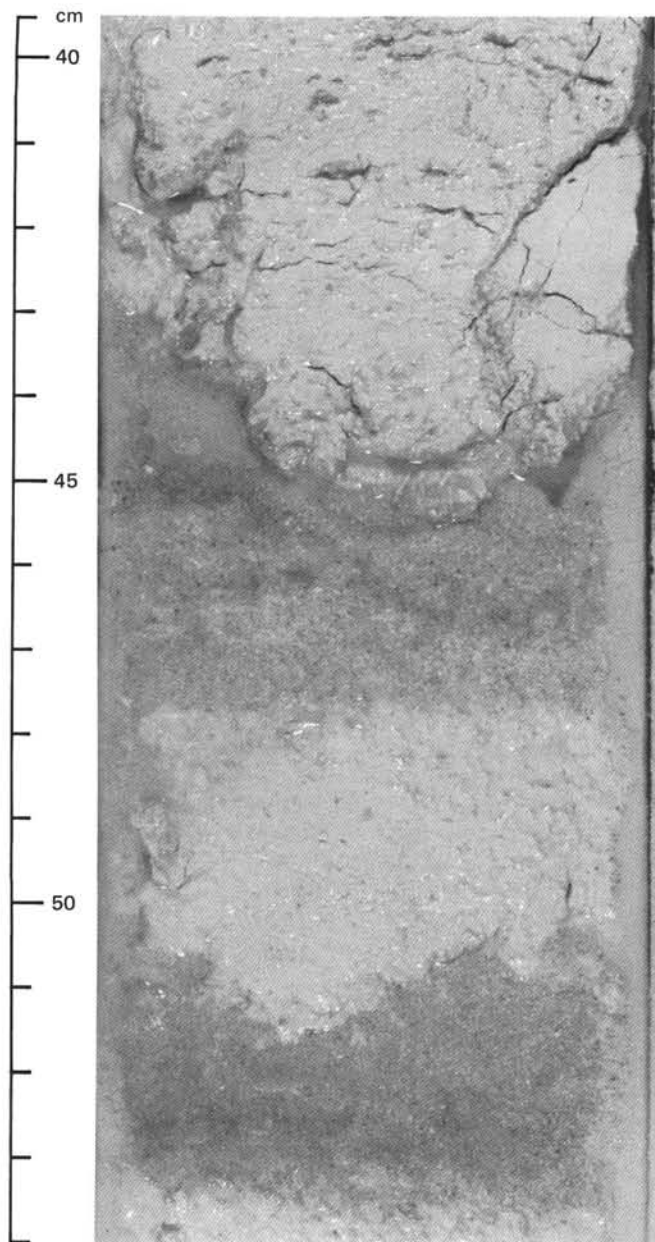


Figure 2. Thin, medium- to fine-grained turbidites, with flat erosional bottoms and irregular, abrupt tops, in Unit I. Grains are composed principally of planktonic foraminifers and pteropods, with minor amounts of platform-derived skeletal fragments. Section 632A-2H-4.

nearly 2 m thick. Most bases of grainstones and packstones are planar, although some of the tops are either irregular or abrupt, possibly as a result of drilling deformation (Fig. 2). Some grainstones and packstones grade into overlying ooze. Layers 10–20-cm thick exhibit grading, whereas the thickest layers show reverse grading and poor sorting (Fig. 3). These grainstone and packstone layers are interpreted as being turbidites owing to the presence of flat bases and grading and the occurrence of abundant skeletal debris derived from the shallow platform, including *Halimeda* plates and *Homotrema*. Abundant echinoid spines and bivalve fragments in these layers may also be platform derived. Neritic debris is particularly abundant in unlithified grainstones and in coarse- to medium-grained sand layers (Fig. 3), which also contain abundant pteropods. Turbidites containing medium-to-fine-sand-sized grains consist principally of planktonic foraminifers and pteropods and of smaller amounts of platform-derived material (Fig. 2). Packstones are dominant at the top (Core 632A-1H) and bottom (Cores 632A-4H to 632A-6H) of this unit. Pyrite and laminations are rare in the turbidites.

Unit II (54.7–104.7 m sub-bottom; Cores 632A-6H-7, 28 cm, to 632A-13X-2)

Unit II is late Pliocene to latest Miocene in age (see “Biostratigraphy” section, this chapter). Although both Units I and II contain sediment gravity flows, Unit II differs from Unit I in that these sediment gravity flows are not evenly distributed throughout the unit as they are in Unit I, which results in thicker ooze and chalk intervals in Unit II than those in Unit I. Unit II consists of alternating calcareous ooze and chalk, interbedded with unlithified floatstone, unlithified to partly lithified packstone, and limestone (with wackestone texture). All lithologies are various shades of white (5Y 8/1, 5Y 8/2, 2.5Y 8/0, 2.5Y 8/2, 10YR 8/1, and 10YR 8/2). Unit II can be divided into three subunits on the basis of the presence or absence of sediment gravity flows.

Subunit IIA (54.7–68.6 m sub-bottom; Cores 632A-6H-7, 28 cm, to 632A-8H-3, 108 cm) is early to late Pliocene in age (see “Biostratigraphy” section, this chapter). This subunit consists of alternating calcareous ooze (80%) and chalk (20%), similar to the periplatform ooze and chalk occurring in Unit I. Burrows are not conspicuous and generally are indicated by flecks and streaks of pyrite. Laminations are rare.

Subunit IIB (68.6–84.9 m sub-bottom; Cores 632A-8H-3, 108 cm, to 632A-10H) is early Pliocene in age (see “Biostratigraphy” section, this chapter). Unlithified floatstone and unlithified to partly lithified packstone, interpreted as being sediment gravity flows, characterize this subunit. Unlithified floatstone in Cores 632A-8H and 632A-9H contains large, rounded clasts (1–5 cm in diameter) of stiff ooze, chalk, and limestone in a calcareous-ooze matrix (Fig. 4). The rounded nature of the clasts and the presence of stained, flat surfaces on some clasts (hardgrounds?) indicate that these floatstones are debris flows. Clasts are distributed unevenly throughout the matrix. At some places, spacing between clasts is small (about 5 cm), whereas at others, spacing is large (about 25–50 cm). However, intervals having clasts spaced about 25–50 cm apart may not be debris flows, but instead may be perennial periplatform ooze and minor chalk interbeds between debris flows. Individual debris flows are 50–150 cm thick and are separated by 70–105-cm-thick intervals of alternating periplatform ooze and chalk.

Core 632A-10H contains a 75-cm-thick interval of unlithified to partly lithified packstone. Although this interval is not graded, the conspicuous absence of planktonic foraminifers and the abundance of skeletal debris (in part neritic)—including fragments of red algae, mollusks, and echinoids—in the medium-to-fine-sand-sized fraction indicate that this packstone is a turbidite.

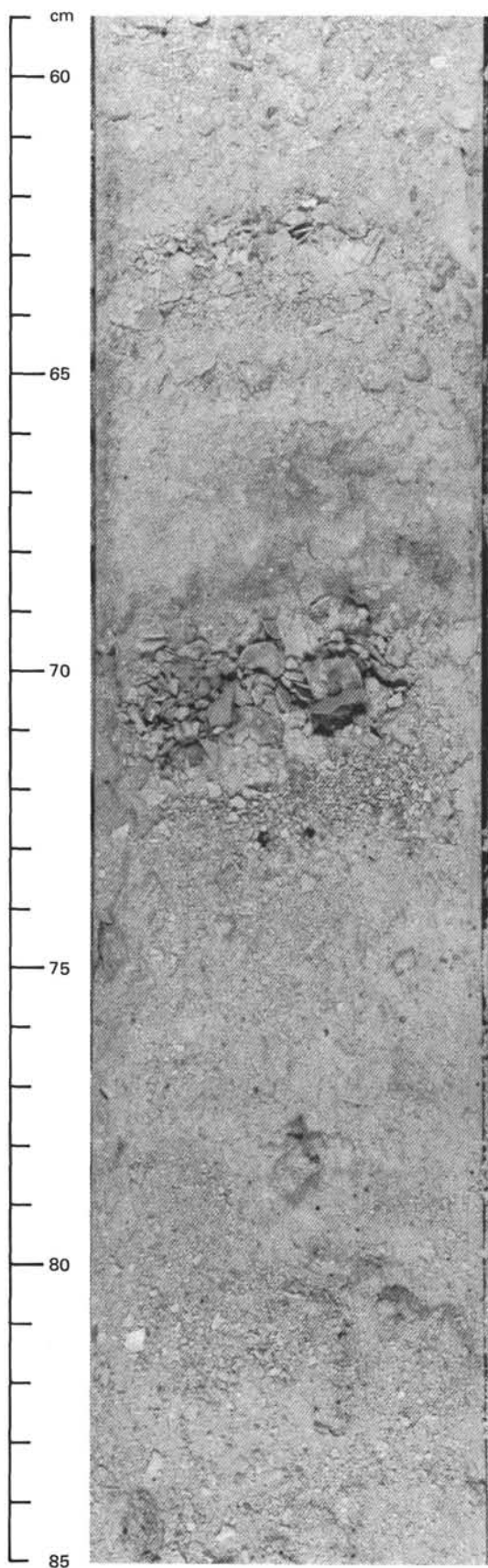


Figure 3. Reverse grading and poor sorting in thick, coarse-grained turbidite of Unit I. Grains consist of neritic debris, including *Halimeda* plates. Section 632A-1H-5.

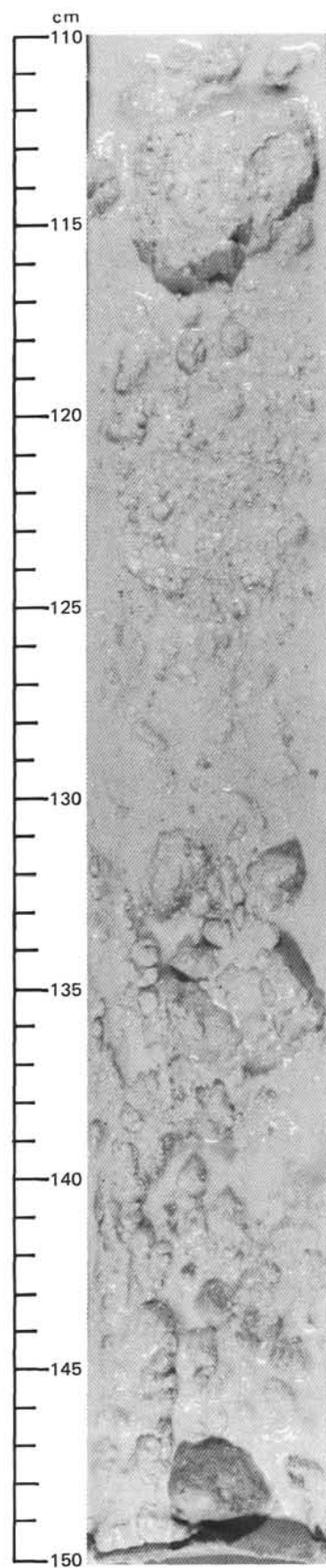


Figure 4. Debris-flow deposit (unlithified floatstone) with rounded chalk clasts at the top of Subunit IIB. Section 632A-8H-3.

Subunit IIC (84.9–104.7 m sub-bottom; Cores 632A-11H to 632A-13X-2) is latest Miocene to earliest Pliocene in age (see “Biostratigraphy” section, this chapter). This subunit is dominated, as is Subunit IIA, by alternating periplatform ooze (25%–40%) and chalk (60%–75%). This interval is, however, considerably more lithified than the overlying section, the amount of chalk being greater than the amount of ooze. Furthermore, well-lithified limestone was recovered in Core 632A-11H. This increase in lithification forced a switch from HPC to XCB techniques beginning with Core 632A-12X (93.9 m sub-bottom). An unlithified to partly lithified packstone composed of planktonic foraminifers occurs at the bottom of this subunit. The upper part of this interval was slightly burrowed and had flecks and stains of pyrite and an odor of H₂S.

Unit III (104.7–283.3 m sub-bottom; Cores 632A-13X, CC to 632A-16X; Cores 632B-1R to 632B-17R)

Unit III is latest Miocene in age (see “Biostratigraphy” section, this chapter) and includes all cores recovered in Hole 632B. Unit III is differentiated from Unit II by the first occurrence of well-lithified packstone in Core 632A-13X, CC. The change in lithification coincides with a decrease in foraminifers and nanofossils in smear slides. Unit III consists entirely of alternating limestone (lithified periplatform ooze) and hard, lithified grainstone and packstone (lithified turbidites). The limestone is various shades of white (principally 5Y 8/1, 2.5Y 8/0, and 2.5Y 8/2) and is a lighter color than the grainstone and packstone, which are principally light gray (2.5Y 7/2 and 10YR 7/2) to pale yellow (5Y 7/3).

The most striking characteristic of this unit, both in limestone and turbidites, is the presence of several generations of well-defined burrows covering 30%–60% of core surfaces; some core pieces larger than 5 cm are 100% burrows (Figs. 5 and 6). The burrows range in diameter from 1 mm to 5 cm, although most are 1–3 cm in diameter. Burrows are generally horizontal, but a few extend vertically over at least 15 cm (see Section 632A-12R-2). Typically, darker packstones and coarse to medium grainstones fill these burrows, making them most obvious in the lighter limestone. A few burrows in turbidites contain fine-grained sediment similar to that composing the limestone. The youngest generation of burrows contains the coarsest fill. Several burrows are of the *Zoophycos* or *Teichichnus* type (Frey, 1975; Wetzel, 1981) (Figs. 6 and 7), and a few contain pyrite and rare glauconite.

The limestone has a dominantly wackestone texture, although small patches of packstone do occur. Sand-sized grains in the limestone (exclusive of burrows) are coarse to fine and consist of skeletal fragments and planktonic and benthic (miliolid) foraminifers, which create intraparticle porosity.

Grainstones and packstones consist of well-sorted, coarse-to-fine-sand-sized skeletal fragments; platy grains are oriented parallel to bedding. These lithologies commonly exhibit horizontal lamination and cross-lamination with sharp, erosional bases (Figs. 7 and 8) in Cores 632B-4R to 632B-17R. These features are particularly well developed in Cores 632B-4R to 632B-8R and 632B-16R to 632B-17R. Grainstones and packstones also show normal grading, which is commonly disrupted by burrowing. These characteristics indicate that grainstone and packstone layers are turbidites. Interparticle porosity and minor moldic porosity is well developed in these turbidites.

The relationship between periplatform limestone and turbidites is well illustrated in Cores 632B-4R, 632B-6R, 632B-9R, and 632B-17R, which show upward-fining sequences, turbidites being at the base and limestone at the top (Fig. 8). These sequences are 20–60 cm thick; turbidites range from 5 to 20 cm and periplatform limestones from 5 to 40 cm in thickness. The

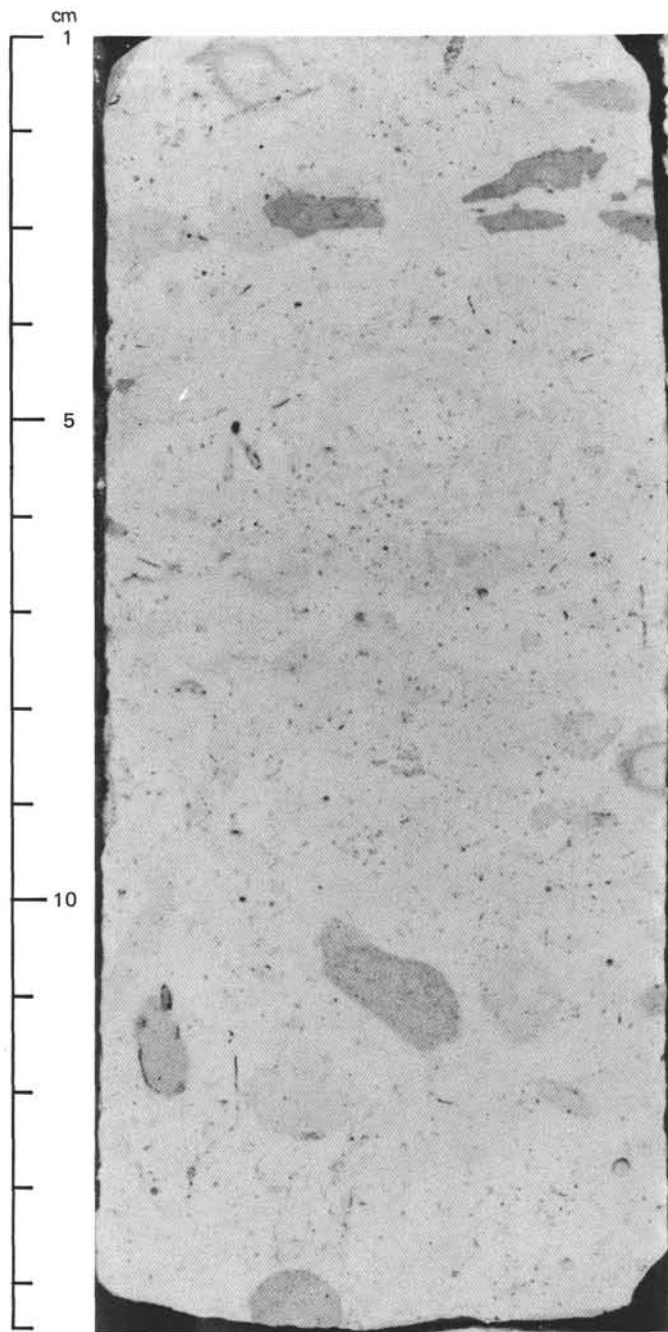


Figure 5. Well-defined burrows in limestone of Unit III. Darker burrows are filled with coarser sediment. Section 632A-14X, CC.

contact between these lithologies is gradational and is commonly obscured by burrowing (Fig. 7). The coarse fill in the limestone burrows appears to be turbidite sand reworked downward by burrowing organisms. In a few cores near the top of the unit, where only limestone was recovered, the only evidence of turbidites is preserved in such coarse burrow fill.

An unusual feature of Unit III is the presence of celestite (SrSO₄)-filled fractures in Cores 632B-2R, 632B-3R, and 632B-7R (Fig. 9). The angularity of these fractures indicates that they developed after consolidation, or lithification, of this unit.

Another important aspect of this part of the section is the presence of hydrocarbons. Asphalt flecks and tarry blebs occur in laminated grainstone and in burrow fill of Core 632B-4R

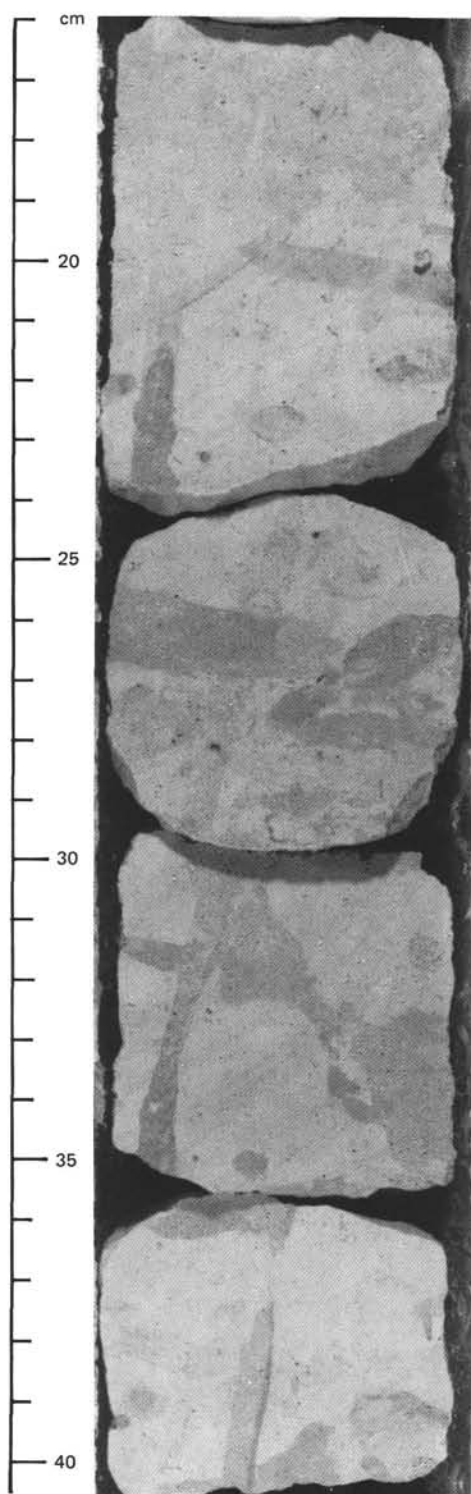


Figure 6. Several generations of well-defined burrows (horizontal and vertical) in limestone of Unit III. Vertical burrows, 24–35 cm, exhibit *Zoophycos* or *Teichichnus* type of structure. Section 632B-4R-1.

(149.6 m sub-bottom) to the bottom of the hole (283.3 m sub-bottom). These hydrocarbons occur only in the coarsest sediment, where interparticle and moldic porosity is best developed. More abundant hydrocarbons in Cores 632B-16R and 632B-17R forced abandonment of the hole at 283 m, well short of the target depth of about 1300 m.

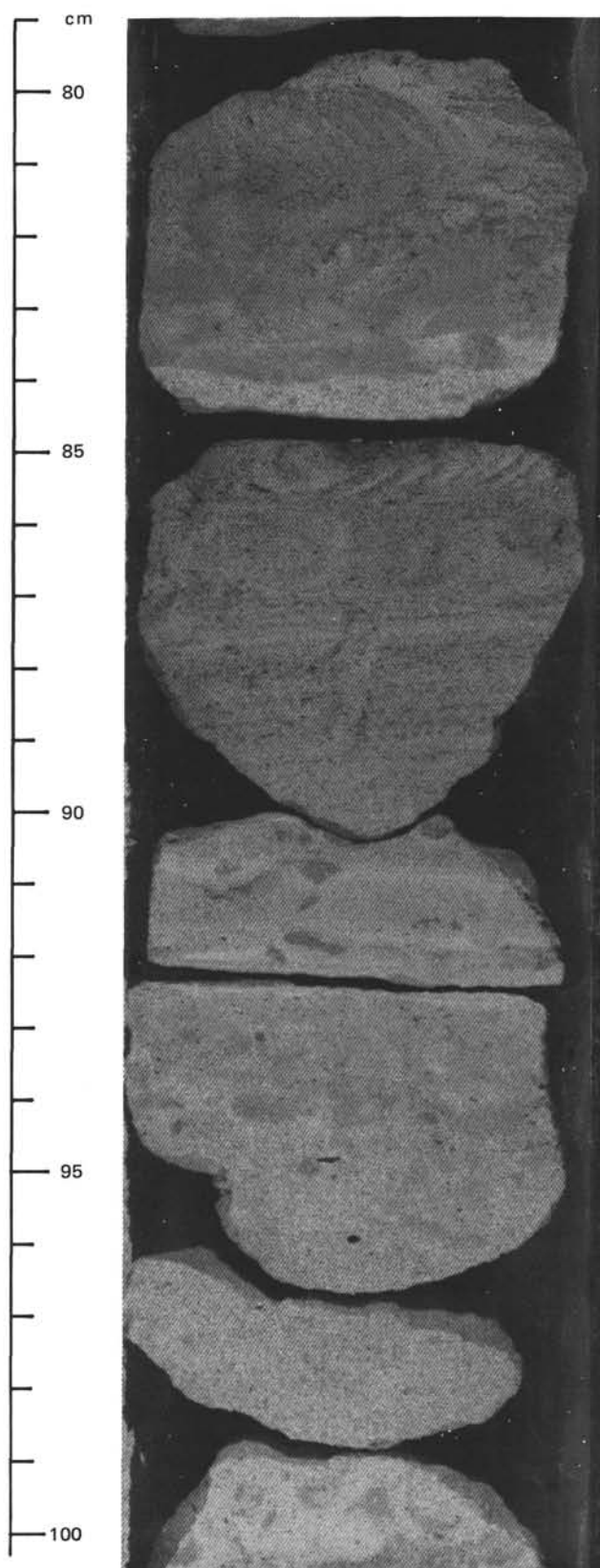


Figure 7. Lithified graded and laminated turbidite (grainstone) of Unit III. Grain size is coarse to medium sand, which consists of skeletal fragments. *Zoophycos* or *Teichichnus* type of burrows disrupts lamination at the top of this grainstone (80–86 cm). Sedimentary structures are enhanced by hydrocarbon flecks in coarse-grained sediment. Section 632B-17R-1.

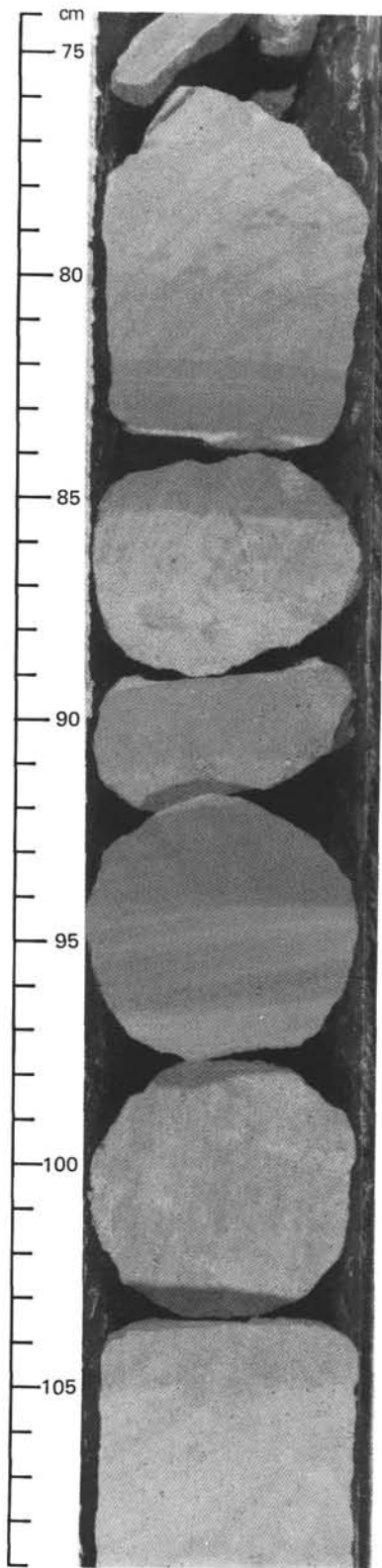


Figure 8. Upward-fining sequences of Unit III, consisting of interbedded periplatform limestone and lithified turbidites (grainstone-packstone). Turbidites have sharp, eroded bases, cross-lamination, and grading. Grain size is medium to fine sand, consisting of skeletal fragments. Burrowing is most intense in the limestone, although the turbidite at 85 cm exhibits a well-defined burrow cutting across lamellae. Photograph shows two and one-half sequences (bases of upward-fining sequences at 86 and 98 cm). Section 632B-4R-1.

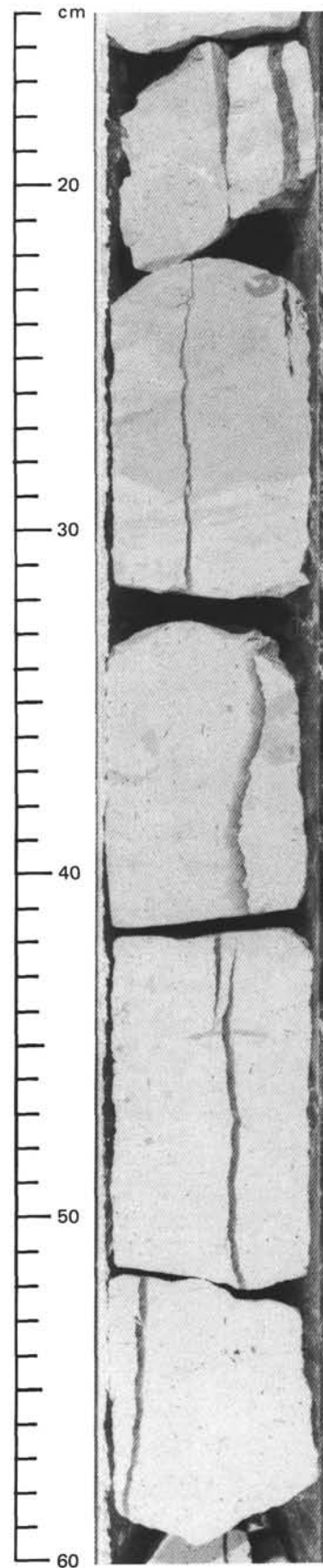


Figure 9. Celestite-filled fractures in periplatform limestone and lithified turbidite in Unit III. The fracture at 45 cm cuts a burrow with no displacement. Section 632B-7R-1.

Discussion

The section drilled at Site 632 in Exuma Sound is, in general, a turbidite basin fill, deposited at moderate (about 25 m/m.y.) to high (210 m/m.y.) accumulation rates (see "Sediment-Accumulation Rates" section, this chapter). Thick (50–200-cm) to thin (5–20-cm) turbidites are interbedded with perennial periplatform ooze, chalk, and limestone (Units I and III). The turbidite-ooze sequence is interrupted by a 50-m-thick interval of debris flows and periplatform ooze and chalk with rare turbidites (Unit II). Although the sediment gravity flows of Unit II were deposited at rates comparable to those of the basin-fill sediments of Units I and III, the associated oozes and chalks of Unit II have lower (5–10 m/m.y.) accumulation rates. In contrast, similar ooze-chalk deposits at Sites 628, 630, and 631 have high sedimentation rates (30–120 m/m.y.).

Periplatform limestone and lithified turbidites recovered in Unit III have higher seismic velocities (3000–4500 m/s) than interval velocities calculated from multichannel seismic data (about 1800 m/s) (see "Physical Properties" and "Seismic Stratigraphy" sections, this chapter). Because core recoveries in Unit III ranged only from 1% to 20% (exclusive of downhole contamination), Unit III clearly must contain significant thicknesses of less indurated, lower velocity sediments as well as the well-lithified, higher velocity deposits actually recovered.

As noted previously, aragonite is present throughout this section (see "Inorganic Geochemistry" section, this chapter), even in limestones and lithified grainstones and packstones of late Miocene age. It is not clear why this aragonite has survived lithification here or in the sediments at Site 631. The downhole decrease of aragonite (see "Inorganic Geochemistry" section, this chapter) does suggest that some dissolution of aragonite has occurred. Aragonite-derived strontium probably accounts for the celestite that fills fractures in Unit III, although further documentation is needed. Whether or not the presence of hydrocarbons in Unit III has anything to do with preservation of aragonite to 283 m sub-bottom is also unclear.

Summary

The section recovered at Site 632 was divided into three lithologic units: Unit I (0–54.7 m sub-bottom); interbedded periplatform ooze and unlithified turbidites (packstone and grainstone); basin fill; moderate accumulation rate; (2) Unit II (54.7–104.7 m sub-bottom); periplatform ooze and chalk with a 15-m-thick interval of sediment gravity flows (Subunit IIB); low accumulation rate in periplatform deposits, high accumulation rate in sediment gravity flows; and (3) Unit III (104.7–283.3 m sub-bottom); interbedded burrowed periplatform limestone and lithified turbidites (grainstone and packstone); basin fill; high accumulation rate.

BIOSTRATIGRAPHY

Introduction

The two holes drilled at Site 632 yielded a composite section that spans the late Miocene through the Quaternary. The section consists of a sequence of oozes, turbidites, and debris flows having major variations in rates of sediment accumulation. These variations in sedimentation somewhat complicate the paleontological record, as does downhole contamination. At least two intervals in the sequence appear to be condensed (see "Sediment-Accumulation Rates" section, this chapter), so that some age assignments are tentative. All references to cores are based on core-catcher samples, and depths refer to sub-bottom depths, unless otherwise specified.

Calcareous Nannofossils

Hole 632A

Two samples were studied from Core 632A-1H. Sample 632A-1H-1, 1 cm, contains abundant *Emiliana huxleyi*, indicating the *E. huxleyi* Acme Subzone. This subzone, which occupies the youngest part of Zone NN21, correlates with the late Pleistocene and Holocene. The recovery of this subzone suggests that the mud line was successfully retrieved. Sample 632A-1H, CC also contains *E. huxleyi*, but *Gephyrocapsa oceanica* dominates. Therefore, the assemblage belongs to the oldest part of Zone NN21 and correlates with the early to latest middle Pleistocene.

Emiliana huxleyi is not present in Cores 632A-2H through 632A-5H, but *Pseudoemiliana lacunosa* occurs. The assemblage is assigned to Zone NN19, which correlates with the latest Pliocene to earliest middle Pleistocene. Reworking of older nannofossils is common throughout this part of the hole. The presence of planktonic foraminifers indicates that only the top of NN19 has been recovered, and even the occurrence of *Cyclococcolithina macintyreii* must be considered the result of reworking. In Core 632A-4H, Oligocene nannofossils are common reworked elements of the assemblages.

The late Pliocene was recognized tentatively in a poorly preserved assemblage in Core 632A-6H. The presence of *Discoaster brouweri*, *D. surculus*, *D. asymmetricus*, and *D. pentaradiatus* and the absence of *P. lacunosa* and *Reticulofenestra pseudoumbilica* indicate Zone NN16. Reworked (early) Oligocene nannofossils are abundant.

Sample 632A-7H-CC differs from the overlying sample by the presence of *R. pseudoumbilica* and is therefore assigned to Zones NN14/15. A subdivision between these two zones is difficult, because the presence or absence of the rare marker species *Amaurolithus tricorniculatus* cannot be reliably ascertained. These zones (NN14/15) correlate with the latest part of the early Pliocene. The same assemblage is present in core catchers from Cores 632A-8H and 632A-9H, in which Oligocene elements occur as reworked components. No age-diagnostic assemblages have been retrieved from the core catchers of Cores 632A-10H and 632A-11H.

Discoaster quinqueramus is present in Cores 632A-12X and 632A-13X, indicating Zone NN11, which correlates with the late Miocene. Oligocene nannofossils occur as rare, reworked components of these assemblages. Sample 632A-14X, CC contains only reworked Oligocene nannofossils. In Sample 632A-15X-1, 32 cm, *D. quinqueramus* was encountered (with thanks to G. Kuhn for sample advice), indicating that this sample also belongs to Zone NN11 of late Miocene age. Core 632A-16X contains only reworked Oligocene nannoplankton.

Hole 632B

Hole 632B (rotary drilled), the continuation of Hole 632A, was washed down to 120.7 m before coring commenced, creating an overlap of about 20 m with Hole 632A. Most of the cores contained only hard rock from which nannofossils were impossible to extract. The few zones that yielded nannofossils generally contained very poorly preserved assemblages. *Discoaster quinqueramus*, indicating Zone NN11, is present in all samples that yielded usable assemblages. Zone NN11 correlates with the late Miocene. Contrary to the general preservational trend in this sequence, two samples contain abundant and well-preserved assemblages (632B-8R, CC and 632B-13R-1, 74–75 cm). Both of these well-preserved assemblages contain *Discoaster berggreni* and *Ceratolithus primus*, indicating that these assemblages belong to the upper part of NN11 (CN 9b of Okada and Bukry, 1980), which correlates with the latest Miocene.

The hard limestones in the basal four cores did not yield any usable nannofossil assemblages. Thus, the lower 40 m of the hole has no age assignment.

Planktonic Foraminifers

Planktonic foraminifers of the Pleistocene *Globorotalia truncatulinoides* Zone (N22/N23) are present in Cores 632A-1H to 632A-4H (35.9 m sub-bottom). The co-occurrence of *G. truncatulinoides* and *G. tosaensis* in Section 632A-4H-1 suggests a latest Pliocene–early Pleistocene age for this level. Core 632A-5H contains only downhole debris. Sample 632A-6H-5, 72–74 cm, yielded a late Pliocene age, based on the presence of *Globigerinoides extremus* and *Globorotalia crassula* and the absence of *G. truncatulinoides* and early Pliocene species. The core catcher from Core 632A-6H (55.0 m sub-bottom) contains a planktonic-foraminiferal assemblage indicative of the early late Pliocene *Globorotalia miocenica* Zone (upper N19), whereas an early Pliocene age (*Globorotalia margaritae* Zone, N19) is suggested for Core 632A-7H (64.6 m sub-bottom). Diagnostic taxa include *Globorotalia plesiotumida*, *Globoquadrina altispira*, and *Globigerina nepenthes*.

The nominate taxon of the *Globorotalia margaritae* Zone occurs in Cores 632A-8H, 632A-9H, 632A-12X, and 632A-13X (64.6–112.3 m sub-bottom). Core 632A-10H contains shallow-water debris of indeterminate age, and Core 632A-11H contains limestone. The co-occurrence of *Globorotalia margaritae* and *G. cibaoensis* in Cores 632A-12X and 632A-13X indicates an earliest Pliocene age (N18/N19). Rare, poorly preserved planktonic foraminifers were extracted from the limestones of Cores 632A-14X to 632A-16X and Cores 632B-1R to 632B-17R (112.3–283.3 m sub-bottom); age-diagnostic taxa generally could not be identified. A latest Miocene age (N17), however, is suggested for Cores 632B-8R, 632B-10R, 632B-12R, and 632B-13R. Diagnostic species include *Globorotalia cibaoensis*, *Globigerinoides extremus*, *Globigerina nepenthes*, *Sphaeroidinellopsis paenedehiscens*, *S. subdehiscens*, and *Globorotalia* sp. cf. *G. plesiotumida*.

Benthic-foraminiferal assemblages are characterized by a mixture of neritic and bathyal species.

Larger Foraminifers

Larger benthic foraminifers are present in core-catcher samples from Cores 632A-1H, 632A-3H, and 632A-4H, and in Samples 632A-5H-3, 50–52 cm, and 632A-5H-4, 50–52 cm. Preservation is generally good. The foraminifers present include *Amphistegina* sp. gr. *lessonii*, *Archaias angulatus*, *Cyclorbiculina compressa*, and *Cyclorbiculina americana*, which occur with other benthic foraminifers such as *Textulariella barretii*, *Cymballoporella squamosa*, *Articulina* sp. cf. *A. pacifica*, *Quinqueloculina* sp. cf. *Q. reticulata*, *Pyrgo* sp., and *Vertebralina mucronata*. The larger foraminifers (*Archaias*, *Cyclorbiculina*) occur with planktonic foraminifers and nannofossils, which indicate a late Pleistocene (N23) age for the interval. These larger foraminifer species, typical of shallow-water environments, are considered to have been deposited penecontemporaneously in deep water by turbidites.

SEDIMENT-ACCUMULATION RATES

A nearly complete section of uppermost Miocene to Holocene basinal sediments is present at Site 632 (Fig. 10). The uppermost Pliocene and Pleistocene sequence of ooze and calciturbidites accumulated at an average rate of 22 m/m.y. Mid-Pliocene ooze in Cores 632A-6H and 632A-7H accumulated at a rate of 6 m/m.y. A sequence of lower Pliocene calciturbidites and debris flows in Cores 632A-8H to 632A-10H accumulated at a rate of about 44 m/m.y. A hard layer of limestone in Core

632A-11H may correspond to a minor stratigraphic break within lower Pliocene strata. Uppermost Miocene–lowermost Pliocene ooze in Cores 632A-12X and 632A-13X again accumulated at a reduced rate, on the order of 10 m/m.y. A thick sequence of uppermost Miocene periplatform chalk and calciturbidites in Cores 632A-14X through 632A-16X and Cores 632B-1R through 632B-17R accumulated at a rate of about 210 m/m.y., as indicated by nannofossil biostratigraphy.

INORGANIC GEOCHEMISTRY

Interstitial Water

Concentrations of Ca, Mg, pH, alkalinity, salinity, chlorinity, and sulfate in the interstitial waters show slight changes with increasing depth in Hole 632A (see Figs. 11 and 12 and Tables 2 and 3). Calcium and alkalinity values reach a minimum and maximum of 8.8 mm/L and 4.1 meq/kg, respectively, at 33.7 m sub-bottom, and Mg, after showing an initial decline, increases to a maximum of 56.82 mm/L at 43.3 m sub-bottom. Sulfate values decrease to a minimum of 21.16 mm/L at 14.3 m sub-bottom.

Changes in the Ca and Mg concentrations are believed to be related to cementation, produced by the addition of CO₂ from sulfate reduction. However, increases in alkalinity are not directly related to CO₂ addition, as seen in the relationship between sulfate and alkalinity (Fig. 12). The maximum rate of sulfate reduction occurs much shallower than does the maximum in alkalinity. Perhaps this initial rise is a result of sulfate reduction, whereas the final change is caused by processes such as methanogenesis. The magnitude of the alkalinity rise is reduced by the precipitation of calcium carbonate.

X-Ray Studies

The main trend in the carbonate mineralogy of Holes 632A and 632B is a gradual reduction in the percentage of aragonite (see Figs. 13 and 14 and Tables 4 and 5). The first-order pattern indicates diagenetic replacement of aragonite by calcite, although a strong second-order cyclicity may reflect processes such as periodic input or dissolution (see Droxler et al., 1984). The persistence of aragonite in considerable amounts was a surprising feature of Holes 632A and 632B. Even in well-cemented rocks, which had been fractured and filled with celestite (SrSO₄), aragonite was a major component. The origin of the celestite is unknown but may be related to the diagenesis of aragonite, which can contain between 7000 and 8000 ppm Sr. During dissolution of aragonite and precipitation of calcite, Sr becomes enriched in the pore waters to a point that SrSO₄ could precipitate.

Carbonate-Bomb Data

The percentage of carbonate was between 95% and 100% throughout the entire length of the section (see Fig. 15 and Table 6).

ORGANIC GEOCHEMISTRY

Twenty-four rock samples were taken from Hole 632A for analysis by the Rock-Eval method. Some gas data were also obtained from unsplit cores (through the liner). In Hole 632B, near terminal depth, petroleumlike substances were encountered. This material, which occurred both as free blebs and as bitumen impregnating the rock, were analyzed by thin-layer chromatography (TLC) and gas chromatography (GC).

Rock-Eval Data

The lithology in Hole 632A is subdivided into three major lithotypes (see Fig. 16 and "Sedimentology" section, this chapter): (1) upper Pliocene–Pleistocene periplatform ooze (Unit I);

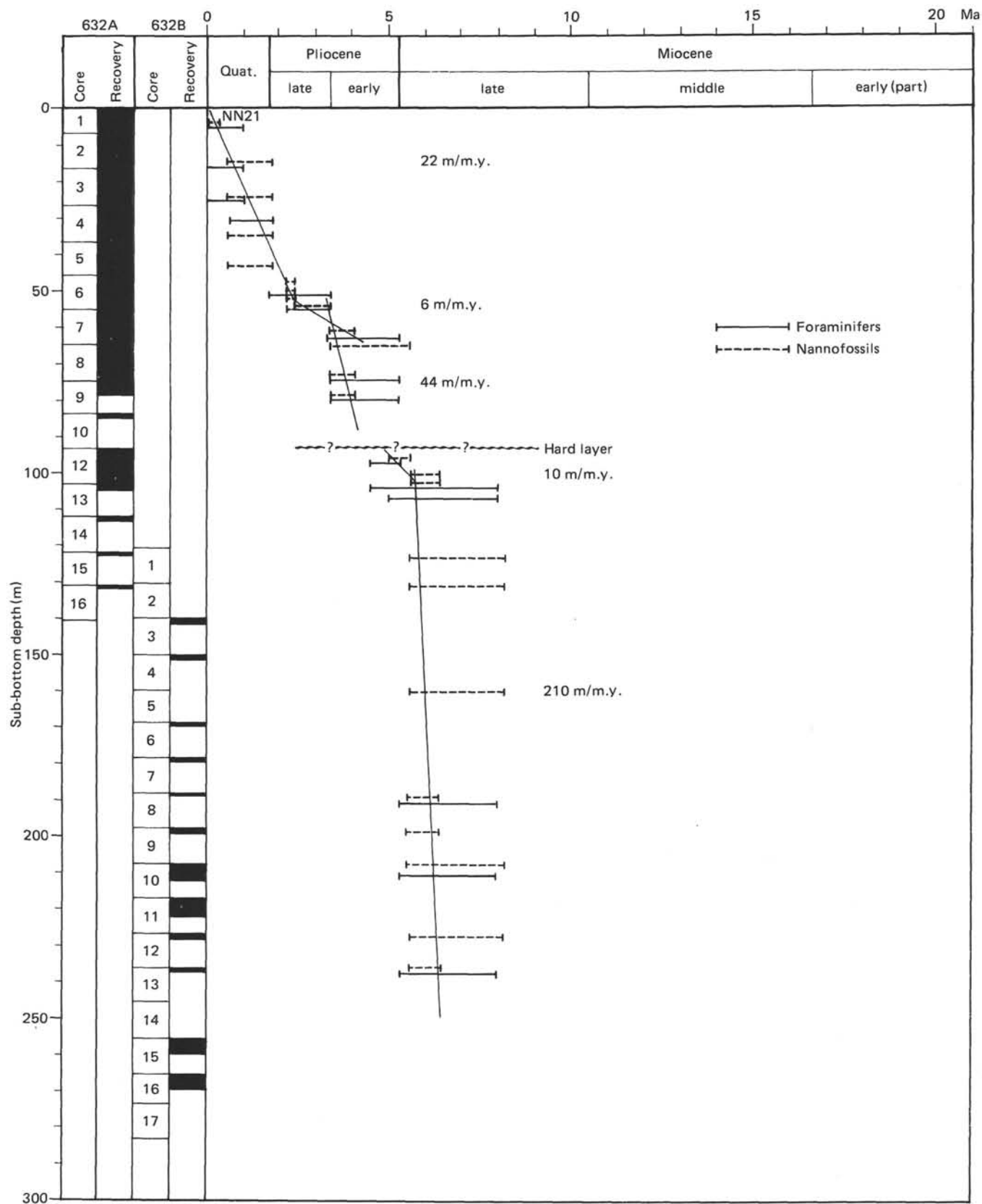


Figure 10. Sediment-accumulation rates, Site 632.

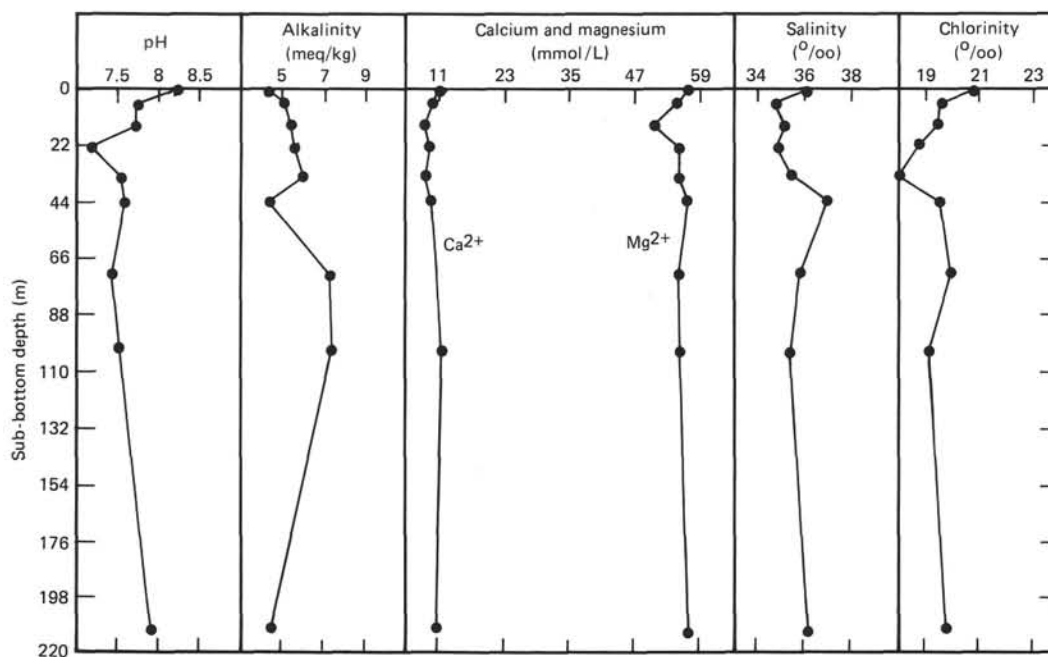


Figure 11. Summary of interstitial-water analyses, Holes 632A and 632B.

(2) upper Miocene–Pliocene mixed lithologies: periplatform ooze–debris flows–turbidites, etc. (Unit II); and (3) upper Miocene chalky lime mudstones (Unit III).

The S_2 content (see Fig. 16) of Unit I was generally low (0.1–0.2), corresponding to lipid-poor kerogens (types III and IV). Units II and III showed more variation in lipid-rich kerogen content, values of 0.4–0.55 being common. However, S_2 values in Units II and III were generally lower than those of Site 631 (see “Organic Geochemistry” section, Site 631 chapter).

The S_2/S_3 ratio (see Fig. 17), though unreliable as a kerogen-typing guide, indicated the generally low source potential of this site. Kerogens of Hole 632A would be capable of generating mainly gas.

The S_1 content (free bitumen) was also generally very low, i.e., less than 0.1, further signifying the low hydrocarbon potential of the site (see Fig. 18).

T_{max} (see Fig. 19) showed a similar pattern to that of Site 631, but more scatter was present in the data. Most of the Pleistocene and Neogene parts of the section showed the anomalously high T_{max} values seen at Site 631, but the trend was less uniform. This was interpreted as being a significant input of sea grass (*Thalassia* sp.), along with a greater admixture of other marine materials (probably algal) than at Site 631.

Gas Analyses

Gas analyses were run routinely on samples from Hole 632A. Graphs for total methane, ethane, and carbon dioxide content are shown in Figures 20–22. Carbon dioxide content fluctuated downhole but never fell below 1200 ppm and often rose to values of 3600 ppm.

The methane concentration, except for the top sample and the sample at 67 m sub-bottom, appeared to vary antipathetically in relation to the carbon dioxide concentration. Methane concentrations, even where high, were commonly 20 times less abundant than carbon dioxide concentrations. Ethane concentrations were, at most, 20 times less than the methane but showed a similar trend.

The gas data are interpreted as showing mutual exclusivity of methanogenesis and sulfate reduction. Fermentation of organic matter evidently had occurred where sulfate reduction was low.

The ethane concentration was interpreted as exclusively bio-synthetic because it mimicked the fluctuations in methane (except for the bottom sample).

An attempt was made to correlate these data with the inorganic-geochemistry data of Site 632 (see “Inorganic Geochemistry” section, this chapter). A crude correlation of CO_2 was noted with interstitial sulfate content (see Figs. 12 and 22). However, samples chosen for inorganic and organic analysis did not coincide in depth, and the gas data were affected by proportions of air left in the core liner. Seemingly, the higher the concentration of dissolved sulfate, the more actively the sulfate reducers evolved CO_2 . No other clear correlations were noted with the inorganic data.

Hydrocarbon Monitoring by Gas Chromatography and Rock-Eval Techniques

Numerous tar blebs were noted in the Pleistocene downwash of Core 632B-16X (4–5 cm). This material was immediately analyzed by thin-layer chromatography (TLC) to separate the aliphatic hydrocarbons using the methodology of Barnes et al. (1979). The aliphatic hydrocarbons were analyzed by gas chromatography on the shipboard Hewlett-Packard 5890, which contains a 25-m cross-linked methyl silicone fused silica capillary column (results are shown in Fig. 23).

After a discussion with drilling personnel, contamination from a drilling lubricant was suspected. Several of these greases were analyzed for comparative purposes. Line tar and Sedco/BP “pipe dope” (zinc-based) were analyzed. Core-liner lubricant was also investigated but not analyzed, as it is silicone-based. The line tar aliphatic hydrocarbons (Fig. 24) have an *n*-alkane pattern similar to that of the blebs in Core 632B-16R-1. Slight differences may reflect changes in work-up procedures, particularly because “blow-down” (i.e., exploration of the liquid surface by gently blown nitrogen gas) methodology could not be used. Instead, the sample was gently warmed on a stove, possibly resulting in a preferential slight loss of the “light ends,” i.e., nC_{10} – nC_{20} . The “pipe dope,” however, showed a completely different pattern, consisting almost entirely of a petroleum “hump” of branched cyclics in which *n*-alkanes were lacking (see Fig. 25). Biodegradation of petroleum produces this kind of

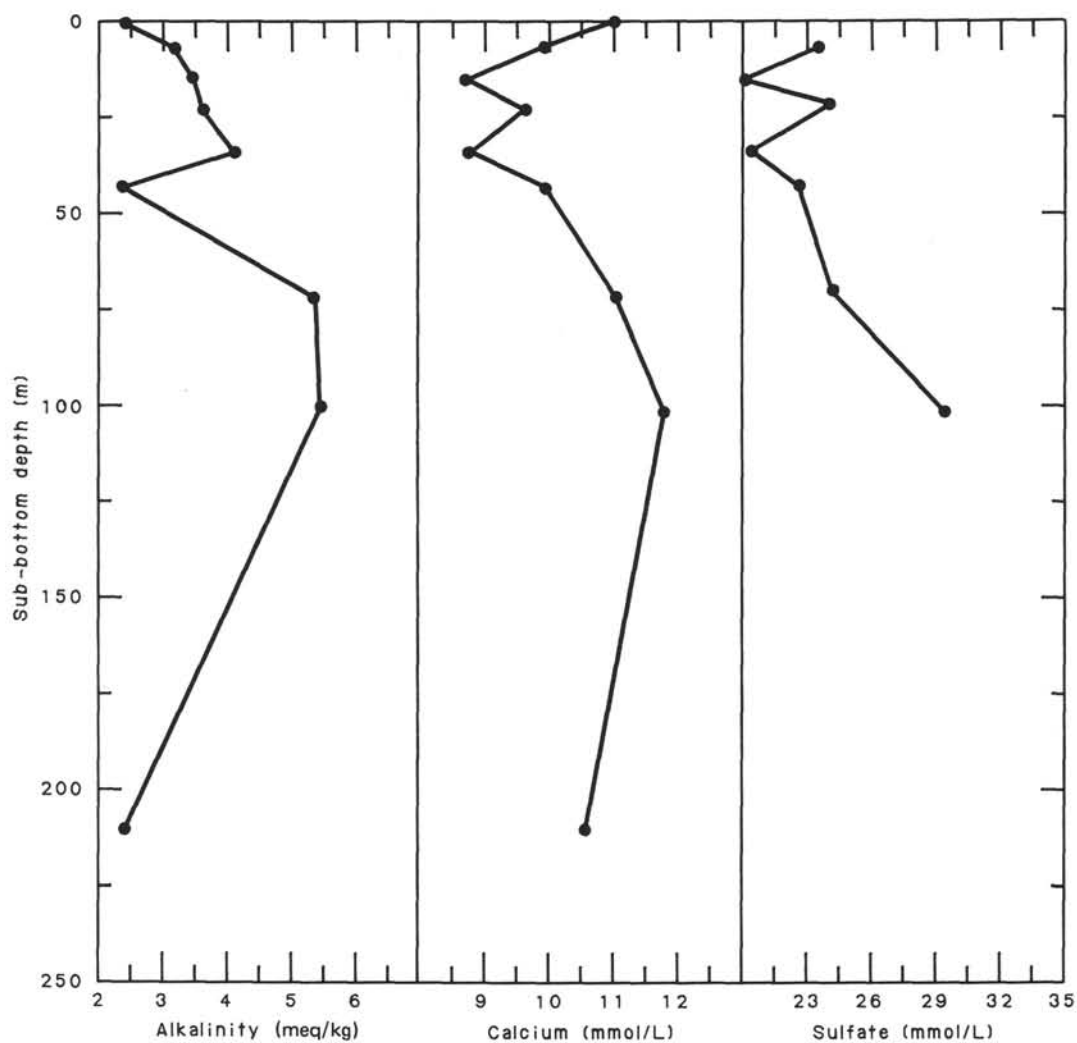


Figure 12. Interstitial-water alkalinity, calcium, and sulfate concentrations, Holes 632A and 632B.

Table 2. Analyses of interstitial waters from Hole 632A.

Sub-bottom depth (m)	pH	Alkalinity (meq/kg)	Salinity (‰)	Chlorinity (‰)	Ca (mmol/L)	Mg (mmol/L)	SO ₄ (mmol/L)
Surface seawater	8.21	2.42	36.2	20.83	10.93	56.67	—
5.9	7.73	3.16	34.8	19.52	9.94	54.72	23.44
14.3	7.74	3.47	35.2	19.48	8.72	50.51	20.16
22.6	7.18	3.62	34.8	18.72	9.60	55.06	24.37
33.7	7.54	4.11	35.5	18.00	8.80	55.04	20.73
43.3	7.60	2.37	37.0	19.55	9.90	56.82	22.52
72.0	7.42	5.37	35.8	19.96	11.01	54.94	24.58
101.3	7.52	5.44	35.4	19.17	11.77	55.24	28.91

Table 3. Analyses of interstitial waters from Hole 632B.

Sub-bottom depth (m)	pH	Alkalinity (meq/kg)	Salinity (‰)	Chlorinity (‰)	Ca (mmol/L)	Mg (mmol/L)	SO ₄ (mmol/L)
210.4	7.91	2.43	36.2	19.82	10.59	57.0	27.31

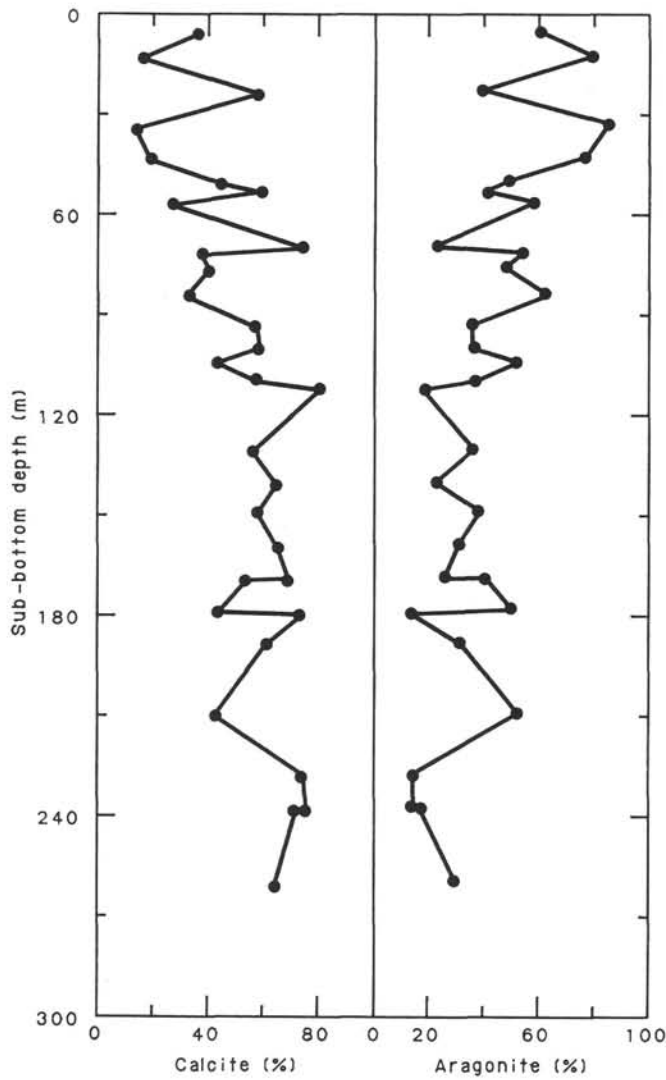


Figure 13. Percentages of calcite and aragonite in sediments from Holes 632A and 632B.

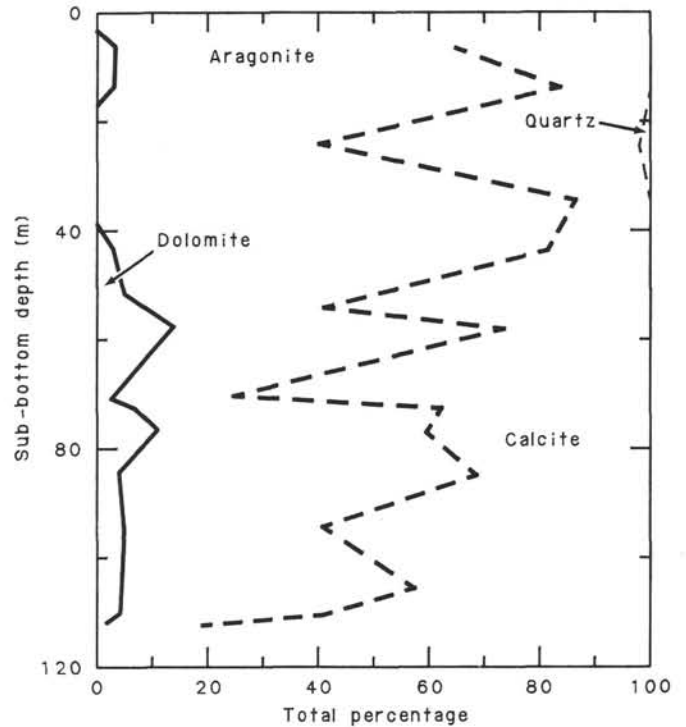


Figure 14. X-ray data, Hole 632A.

material. The blebs did not, therefore, appear to originate from "pipe dope" and were tentatively interpreted as being line tar.

In Sample 632B-17X, CC, bitumen-impregnated packstones were encountered. This well-lithified limestone contains a dull fluorescent bitumenlike substance with very little organic material extracted. A 20-g rock sample yielded only 1.2 mg on TLC separation, and gas-liquid chromatography (GLC) of the aliphatics resulted in a pattern unlike that of any of the contaminants previously considered. A blank was also run. Only nC_{16} - nC_{19} and pristane/phytane were significant components of this fraction. The bitumen was tentatively interpreted as being possibly of algal derivation and of unknown maturity. Shore-based studies are planned.

Table 4. X-ray analyses of samples from Hole 632A.

Sub-bottom depth (m)	Calcite (%)	Aragonite (%)	Dolomite (%)	Quartz (%)	Comments
5.9	36	61	3	0	
13.3	16	80	3	0	Illite-montmorillonite present
24.1	59	40	0	2	
33.7	14	86	0	0	Low-Mg calcite, 70%; high-Mg calcite, 30%
43.3	19	78	3	0	Palygorskite(?) present; low-Mg calcite, 62%; high-Mg calcite, 38%
50.6	45	50	5	0	
53.6	59	41	0	0	
57.2	27	59	14	0	Palygorskite(?) present
70.2	75	22	3	0	Palygorskite(?) present
72.0	38	55	7	0	Palygorskite(?) present
76.4	41	48	11	0	
84.5	32	64	4	0	Illite-montmorillonite present
93.9	58	36	5	0	Illite-montmorillonite present
104.9	43	53	4	0	
110.1	58	38	4	0	
112.7	81	18	2	0	

Table 5. X-ray analyses of samples from Hole 632B.

Sub-bottom depth (m)	Calcite (%)	Aragonite (%)	Dolomite (%)	Quartz (%)	Comments
130.8	56	37	7	0	Illite-montmorillonite present
140.7	65	23	12	0	
149.6	0	0	0	0	Celestite (SrSO ₄) in fissures
149.6	58	39	3	0	Host rock for celestite
159.2	65	31	4	0	Illite-montmorillonite present
168.9	70	26	4	0	
169.2	54	41	5	0	
178.7	44	51	5	0	
179.3	75	14	11	0	
188.6	61	32	7	0	Illite-montmorillonite present
209.5	42	53	5	0	Illite-montmorillonite present
227.4	75	15	9	0	Illite-montmorillonite present
236.9	76	15	8	0	Illite-montmorillonite present
237.1	72	17	11	0	
255.5	63	31	6	0	
258.6	65	30	4	0	
260.0	80	15	4	0	

Table 6. Carbonate-bomb data, Site 632.

Sub-bottom depth (m)	CaCO ₃ content (%)
4.2	95
12.0	91
24.9	94
34.5	96
40.1	97
47.6	100
57.2	95
72.8	102
76.4	98
84.5	100
93.1	100
100.6	98
104.4	103
112.7	99
130.8	99
140.7	97
169.0	100
169.8	95
179.3	94
188.6	96
198.6	97
209.7	96
219.3	96
227.4	99
236.9	97
259.6	99

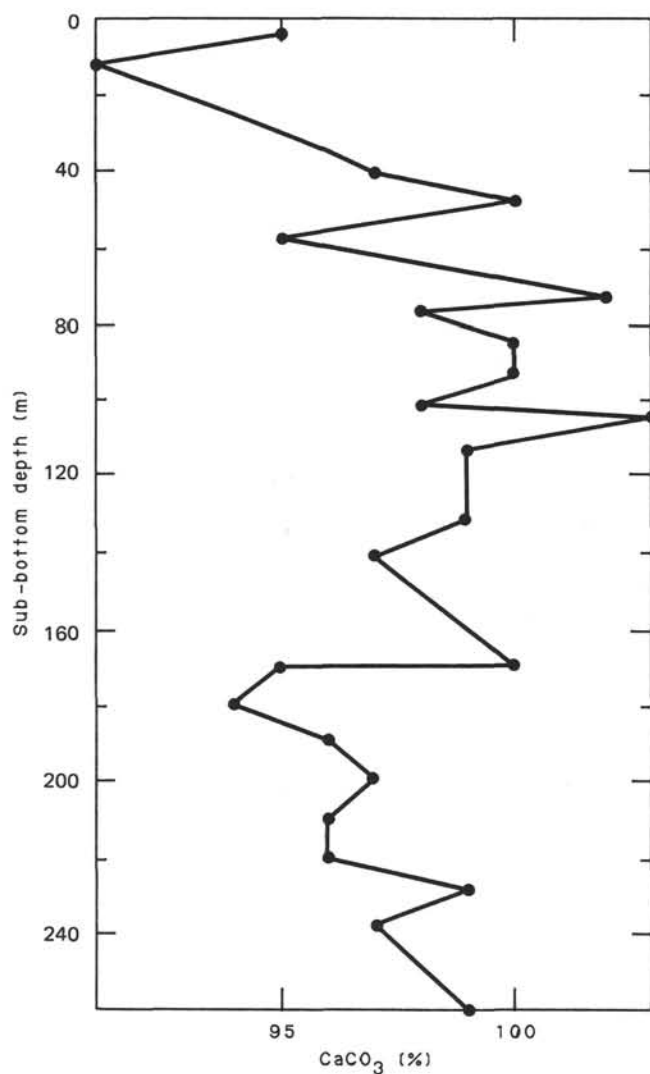


Figure 15. Carbonate-bomb data, Holes 632A and 632B.

Sample 632B-17X, CC, 1 cm, was also analyzed by the Rock-Eval method. The data are given in Table 7. However, bitumen was insufficient within this rock to distinguish it (on the basis of Rock-Eval analysis alone) from the other Miocene samples of Site 632.

A kerogen concentrate was prepared from this sample using hot diluted hydrochloric acid to remove all carbonate. A residue of about 0.5% "kerogen" remained, which was dried and run on the Rock-Eval (as a 10-mg sample; see Table 7). The material gave a production index within the oil-generation zone, and the S₂/S₃ kerogen-typing ratio was that of a mixed oil and gas type (probably equivalent to type II kerogen, but total-organic-carbon [TOC] values were not available). T_{max} showed the sample to be fairly immature. Only ratios are discussed here because the sample was a kerogen concentrate and was extracted (see Barnes et al., 1979) before demineralization, possibly lowering the content of free hydrocarbons.

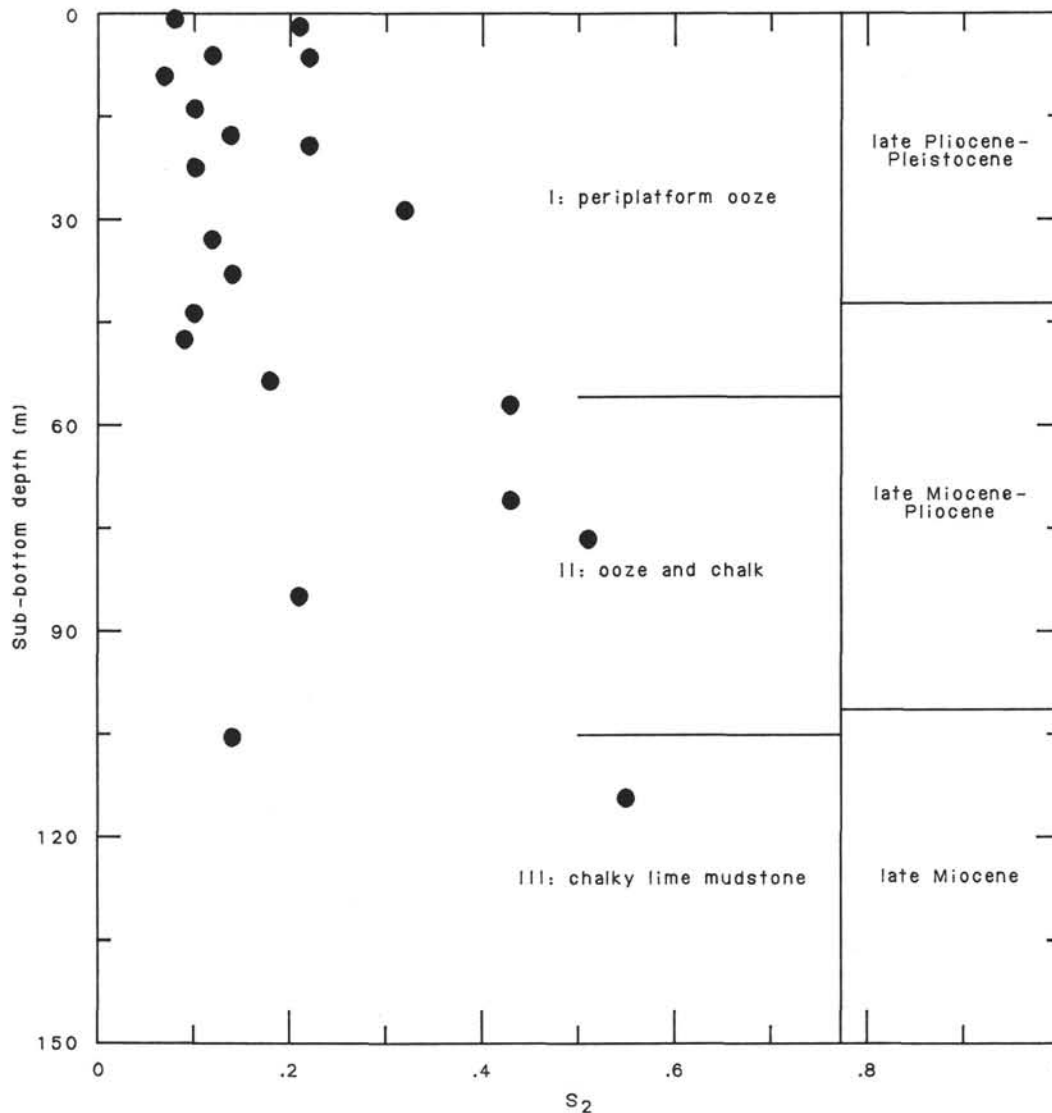


Figure 16. S_2 content of lithologies at Site 632, showing downhole variation.

PALEOMAGNETISM

Natural Remanent Magnetization

Thirty-one oriented 7-cm³ samples were taken from soft sediments recovered from Hole 632A. Twenty-five of these samples were removed from Cores 632A-1H through 632A-3H, of Pleistocene age, and the rest, from Cores 632A-9H, 632A-10X, and 632A-12X, of late Miocene to early Pliocene age (see "Biostratigraphy" section, this chapter). Additionally, sixteen 12-cm³ mini-cores were drilled from upper Miocene limestones obtained from Hole 632B. Although these limestone samples correspond to a wide range of depths in the hole, from 150 to 264 m sub-bottom (Cores 632B-4R to 632B-16R), they were all deposited within a period of less than about 3 m.y. (see "Biostratigraphy" section, this chapter).

Most of these samples, having magnetizations less than 1.5×10^{-6} emu, are too weakly magnetized to be accurately measured with the shipboard Molspin spinner magnetometer. However, the samples from Core 632A-1H and those from Section 1 of Core 632A-2H have magnetizations 1 to 1.5 orders of magnitude higher. The most highly magnetic of these samples has an intensity of 6.2×10^{-5} emu.

From 11 of the more strongly magnetized samples, a mean natural remanent magnetization (NRM) inclination of 61.2° and a standard deviation of 21.5° were calculated. This is considerably steeper than the present geocentric axial dipole field inclination of 41.3° for Site 632. Although the two inclinations seem indistinguishable, given the scatter in the NRM directions, the inclinations measured from these samples probably have been steepened by an overprint magnetization derived from their exposure to large magnetic fields near the drill pipe.

Magnetic Susceptibility

Whole-core magnetic-susceptibility measurements were generally made at 20-cm intervals along each core section recovered from Holes 632A and 632B. Where recovery was low, the sampling interval was 10 cm. A total of 595 measurements were made in both holes; 441 of these are from Hole 632A, and 154 from Hole 632B. Fewer readings were taken from Hole 632B because of lower recovery rates.

Figure 26A is a plot of the raw susceptibility values vs. sub-bottom depth. Many large-amplitude spikes are evident, most corresponding to the top of the first section of a given core. As

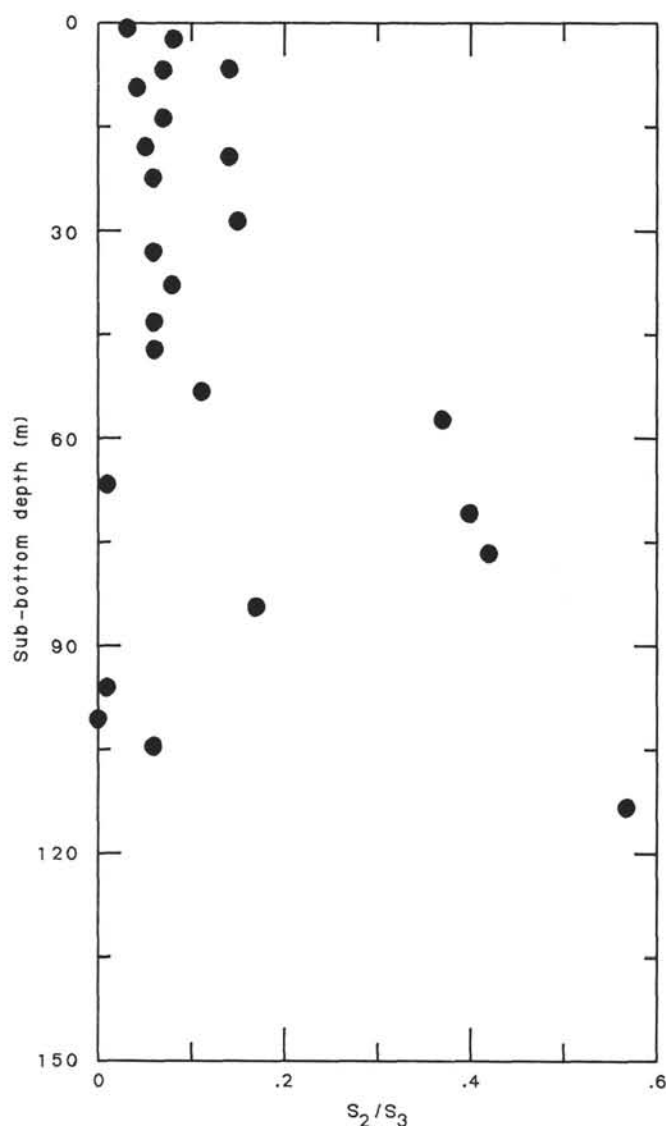


Figure 17. S_2/S_3 ratio of lithologies at Site 632, showing downhole variation. Kerogen becomes more lipid-rich downhole (but S_3 values are unreliable). Kerogen is mainly types III and IV.

with previous Leg 101 holes, metallic contamination as a result of rust from the drill pipe seems to be the most likely explanation for most of the spikes. Rust was detected by eye in Cores 632A-4H, 632A-5H, 632A-10H, and 632B-10R. A bit of metal wire caused one spike in Core 632A-7H. Both Cores 632A-5H and 632B-10R appeared to consist mainly of downhole contamination. As noted in the summary for Site 627, rust often disseminates throughout this sort of material, probably from outside the drill string. Both cores give very high and irregular susceptibility values (Fig. 26A).

Metallic contamination was a greater problem in Holes 632A and 632B than in previous holes on Leg 101. In removing the spikes thought to be caused by this contamination, approximately 20% of the data were excised, compared with about 5% at previous sites. Because the water depth at Site 632 is greater by 915 m than the deepest at the previous sites, the metallic contamination probably stems from the extra stands of drill pipe needed to reach the ocean bottom. Having lain unused for nearly 1.5 yr (according to the drilling engineer), this pipe was most likely coated with rust, which the core barrel managed to dislodge while traveling to and from the bottom of the hole.

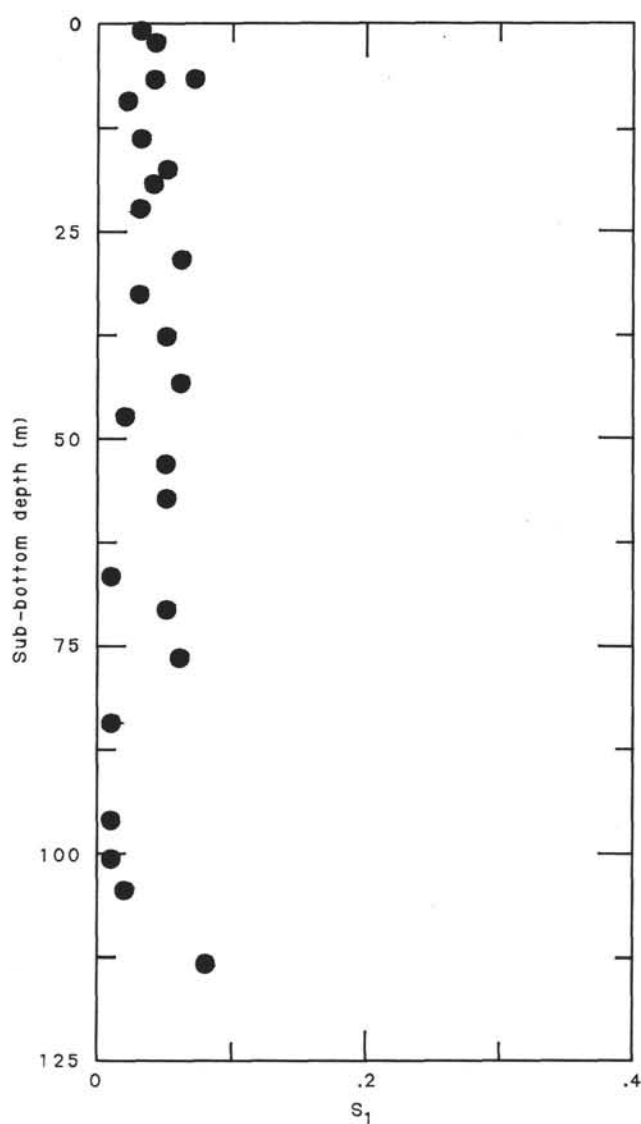


Figure 18. S_1 content (bitumen) of lithologies at Site 632, indicating minor content of free hydrocarbons.

Most of the downhole-contamination values and spikes thought to result from rust were removed in a plot of magnetic susceptibility vs. depth (Fig. 26B; see "Paleomagnetism" section, Site 627 chapter, for explanation of rationale used for removal of spurious values). The most notable feature is a marked decrease in susceptibility in the 15 m below the ocean bottom. In Core 632A-1H the average susceptibility in each section ranged from 1.7×10^{-6} G/Oe to 4.7×10^{-6} G/Oe, whereas in Core 632A-2H the averages ranged from -0.3×10^{-6} G/Oe to 0.2×10^{-6} G/Oe. These high susceptibility values correlate with the larger than average magnetizations found in the oriented paleomagnetic samples, noted previously, from Core 632A-1H. Similar high-magnetic susceptibility readings were also found near the seafloor in Holes 627B and 631A.

Below 35 m sub-bottom, the recovery from both Holes 632A and 632B was low, so trends in the susceptibility data are difficult to define. However, as seen in Figure 26B, most of the deeper cores appear to be slightly diamagnetic (i.e., the susceptibility is negative). Such values seem to be indicative of material that is primarily calcium carbonate and seawater having virtually no magnetic minerals. This trend mirrors the pattern of susceptibility vs. depth in most other Leg 101 holes.

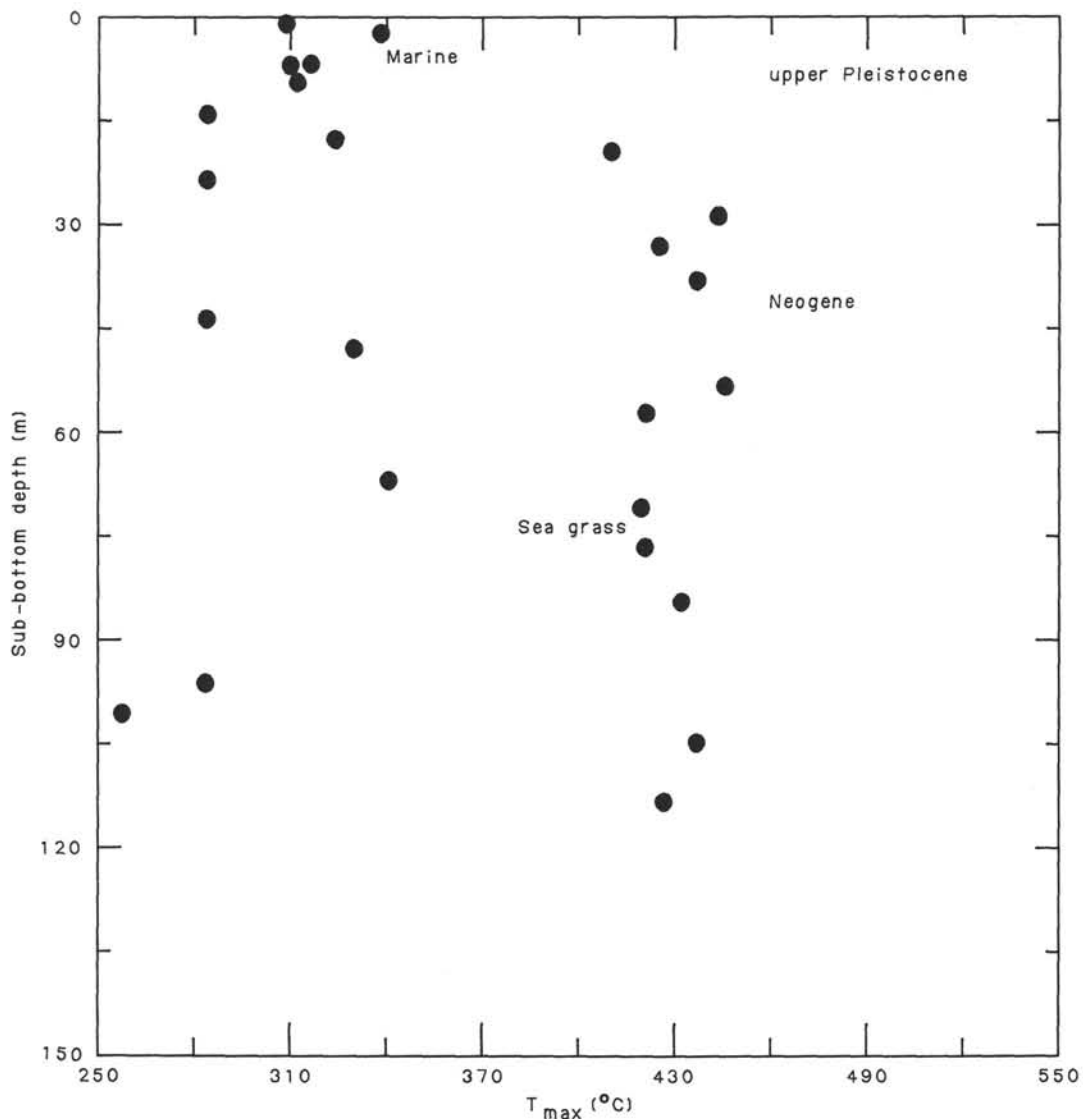


Figure 19. T_{max} values downhole at Site 632, showing highly immature kerogen in top 15 m of section (upper-middle Pleistocene), possibly marine, underlain (15–120 m sub-bottom) by a more “mature” kerogen type (probably from *Thalassia* sp.).

PHYSICAL PROPERTIES

Physical properties were measured for sediment and rock recovered from Site 632, as described in the “Introduction and Explanatory Notes” chapter (this volume). The Gamma Ray Attenuation Porosity Evaluator (GRAPE) was used to take 2-min counts on discrete samples.

Compressional Wave Velocity

Hole 632A

Compressional-wave-velocity values are combined results of measurements taken both in and out of the liner. Between the low values in Core 632A-1H at 1.5 m sub-bottom (1600 m/s) and in Core 632A-13X at 111.8 m sub-bottom (1561 m/s), average values range from 1650 and 1700 m/s (Fig. 27 and Table 8). Parts of Hole 632A above 104.4 m sub-bottom showed drilling disturbance, and these sections correlate with the lowest values recorded. Core 632A-3H-2 (18.4 m sub-bottom) was composed of skeletal sands. In this core, it was difficult to transmit a good compressional wave signal through samples in the liner and im-

possible to make a measurement outside the liner. Skeletal sand in Cores 632A-5H (39.5–42.5 m sub-bottom), 632A-9H, and 632A-10H (75–84 m sub-bottom) also transmitted a poor signal; therefore, actual values may be higher than recorded. Partly indurated chalk was measured in Core 632A-13X (111.8 m sub-bottom).

Between 103 and 113 m sub-bottom, the velocity profile changes noticeably. In Core 632A-14X (112.7 m sub-bottom), recovered sediment was lithified. Compressional wave velocities reflect this change in lithification; values jump to 3786 m/s at this depth. One well-lithified sample, recovered from Sample 632A-14X, CC at 121 m sub-bottom, registered an extreme value of 4735 m/s.

Hole 632B

Compressional wave velocities were measured of lithified limestone recovered from Hole 632B between 130.21 and 274 m sub-bottom. Values are highly variable, and results seem to depend on the particular sample chosen. For example, a high value of 4250 m/s was recorded from a packstone in Core 632B-4 (172 m sub-bottom), whereas at the same depth a brown grainstone reg-

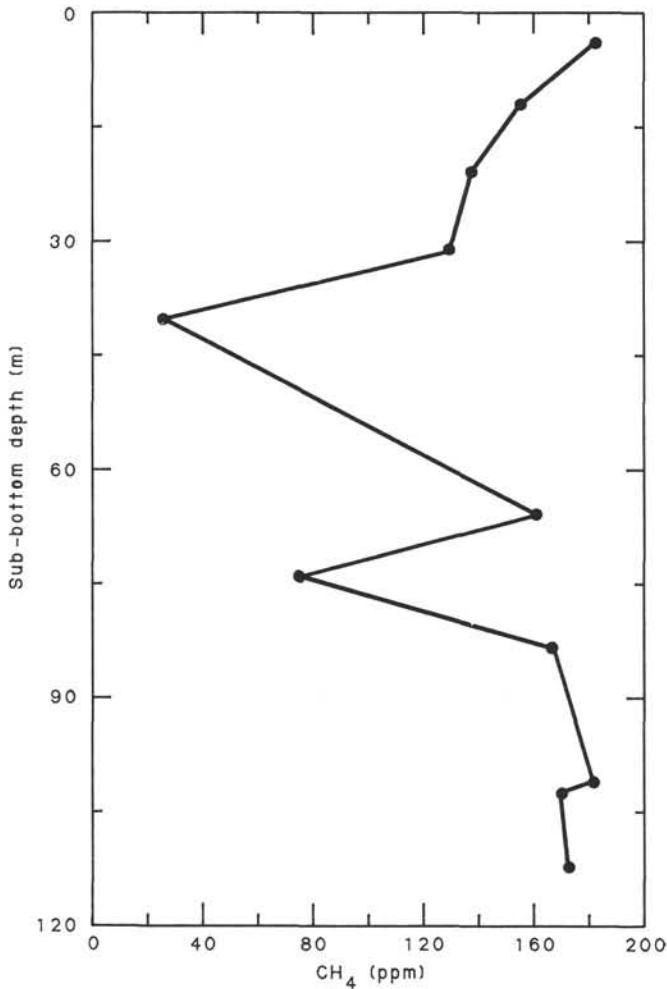


Figure 20. Methane content downhole at Site 632.

istered 3762 m/s. Measurements were made wherever possible, both perpendicular and parallel to bedding (Table 8), but no anisotropy was evident. There is a trend toward increasing velocity with increasing depth (Fig. 27).

Wet-Bulk Density, Porosity, and Dry Water Content

Hole 632A

In general, index properties do reflect the change between unconsolidated and lithified sediments observed between 110 and 120 m sub-bottom (see "Sedimentology" section, this chapter). Wet-bulk-density values increase from 1.57 g/cm³ in Core 632A-1H (2.2 m sub-bottom) to 2.08 g/cm³ in Sample 632A-16X, CC (140.7 m sub-bottom). Dry water content decreases from 75.42% at 2.2 m sub-bottom to 27.56% at 140.7 m sub-bottom. Porosity values show a similar trend, a decrease from 67.82% at 2.2 m sub-bottom to 44.63% at 140.7 m sub-bottom.

Hole 632B

Wet-bulk-density values measured at 139.6 m sub-bottom (2.11 g/cm³), the first sample being from Hole 632B, are similar to those measured at the bottom of Hole 632A. The same trend of increasing values continues until the last index-property measurement is reached at 261.4 m sub-bottom (2.40 g/cm³). Dry water content decreases from 42% to 18.6% in Hole 632B, whereas porosity decreases from 25% to 8.6%.

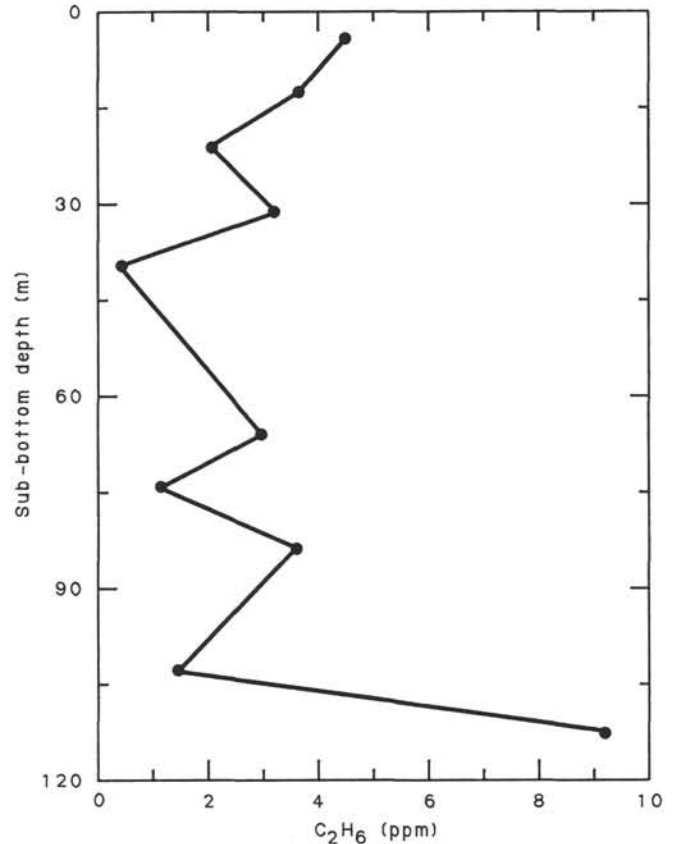


Figure 21. Ethane content downhole at Site 632.

Conductivity

Thermal conductivity was measured in Hole 632A between 0.75 and 113 m sub-bottom. Below this depth the sediment became too stiff for insertion of the temperature probes. Thermal conductivity increased linearly from $2.244 \times 10^{-3} \text{ cal} \times \text{°C}^{-1} \times \text{cm}^{-1} \times \text{s}^{-1}$ at the top of the Hole to $3.091 \times 10^{-3} \text{ cal} \times \text{°C}^{-1} \times \text{cm}^{-1} \times \text{s}^{-1}$ at 120 m sub-bottom.

Shear Strength

Shear-strength values recorded from Hole 632A are low, less than 5 kPa. The higher value of 5.89 kPa recorded at 18.9 m sub-bottom reflects a section of skeletal sand.

Discussion

Physical-property parameters at Site 632 display two different downhole distribution curves. The compressional wave velocity remains low for 110 m downhole. At 119.6 m sub-bottom, a distinct shift in the velocity profile seems to mark the boundary between unconsolidated sediment and well-lithified limestones. Wet-bulk density, water content, and porosity curves, however, suggest a gradual transition in consolidation and lithification. A distinct trend is evident in Hole 632A toward decreasing porosity and water content and increasing density values. Below 140 m sub-bottom, the slope of the profiles changes, but values do not shift sharply as is seen in the velocity profile. Water content and porosity are low in the chalk and skeletal-sand sections of the lower part of Hole 632A, and the trend toward decreasing water content and porosity and increasing density continues but less strongly in the more lithified limestones of Hole 632B. The low-velocity values from Hole 632A reflect the high water content in the upper part of the hole. In

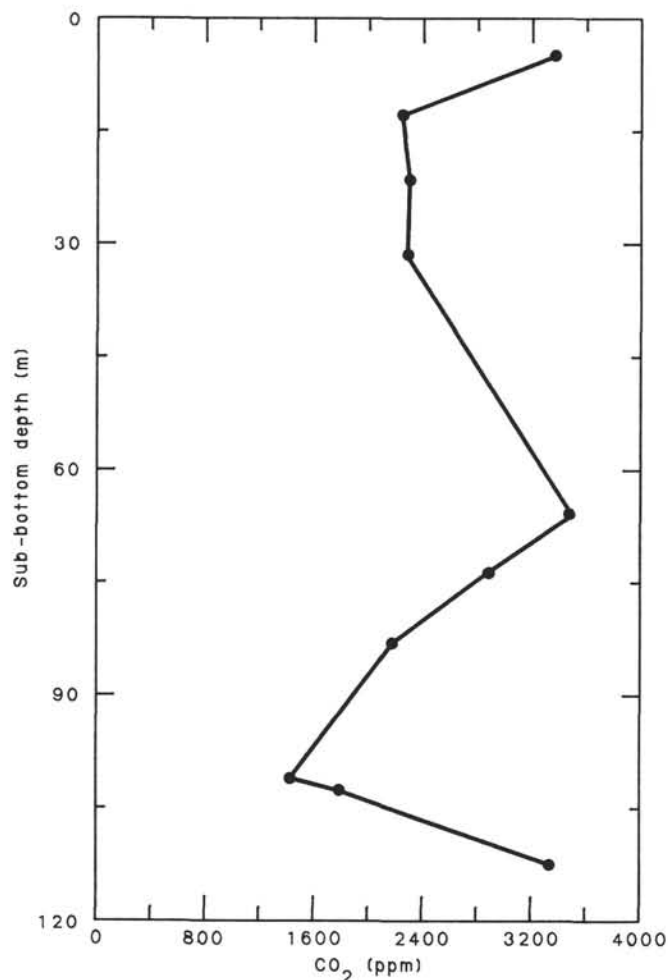


Figure 22. Carbon dioxide content downhole at Site 632.

the lower parts of the hole, the sediment composition, combined with drilling disturbance, may have caused low values. Dry skeletal sands and friable chalks provide a poor medium for transmitting compressional waves. Poor recovery in Hole 632B is reflected in sparse sampling. The recovered sediments consist mainly of dense, fine-grained limestones having high velocities. However, pieces of consolidated skeletal sand could be remnants of the unrecovered sediment. Thus, it seems that the consolidation at Site 632 is gradual yet interrupted by well-lithified layers below 104 m sub-bottom.

SEISMIC STRATIGRAPHY

Introduction

Scientific investigations at Site 632 (BAH-11-C), located at the intersection of site-survey lines ES-05 (Fig. 28) and ES-07 (Fig. 29), had two objectives: (1) to serve as the basinward end of the Exuma Sound slope transect, and (2) to provide additional calibration for long-range seismic stratigraphic correlations between Bahamian deep reentrants and the Gulf of Mexico/East Coast passive continental margin of North America. In this context, comparisons with Sites 626 and 627 were also important, particularly if the acoustic impedance contrast/velocity transition to the interpreted drowned shallow-water-carbonate platform at 1300 m sub-bottom could be reached (see also "Background and Objectives" section, Site 631 chapter).

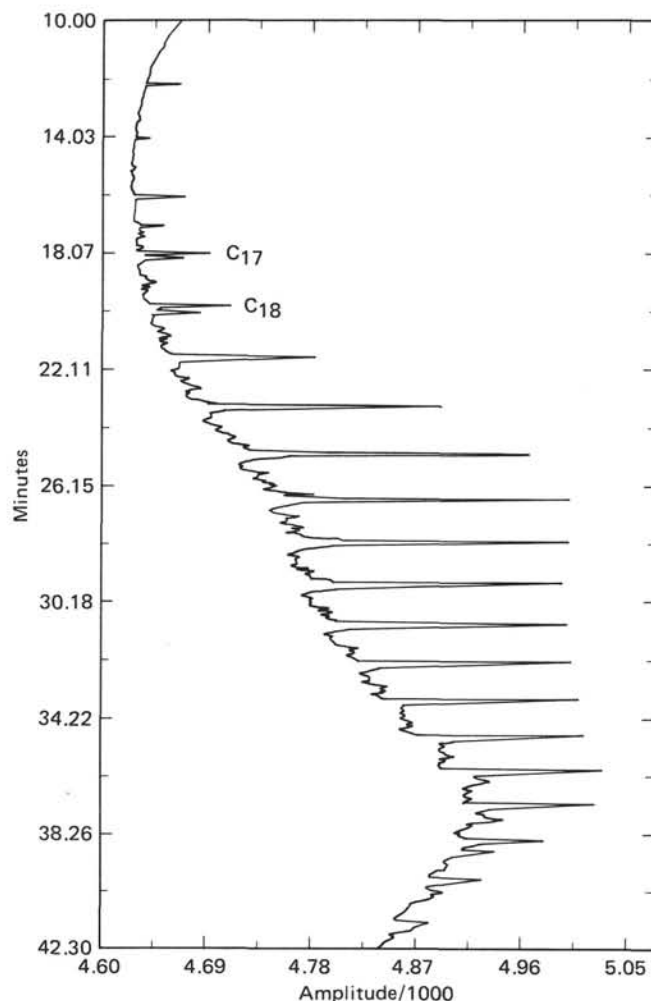


Figure 23. Gas chromatographic analysis of the aliphatic hydrocarbons from Sample 632B-16R-1, 13 cm. Note similarities to line tar (Fig. 24) and distinction from "pipe dope" (Fig. 25).

Acoustic Correlations

Holes 632A and 632B penetrated only to 283.3 m sub-bottom as a result of the presence of migrating hydrocarbons. Three seismic-sequence boundaries were identified within the sampled interval (Figs. 28 and 29 and Table 9).

Sequence 1 (0-95 m sub-bottom) corresponds to lithologic Units I and II, a section composed of alternating ooze and turbidites-debris flows. As shown on both seismic lines, reflectors within this sequence are wavy to subparallel and of varying amplitude. Local channeling approaching the resolution of the data is also evident. However, no hiatuses were detected in the upper 95 m of Hole 632A (see "Biostratigraphy" section, this chapter), although accumulation rates in this section varied substantially (see "Sediment-Accumulation Rates" section, this chapter).

The 1/2 seismic-sequence boundary occurs at 95 m sub-bottom on both lines (Figs. 28 and 29). However, it resembles a channel exhibiting as much as 65 m of relief within several km of the Site 632 location (Fig. 29). The 1/2 boundary horizon correlates in depth with the base of a series of Pliocene-Pleistocene mass flows (lithologic Subunits IIB and IIC; see "Sedimentology" section, this chapter) marked by a partly lithified packstone in Core 632A-10H (83.8-93.4 m sub-bottom). This

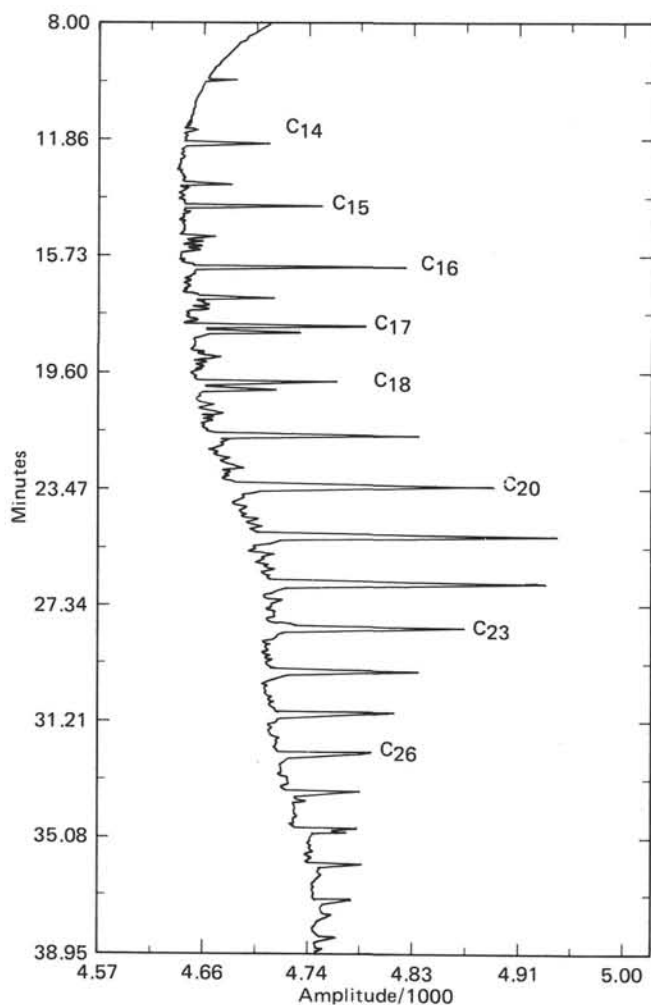


Figure 24. Gas chromatographic analysis of the aliphatic hydrocarbons from line tar. Note large amounts of *n*-alkanes.

packstone is interpreted to be a turbidite, and it may be related to a possible hiatus in the early Pliocene (Core 632A-11H, 93.4–93.9 m sub-bottom; see “Biostratigraphy” section, this chapter).

Seismic sequence 2 (95–109 m sub-bottom) is bounded at its base by the “O” acoustic horizon of J. Ladd and R. Sheridan (unpubl. data). Sequence 2 can be correlated in depth with lithologic Subunit IIC, a succession of periplatform ooze and chalk extending from the aforementioned early Pliocene hiatus in Core 632A-11H to Core 632A-13X-2 (see “Sedimentology” section, this chapter).

Reflector “O,” the 2/3 seismic-sequence boundary, occurs at 109 m sub-bottom on both profiles ES-05 and ES-07. Therefore, it can be interpreted as the Subunit IIC/Unit III boundary, which is identified as a lithified packstone of latest Miocene age occurring at the base of Section 632A-13X-2 (104.7 m sub-bottom). This packstone is probably a turbidite.

Seismic sequence 3 (109–212/222 m sub-bottom) is acoustically similar to sequence 1. It correlates in depth with the upper part of lithologic Unit III (see “Sedimentology” section, this chapter), a rapidly deposited section of chalk and lime grainstone-packstone. However, the 3/4 seismic-sequence boundary, apparently a channel that occurs at 212 m sub-bottom on ES-05 (Fig. 28) and at 222 m sub-bottom on ES-07 (Fig. 29), does not correlate with either a hiatus or a lithologic break at the appro-

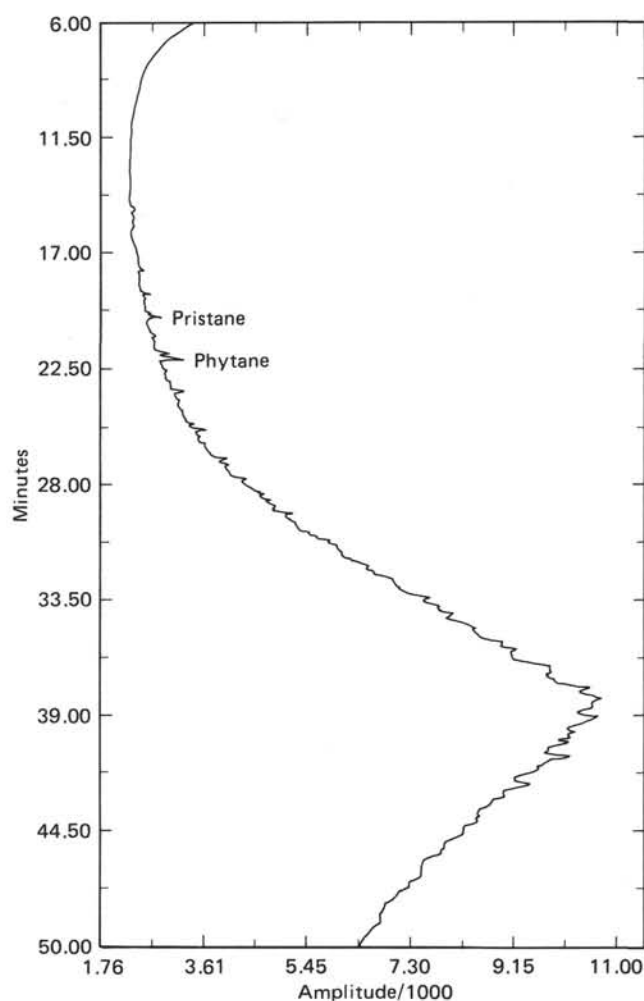


Figure 25. Gas chromatographic analysis of the aliphatic hydrocarbons from “pipe dope.” Note lack of *n*-alkanes and large hump.

Table 7. Organic-geochemical (Rock-Eval) values, Site 632.^a

Sample (levels in cm)	S ₁	S ₂	S ₃	T _{max} (°C)	Production index	
					S ₁ /(S ₁ + S ₂)	S ₂ /S ₃
^b 632B-17X, CC, 1–4	0.07	0.63	0.65	419	0.10	0.96
^c 632B-17X, CC, 1–4	6.37	27.34	6.72	411	0.19	4.06

^a For a more complete explanation, see Table 6, Site 626 chapter.

^b Before demineralization.

^c After demineralization.

appropriate depths within Unit III. Perhaps the 3/4 sequence boundary represents only local scour by turbidity currents traveling along the northwest–southeast axis of Exuma Sound.

Hole 632B did not reach the base of seismic sequence 4, a packet of subparallel reflectors of varying amplitude that must correspond to the alternating periplatform limestones and turbidites of Unit III.

Discussion

The unfortunate encounter with heavy oil in Hole 632B cut short operations at Site 632 and prematurely terminated an attempt to calibrate the regional seismic stratigraphic framework of Exuma Sound (J. Ladd and R. Sheridan, unpubl. data). The hydrocarbons presumably migrated upward from the buried plat-

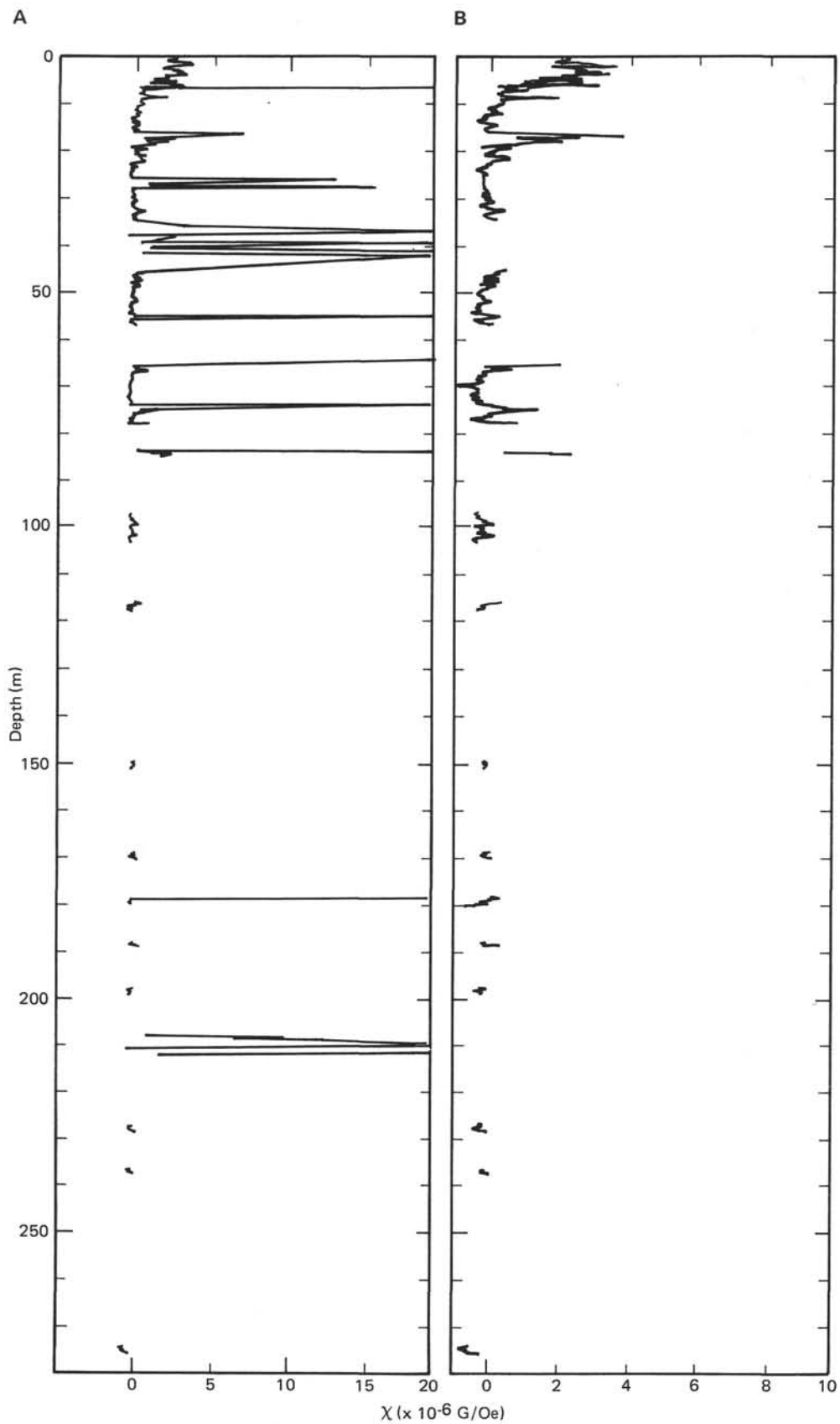


Figure 26. Magnetic-susceptibility values ($\times 10^{-6}$ G/Oe) plotted vs. sub-bottom depth. A. Raw susceptibility values. B. Susceptibility values with spikes, believed to have resulted from metallic contamination, removed (as discussed in the "Paleomagnetism" section, Site 627 chapter).

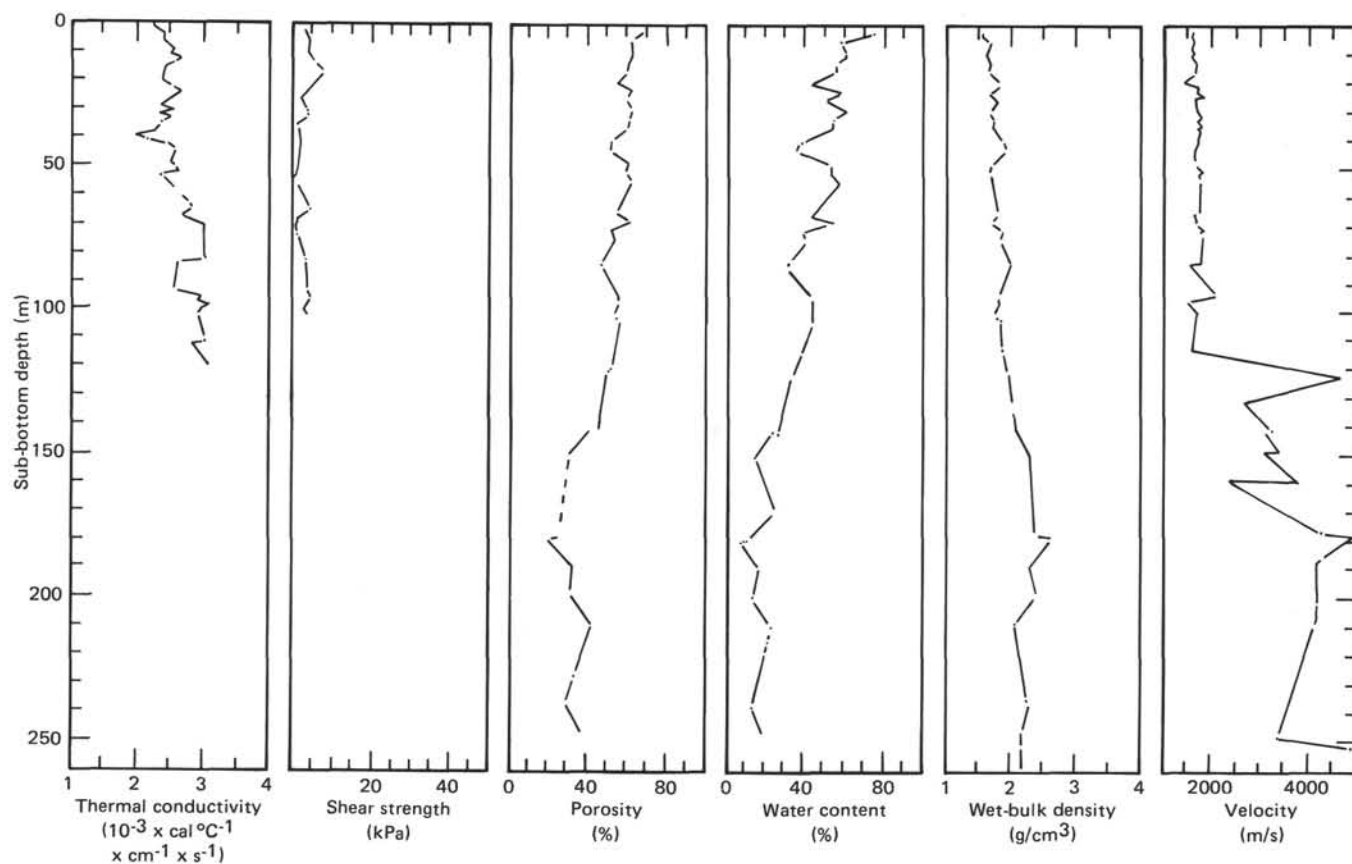


Figure 27. Graphic summary of physical properties, Hole 632A (0–139.1 m sub-bottom), and Hole 632B (130.1–260 m sub-bottom).

form through normal faults, which are common in the sedimentary section at Site 632 at sub-bottom depths greater than about 500 m (Figs. 28 and 29).

Nonetheless, several observations can be made, based on comparison of the available seismic data with the sampled section. First, the acoustic correlations within Exuma Sound advanced by J. Ladd and R. Sheridan (unpubl. data) are accurate in position, but the age of “O,” the 2/3 sequence boundary, needs to be recalibrated according to the drilling results. At Site 632, “O” does tie to a turbidite sequence of apparent regional significance, but J. Ladd and R. Sheridan (unpubl. data) date it as the boundary between the middle and late Miocene, whereas in Hole 632B it is of latest Miocene age. Second, evidence of channeling is present on both profiles ES-05 and ES-07, which cross at approximately right angles (see “Background and Objectives,” Site 631 chapter). This suggests that turbidites have entered the basin from all sides and not just down the axial valley of Exuma Sound. Third, the acoustic facies that characterize sequences 1–4, subparallel reflectors of variable continuity and variable but generally high amplitude, are consistent with a section of mixed pelagic sediments and turbidites. Finally, the channels on the seismic profiles probably correlate in the geologic record with either lithified turbidites or erosional bases of debris flows–slumps, but this cannot be conclusively shown at Site 632.

SUMMARY AND CONCLUSIONS

Two holes were drilled at Site 632. Hole 632A penetrated the top 141 m with HPC/XCB techniques, and Hole 632B rotary-cored to 283 m. The following succession of lithologic units was encountered at the site (Fig. 30; “Sedimentology” and “Biostratigraphy” sections, this chapter): (1) Unit I, periplatform ooze with turbidites (coarse sand) of mainly periplatform material,

late Pliocene to Holocene, 55 m; (2) Unit II, periplatform ooze and chalk with few turbidites and a 7-m debris flow, late Miocene to late Pliocene, 50 m; and (3) Unit III, periplatform chalk and limestone with rhythmic intercalations of turbidites (seismic-interval velocities and poor recovery suggest the presence of large amounts of unrecovered soft sediment), late Miocene, 178 m.

The section at Site 632 represents a basin-floor facies with graded turbidites, a lithology conspicuously absent on the bypass slopes (Unit I of Sites 630 and 631). However, within the constraints of this general setting, the depositional regime has varied considerably, as illustrated by the plot of sedimentation rates and lithologic units in Figure 31. We see a pattern of rapid rates in the late Miocene, early Pliocene, and Quaternary, punctuated by slow rates in the earliest Pliocene and the early late Pliocene. The intervals with high rates commonly contain turbidites; those with low rates have few or none. During the past 4 m.y., this steplike pattern of sedimentation rates and facies changes supports the notion of increased sedimentation during high stands of sea level and flooding of the banks (“high-stand shedding”; Mullins, 1983; Droxler and Schlager, in press). The pattern between 4 and 6.5 Ma is more ambiguous; for instance, the change from rapid turbidite deposition to slow, turbidite-free deposition seems to have occurred during a low stand of sea level in the latest Miocene.

Even though the site could not be drilled to target depth, it provides important calibration for the seismic stratigraphy of Exuma Sound. Most significant is the correlation of the top of Unit III (Miocene turbidites and periplatform limestones) with the regionally traceable reflector “O” of the site-survey stratigraphy (see “Seismic Stratigraphy” section, this chapter; J. Ladd and R. Sheridan, unpubl. data). The overlying seismic sequenc-

Table 8. Physical properties of sediments, Site 632.

Sample (level in cm)	Sub-bottom depth (m)	Velocity ^a (m/s)	Velocity in liner (m/s)	Wet-bulk density (g/cm ³)	Dry water content (%)	Porosity (%)	Thermal conductivity (10 ⁻³ × cal × °C ⁻¹ × cm ⁻¹ × s ⁻¹)	Shear strength (kPa)
Hole 632A								
1-1, 75	0.7						2.244	
1-2, 20			1405					
1-2, 70	2.2	1593		1.57	75.42	67.82	2.261	3.26
1-3, 75	3.7						2.407	
1-4, 20			1616					
1-4, 70	5.2	1632		1.70	58.02	62.53	2.411	4.42
1-4, 100			1609					
1-5, 75	6.7						2.407	
2-2, 20			1600					
2-2, 70	9.1	1621		1.65	61.08	62.79	2.556	4.08
2-2, 100			1581					
2-3, 75	10.6						2.507	
2-4, 20			1680					
2-4, 70	12.1	1682		1.69	56.02	60.77	2.641	7.70
2-4, 100			1682					
2-5, 75	13.6						2.537	
2-6, 20			1665					
2-6, 70	15.1	1637		1.68	55.67	60.11	2.423	5.55
2-6, 100			1665					
3-2, 20			1437					
3-2, 70	18.9	1616		1.86	41.89	54.73	2.378	5.89
3-2, 100			1754					
3-3, 75	20.4						2.385	
3-4, 20			1703					
3-4, 70	21.9			1.68	59.04	62.35	2.541	4.08
3-4, 100			1695					
3-5, 75	23.4						2.637	
3-6, 20			1806					
3-6, 70	24.9	1653		1.79	50.46	59.91	2.548	2.38
3-6, 100			1652					
4-2, 20			1683					
4-2, 70	28.5	1660		1.67	60.36	63.03	2.350	3.74
4-2, 100			1675					
4-3, 75	30.0						2.549	
4-4, 20			1766					
4-4, 70	31.5			1.74	54.42	61.36	2.326	4.08
4-4, 100			1683					
4-5, 45	32.7						2.498	
4-6, 20			1786					
4-6, 70	34.5	1683		1.73	54.03	60.87	2.359	1.47
4-6, 100			1731					
5-1, 75	36.5						2.245	
5-2, 75	38.1		1716	1.90	38.23	52.42	1.967	2.26
5-3, 75	32.5						2.158	
5-4, 75	44.1		1646	1.95	36.14	51.56	2.458	
5-5, 75	42.5						2.575	
6-2, 20			1637					
6-2, 75	47.6			1.73	54.01	60.83	2.539	15.29
6-2, 100			1637					
6-3, 75	49.0						2.505	
6-4, 20			1822					
6-4, 75	50.5			1.72	53.32	59.88	2.587	1.58
6-4, 100			1712					
6-5, 75	52.0						2.627	
6-6, 20			1729					
6-6, 70	53.5	1664		1.74	56.93	63.07	2.355	0.91
6-6, 100			1750					
7-1, 75	55.7						2.787	
7-2, 20			1714					
7-2, 30	55.8	1644	1639	1.81	43.50	54.62	2.821	4.53
8-2, 20			1692					
8-2, 70	66.8	1663		1.72	56.60	62.26	2.667	1.47
8-2, 100			1664					
8-3, 75	68.3						2.790	
8-4, 70	69.8		1844	1.88	38.73	52.37	3.021	1.13
8-4, 110			1732					
8-4, 140		1790						
8-5, 75	71.3						2.999	
8-6, 20			1780	1.86	41.14	54.09		1.69
8-6, 70	72.8	1486						
9-1, 75	75.0						2.997	
9-2, 20			1777					
9-2, 60	76.9		1551	1.99	31.08	46.76	3.027	3.62
9-2, 95			1638					

Table 8 (continued).

Sample (level in cm)	Sub-bottom depth (m)	Velocity ^a (m/s)	Velocity in liner (m/s)	Wet-bulk density (g/cm ³)	Dry water content (%)	Porosity (%)	Thermal conductivity (10 ⁻³ × cal × °C ⁻¹ × cm ⁻¹ × s ⁻¹)	Shear strength (kPa)
Hole 632A (Cont.)								
9-3, 30	77.6						2.613	
10-1, 70	84.5		2101	1.83	44.30	55.96	2.552	3.96
12-2, 30			1491					
12-2, 70	96.1		1491	1.81	44.43	55.61	2.969	4.53
12-3, 75	97.6						2.905	
12-4, 75	99.1						3.066	
12-5, 30			1689					
12-5, 70	100.6		1649	1.75	44.21	53.58	2.960	3.17
12-5, 100			1648					
12-6, 30			1663					
12-6, 70	102.1		1633	1.83	44.89	56.43	2.917	3.85
13-1, 75	103.4						3.035	
13-2, 20	104.4		1561	1.87	39.37	52.5	2.825	26.05
14-1, 10		1786						
14-1, 45	112.7			1.95	34.40	49.64	3.091	
14, CC	121.9	4736						
15-1, 25	122.2	2595						
16-1, 30	131.7	3161		2.08	27.56	44.63		
Hole 632B								
1, CC, 10	130.2	2400 (a) 2220 (c)						
2-1, 50	130.8	2980 (a)		2.11	24.55	41.22		
3-1, 70	140.7	3080 (a) 3380 (c)		2.30	15.56	30.52		
4-1, 70	150.3	2318 (a)						
6-1, 10	169.0	4300 (a) 3700 (c)		2.47	12.03	26.11		
6-1, 87	170.7	4900 (a) 5000 (c)		2.62	8.33	19.79		
7-1, 70	179.3	4100 (a) 4230 (c)		2.30	17.20	32.28		
8-1, 40	188.6	4350 (a) 4180 (c)		2.41	15.06	30.98		
9-1, 75	198.6	4200 (a) 4125 (c)		2.08	24.68	40.67		
10-1, 75	208.2							
10-2, 75	209.7			1.82	44.86	57.20	2.627	
10-3, 75	211.2						2.561	
11-1, 75	217.8						2.601	
11-2, 75				1.81	46.30	57.31	2.647	
11-3, 75	220.8						2.500	
11-4, 75	222.3						2.612	
12-1, 75	227.4	3750 (a) 3622 (b)		2.31	14.92	29.57		
13-1, 65	237.0	3153 (a) 3296 (b)		2.21	20.58	37.27		
15-3, 115	259.6	4472 (a) 4535 (b) 4077 (c)		2.40	8.56	18.60		
16-3, 100	267.9	3087 (b)						
16, CC	274.0	4753 (a)						

^a See footnote to Table 9, Site 627 chapter.

es show distinct channeling in the drilling area, probably caused by migrations of the axial valley of Exuma Sound. The bottom of one channel coincides with a hiatus at 92 m in the borehole.

Rapid burial diagenesis of the periplatform material is indicated by the abundance of limestones below 100 m (earliest Pliocene) and by steep gradients in the downhole profiles of density, porosity, and sonic velocity ("Physical Properties" section, this chapter). However, despite rapid and rather extensive lithification, magnesian calcite is present down to 40 m (upper Pliocene ooze), and aragonite concentrations, although showing a steady decline with depth, exceed 10% throughout the sequence. Celestite-filled fractures in the Miocene limestones of Hole 632B may be related to dissolution of aragonite and to a concomitant increase of strontium in the pore waters (see "Inorganic Geochemistry" section, this chapter).

In contrast to Sites 627 and 628, where turbidite sands remain unlithified even where interlayered ooze turns to chalk, the Miocene section at Site 632 shows no such difference. Turbidites and intervening fine-grained sediments are equally well lithified.

Interstitial waters show a strong negative correlation between alkalinity and sulfate concentration. An alkalinity maximum and a sulfate minimum occur at 150 m (see "Inorganic Geochemistry" section, this chapter). This strongly suggests that the alkalinity profile is largely controlled by sulfate reduction and by associated oxidation of organic matter with attendant production of carbon dioxide in the sediment (see "Inorganic Geochemistry" and "Organic Geochemistry" sections, this chapter).

The limestones and chalks from 160 m down contain small amounts of hydrocarbons (see "Organic Geochemistry" section, this chapter). Small quantities of tar were detected in the inter-

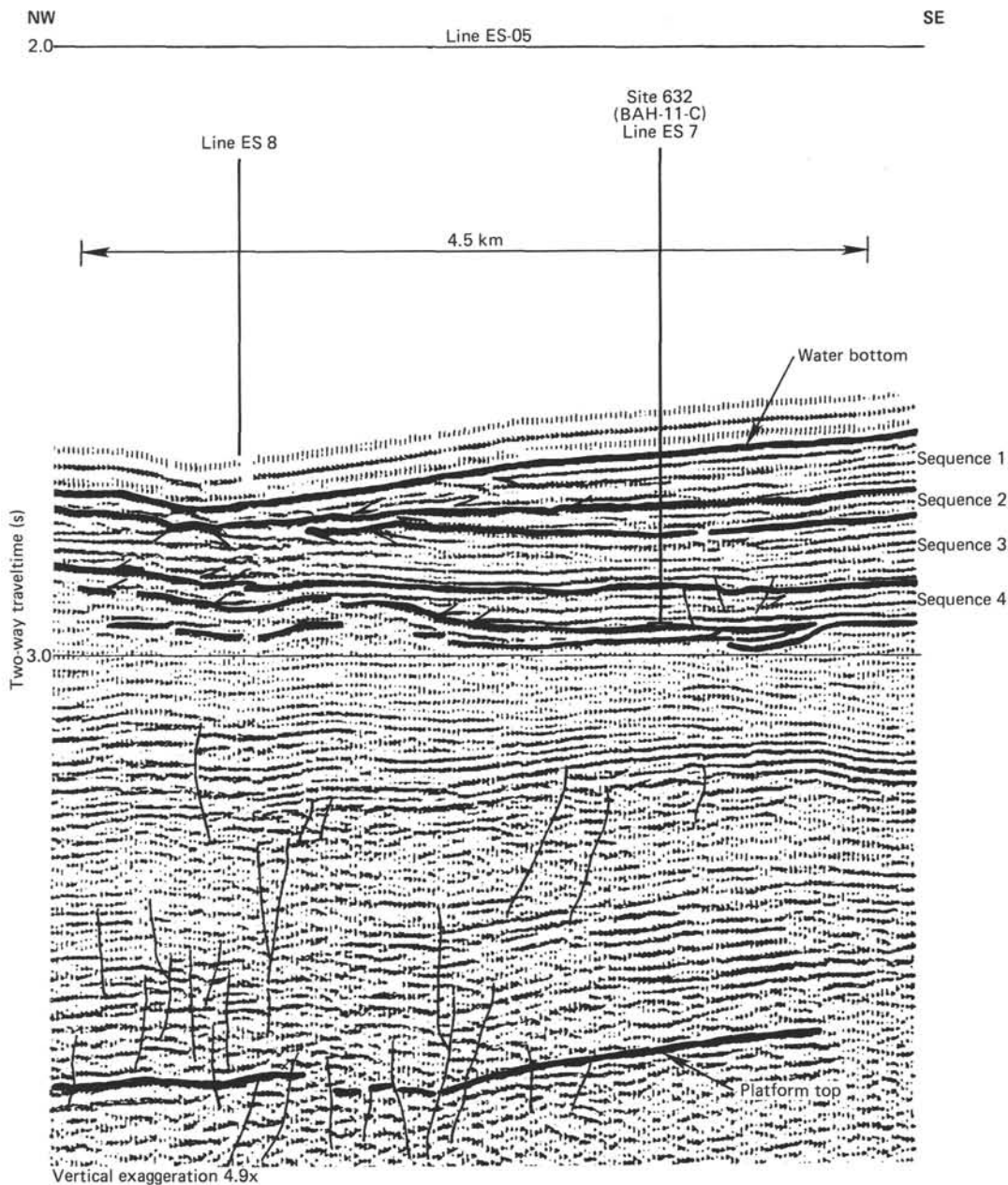


Figure 28. Part of line ES-05 over Site 632. The vertical line segment records depth of penetration. The 2/3 seismic-sequence boundary is the "O" reflector of J. Ladd and R. Sheridan (unpubl. data). Note faults cutting the interpreted platform top and overlying section.

val between 265 and 283 m in primary and secondary (moldic) porosity in turbidite grainstones. Gas chromatography indicates marine organic matter of uncertain maturity that may have migrated from deeper in the section. More problematic is the origin of tar lumps in Pleistocene sand that ran into the borehole. These lumps were recovered at 265 m from an interval that contains indigenous bitumen, yet their chemical composition (heavy oil) resembles that of the line tar used to grease the sand line. Whether these lumps of tar represent indigenous hydrocarbons or downhole contamination is uncertain.

REFERENCES

- Barnes, P. J., Brassell, S. C., Comet, P. A., Eglinton, G., McEvoy, J., Maxwell, J. R., Wardroper, A. M. D., and Volkman, J. K., 1979. Preliminary lipid analyses of core sections 18, 24 and 30 from Hole 402A. In Montadert, L., Roberts, D. G., et al., *Init. Repts. DSDP*, 48: Washington (U.S. Govt. Printing Office), 965-976.
- Beach, D., 1982. Depositional and diagenetic history of Pliocene-Pleistocene carbonates of northwestern Great Bahama Bank; evolution of a carbonate platform [Ph.D. dissert.]. Univ. Miami, Coral Gables.
- Droxler, A. W., Schlager, W., and Whallon, C. C., 1984. Quaternary aragonite cycles and oxygen-isotope record in Bahamian carbonate ooze. *Geology*, 11:235-239.
- Droxler, A. W., and Schlager, W., in press. Glacial/interglacial sedimentation rates and turbidite frequency in the Bahamas. *Geology*.
- Frey, R. W. (Ed.), 1975. *The Study of Trace Fossils*: New York (Springer-Verlag).
- Mullins, H. T., 1983. Comments and reply on "Eustatic control of turbidites and winnowed turbidites" [Comment]. *Geology*, 11:57-58.

- Okada, H., and Bukry, D., 1980. Supplementary modification and introduction of code numbers to the low-latitude coccolith biostratigraphic zonation (Bukry, 1973; 1975). *Mar. Micropaleontol.*, 5: 321-325.
- Schlager, W., and James, N. P., 1978. Low-magnesian calcite limestones forming at the deep-sea floor, Tongue of the Ocean, Bahamas. *Sedimentology*, 25:675-702.
- Vail, P. R., Mitchum, R. M., Jr., and Thompson, S., III, 1977. Seismic stratigraphy and global changes of sea level, Part 4: Global cycles of relative changes of sea level. In Payton, C. E. (Ed.), *Seismic Stratigraphy—Applications to Hydrocarbon Exploration*: AAPG Mem., 26: 83-97.
- Wetzel, A., 1981. Oekologische und stratigraphische Bedeutung biogener Gefuege in quartaeren Sedimenten am NW-afrikanischen Kontinentalrand. *"Meteor" Forsch. Ergeb.*, C-34:1-47.

Table 9. Seismic stratigraphy and velocity structure of site-survey profiles ES-05 and ES-07, Site 632.

Sequence	Sequence boundary	Sub-bottom depth (m)	Sequence thickness		Sequence velocity (km/s)
			(s)	(m)	
ES-05					
1	1/2	95	0.1	95	1.9
2			0.015	14	1.9
2/3	109				
3			0.1	103	2.05
4	^a 3/4	212	0.07	72	2.05
ES-07					
1			0.1	95	1.9
2	1/2	95			
			0.015	14	1.9
3	2/3	109			
			0.11	113	2.05
4	^a 3/4	222			
			0.075	77	2.05

^a This boundary was not specifically recognized in Hole 632B. Water depth for profile ES-05 = 2.67 s or 2002 m; water depth for profile ES-07 = 2.66 s or 1995 m; total depth for profile ES-05 = 284 m sub-bottom, and total depth for profile ES-07 = 299 m sub-bottom; total penetration at Site 632 = 283.3 m.

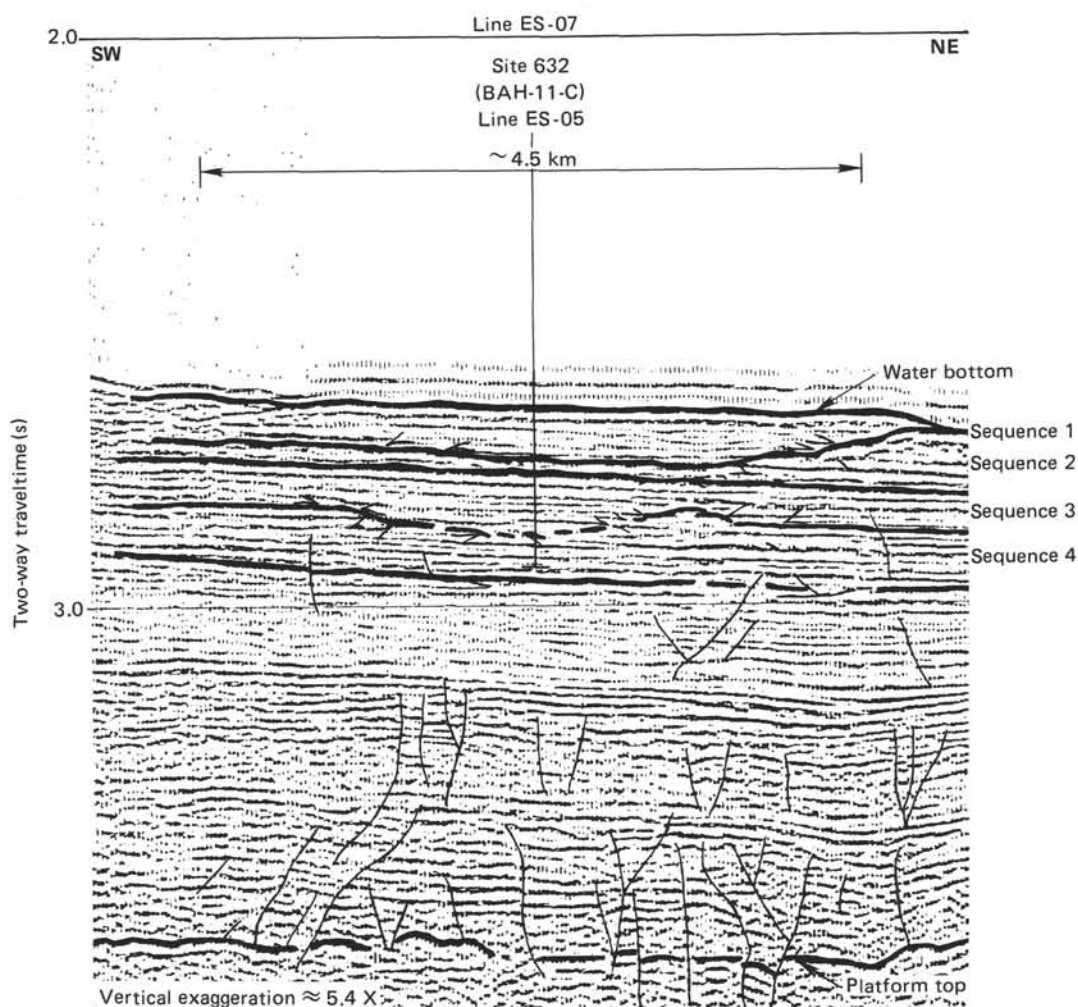


Figure 29. Part of line ES-07 over Site 632. The vertical line segment records depth of penetration. The 2/3 seismic-sequence boundary is the "O" reflector of J. Ladd and R. Sheridan (unpubl. data). Note faults above the interpreted platform.

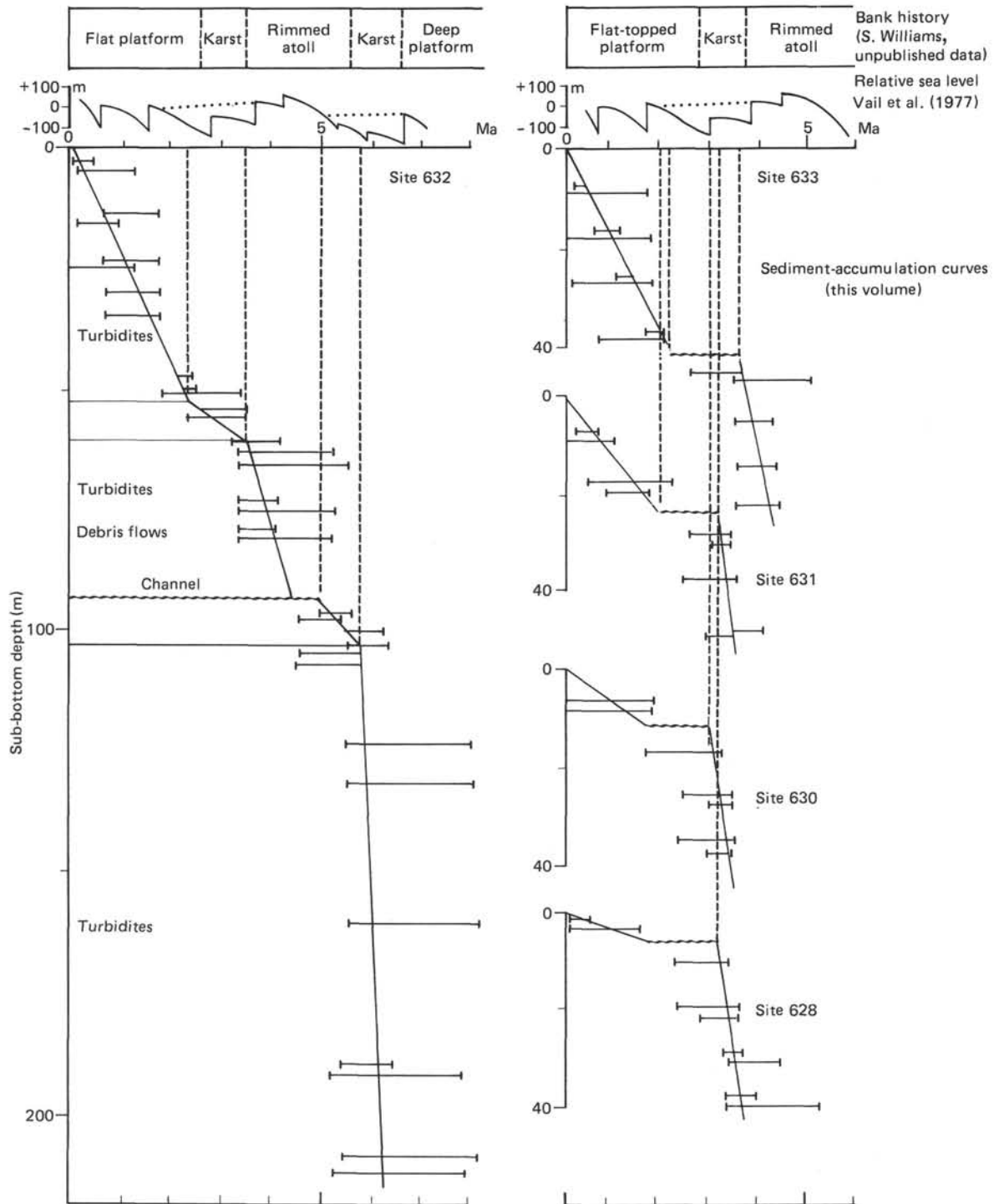
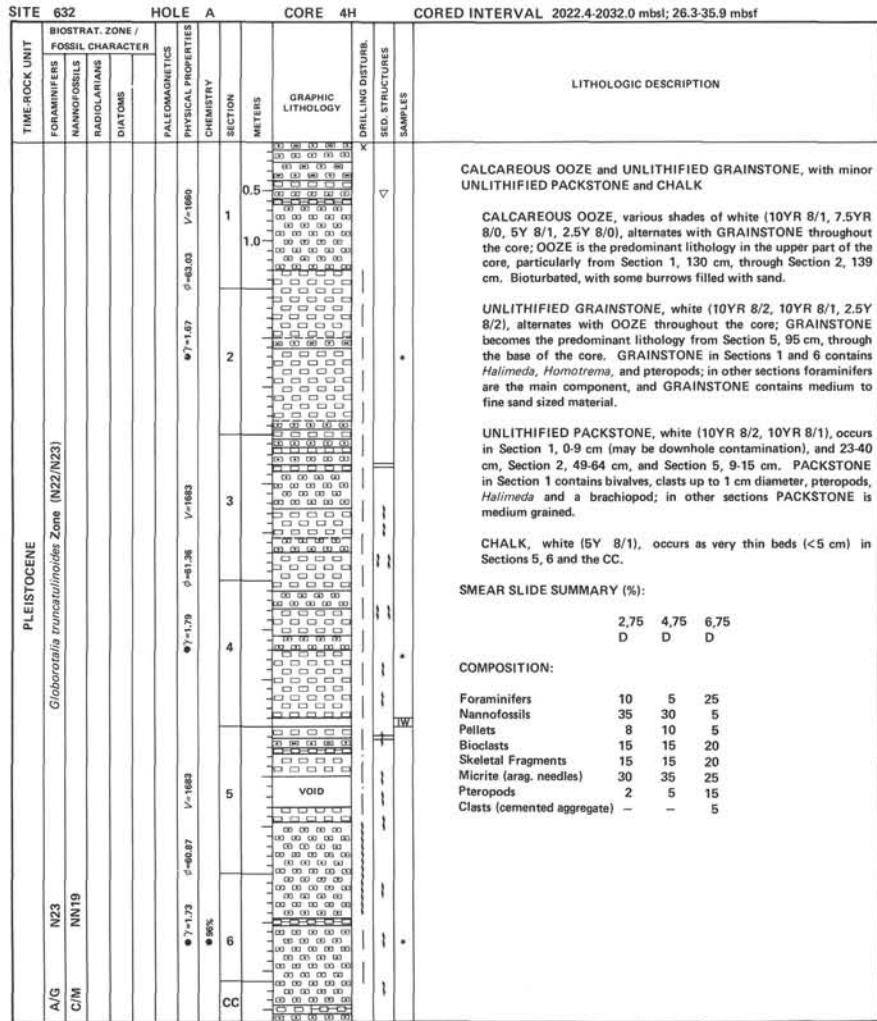
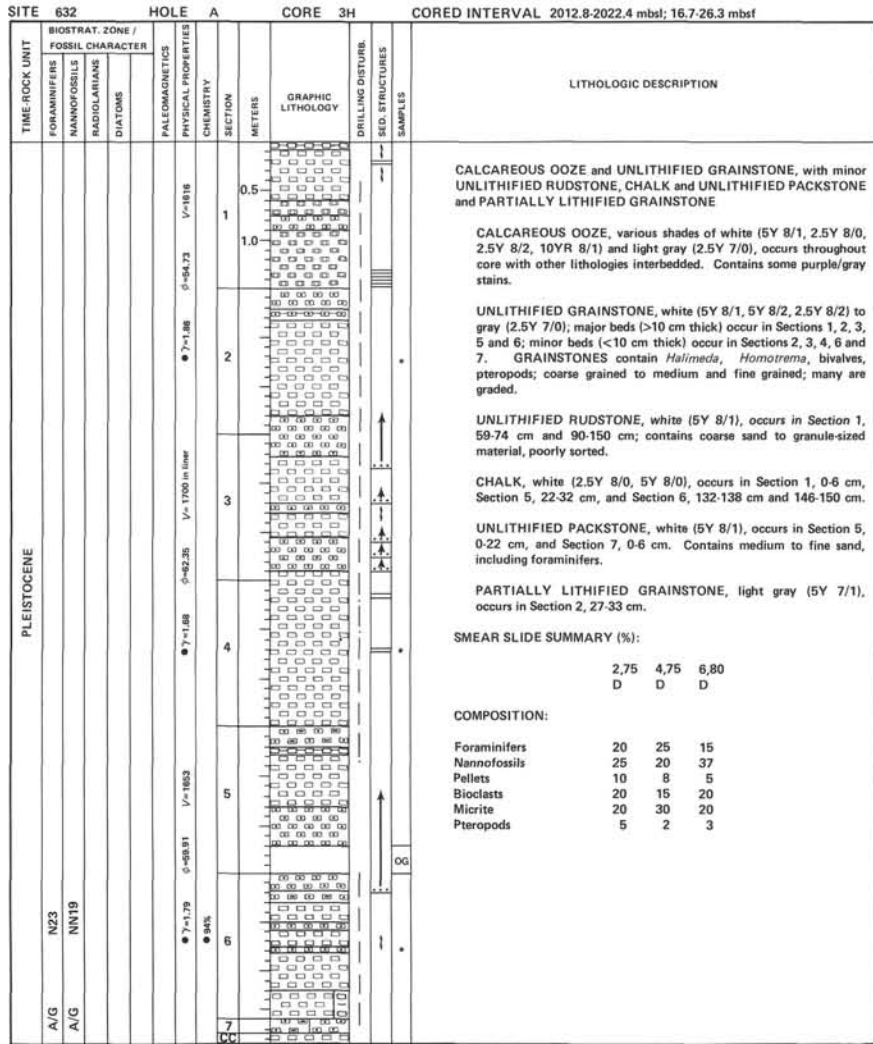
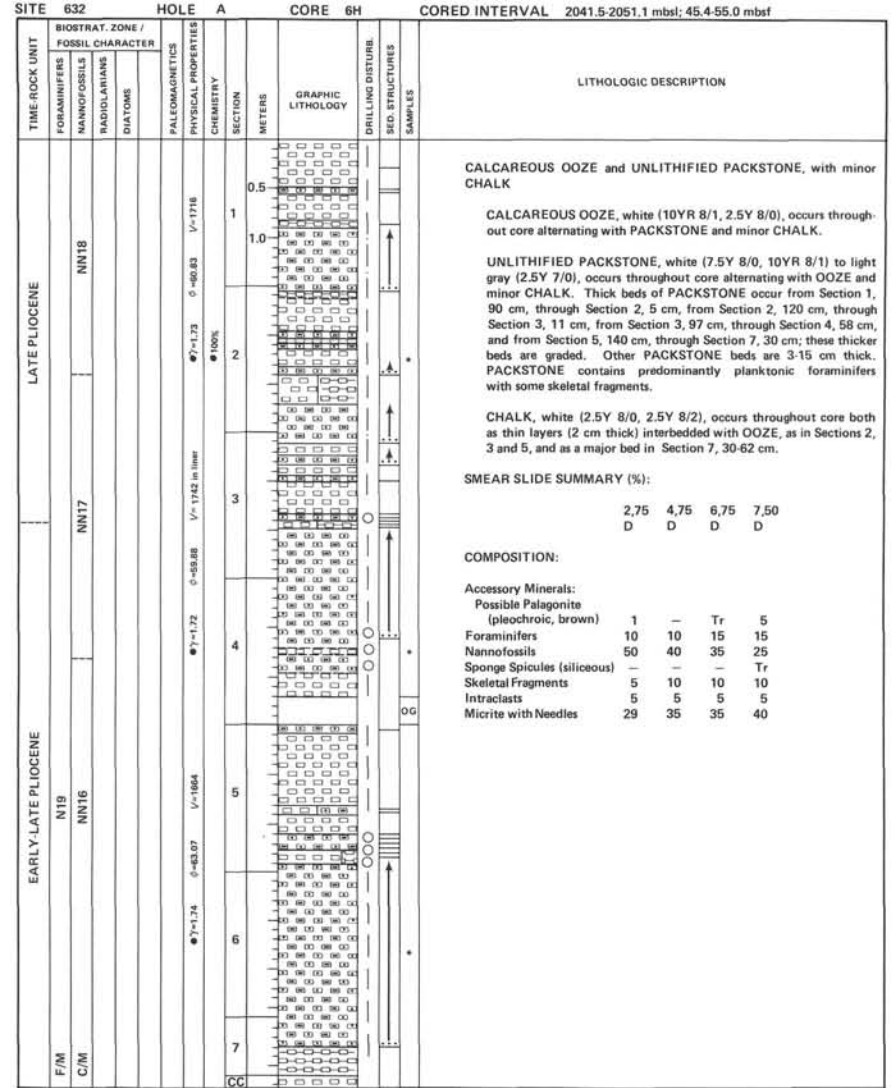
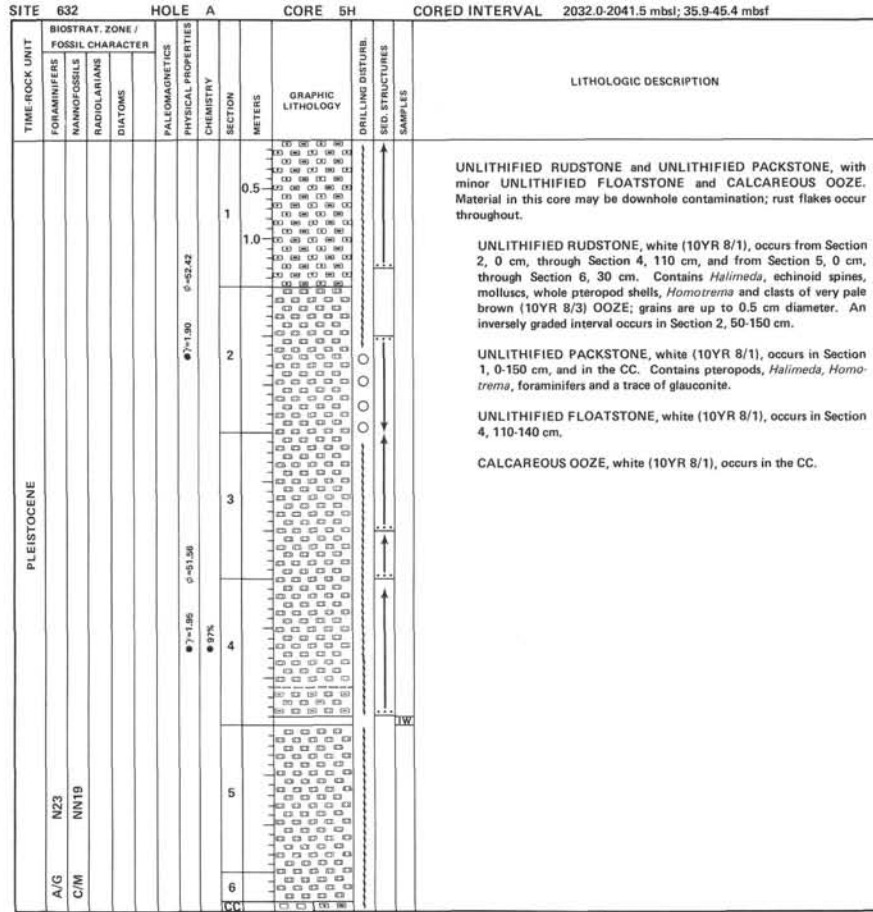


Figure 31. Comparison of facies and accumulation rates at basinal ODP sites with sea-level curve of Vail et al. (1977) and bank stratigraphy of S. Williams (unpubl. data). At Site 632, intervals of slow accumulation and scarce turbidites correspond to sea-level lows on the Vail curve and with exposure horizons and major facies changes on the banks. Sites 628, 630, 631, and 633 confirm this trend for the lowstand at 2–3.3 Ma, corresponding to rapid ice buildup in the Northern Hemisphere. The dotted line on the Vail curve represents the long-term subsidence curve of the Bahama Banks and brackets the duration of bank exposure, assuming that banks had built to sea level during the preceding highstand.





SITE 632		HOLE A		CORE 13X		CORED INTERVAL 2098.8-2108.4 mbsl; 102.7-112.3 mbsf																			
TIME ROCK UNIT	BIOSTRAT. ZONE / FOSSIL CHARACTER			PALEOMAGNETICS	PHYSICAL PROPERTIES	CHEMISTRY	SECTION	METERS	GRAPHIC LITHOLOGY	DRILLING DISTURB.	SED. STRUCTURES	SAMPLES	LITHOLOGIC DESCRIPTION												
	FORAMINIFERS	NANNOFOSSILS	RADIOLARIANS											DIATOMS											
LATE MIOCENE	A/G	NT7			V-1561		1	0.5					<p>CHALK and CALCAREOUS OOZE, UNLITHIFIED to PARTIALLY LITHIFIED PACKSTONE, and minor UNLITHIFIED FLOATSTONE and LITHIFIED PACKSTONE. Odor of hydrogen sulfide noted in some sections.</p> <p>CHALK and CALCAREOUS OOZE, mottled white (2.5Y 8/0 and 5Y 8/1, 2.5Y 8/2), occurs from Section 1, 0-20 cm and 30-150 cm. CHALK may be in the form of "drilling biscuits" with OOZE in between as "drilling paste."</p> <p>UNLITHIFIED to PARTIALLY LITHIFIED PACKSTONES, white (2.5Y 8/2), occurs in Section 2, 0-40 cm. Bioturbated, slightly graded from medium to fine sand. UNLITHIFIED PACKSTONE also occurs in the CC, 0-4 cm and 24-30 cm.</p> <p>UNLITHIFIED FLOATSTONE, white (10YR 8/1), occurs in Section 1, 20-30 cm. Contains angular clasts of CHALK in matrix of OOZE; could be either a debris flow or drilling breccia.</p> <p>LITHIFIED PACKSTONE, white (2.5Y 8/2), occurs in the CC, 4-24 cm; is possibly drilling breccia.</p> <p>SMEAR SLIDE SUMMARY (%):</p> <p style="text-align: center;">2,20 D</p> <p>COMPOSITION:</p> <table border="0"> <tr><td>Foraminifers</td><td>5</td></tr> <tr><td>Nannofossils</td><td>5</td></tr> <tr><td>Pellets</td><td>10</td></tr> <tr><td>Skeletal Fragments</td><td>20</td></tr> <tr><td>Cemented Aggregates</td><td>25</td></tr> <tr><td>Micrite (with aragonite)</td><td>35</td></tr> </table>	Foraminifers	5	Nannofossils	5	Pellets	10	Skeletal Fragments	20	Cemented Aggregates	25	Micrite (with aragonite)	35
Foraminifers	5																								
Nannofossils	5																								
Pellets	10																								
Skeletal Fragments	20																								
Cemented Aggregates	25																								
Micrite (with aragonite)	35																								
	A/B	NN11			102K		2	1.0																	
							CC																		

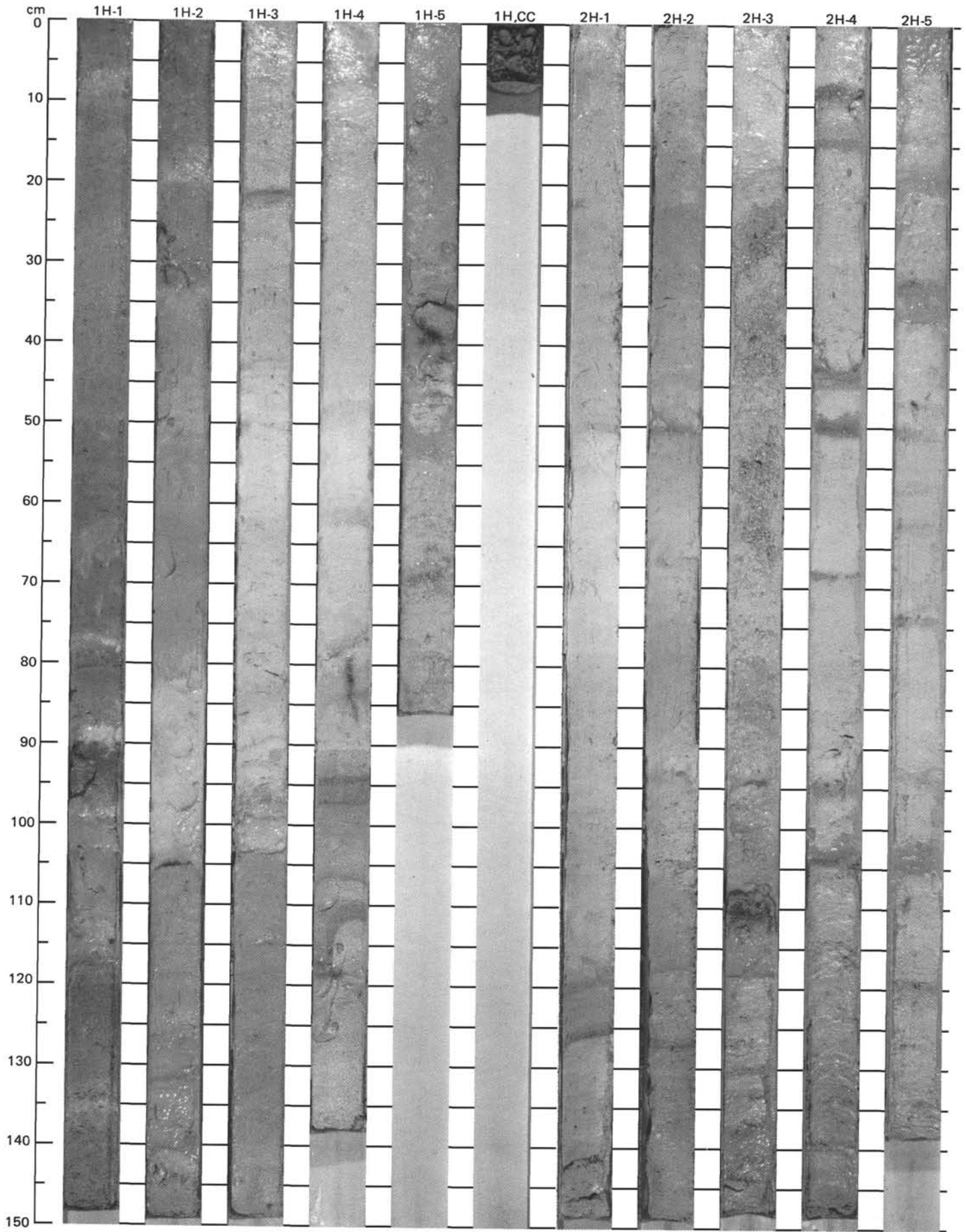
SITE 632		HOLE A		CORE 15X		CORED INTERVAL 2118.0-2127.4 mbsl; 121.9-131.3 mbsf																	
TIME ROCK UNIT	BIOSTRAT. ZONE / FOSSIL CHARACTER			PALEOMAGNETICS	PHYSICAL PROPERTIES	CHEMISTRY	SECTION	METERS	GRAPHIC LITHOLOGY	DRILLING DISTURB.	SED. STRUCTURES	SAMPLES	LITHOLOGIC DESCRIPTION										
	FORAMINIFERS	NANNOFOSSILS	RADIOLARIANS											DIATOMS									
LATE MIOCENE	R/P	?					1						<p>LIMESTONE</p> <p>LIMESTONE, white (7.5YR 8/0), throughout core; bioturbated.</p> <p>SMEAR SLIDE SUMMARY (%):</p> <p style="text-align: center;">1,32 D</p> <p>COMPOSITION:</p> <table border="0"> <tr><td>Foraminifers</td><td>2</td></tr> <tr><td>Nannofossils</td><td>20</td></tr> <tr><td>Skeletal Fragments</td><td>15</td></tr> <tr><td>Clasts (cemented aggregates)</td><td>35</td></tr> <tr><td>Micrite</td><td>28</td></tr> </table>	Foraminifers	2	Nannofossils	20	Skeletal Fragments	15	Clasts (cemented aggregates)	35	Micrite	28
Foraminifers	2																						
Nannofossils	20																						
Skeletal Fragments	15																						
Clasts (cemented aggregates)	35																						
Micrite	28																						
	F/R	NN11					CC																

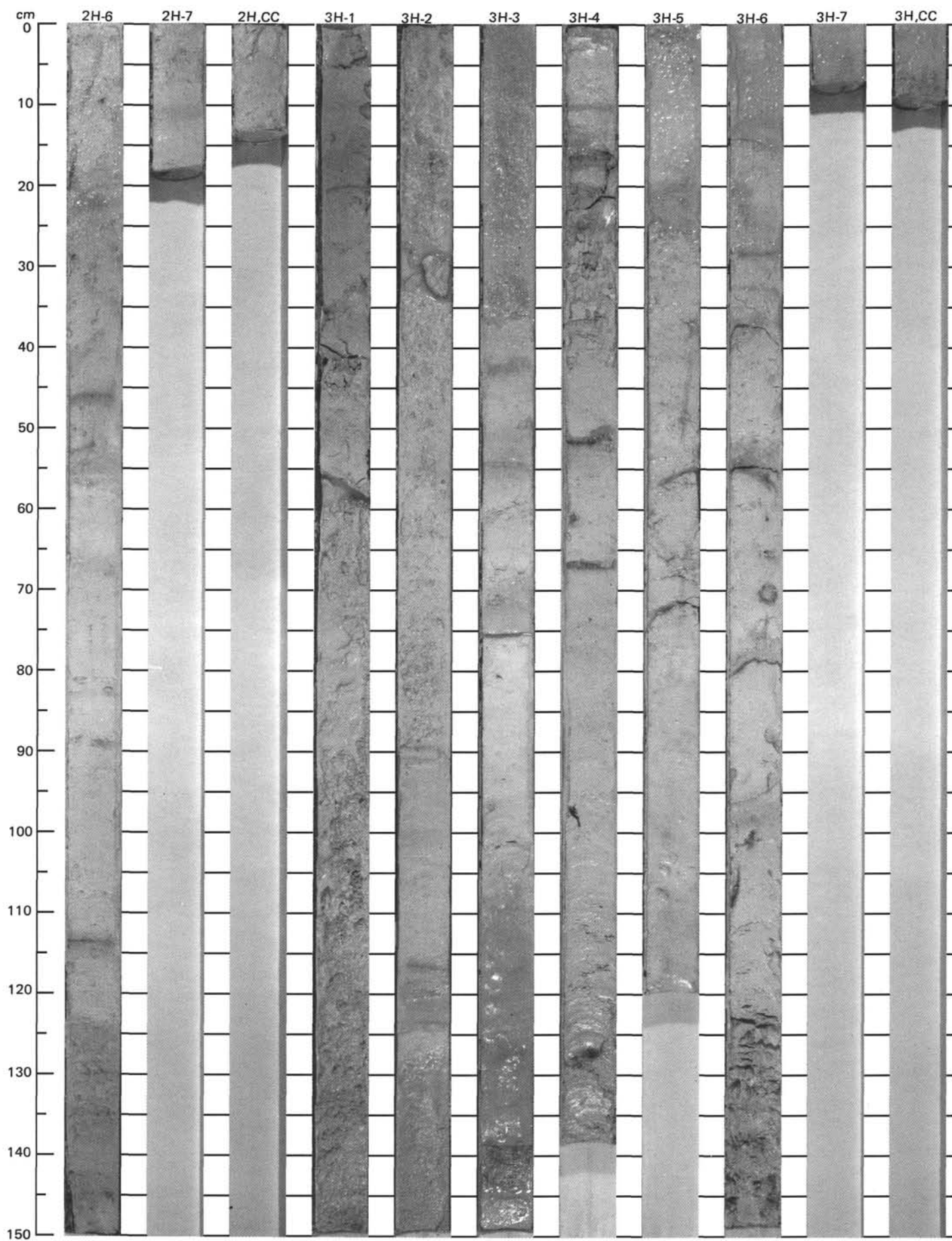
SITE 632		HOLE A		CORE 14X		CORED INTERVAL 2108.4-2118.0 mbsl; 112.3-121.9 mbsf																										
TIME ROCK UNIT	BIOSTRAT. ZONE / FOSSIL CHARACTER			PALEOMAGNETICS	PHYSICAL PROPERTIES	CHEMISTRY	SECTION	METERS	GRAPHIC LITHOLOGY	DRILLING DISTURB.	SED. STRUCTURES	SAMPLES	LITHOLOGIC DESCRIPTION																			
	FORAMINIFERS	NANNOFOSSILS	RADIOLARIANS											DIATOMS																		
?	B	?			V-581		1	0.5					<p>LITHIFIED PACKSTONE, CALCAREOUS OOZE and LIMESTONE (probably drilling breccia)</p> <p>LITHIFIED PACKSTONE and CALCAREOUS OOZE, light gray (10YR 7/2), occur in Section 1 and in the CC, 30-40 cm; probably drilling breccia. Burrows evident in larger fragments of PACKSTONE. Skeletal molds visible in fragment in CC.</p> <p>LIMESTONE, white (10YR 8/1, 2.5Y 8/2), contains foraminifers, bioturbated, some burrows have marcasite/pyrite fill.</p> <p>SMEAR SLIDE SUMMARY (%):</p> <table border="0"> <tr><td>1,29</td><td>CC,19</td></tr> <tr><td>D</td><td>D</td></tr> </table> <p>COMPOSITION:</p> <table border="0"> <tr><td>Foraminifers</td><td>5</td><td>-</td></tr> <tr><td>Nannofossils</td><td>2</td><td>5</td></tr> <tr><td>Skeletal Fragments</td><td>50</td><td>10</td></tr> <tr><td>Clasts (cemented aggregates)</td><td>30</td><td>20</td></tr> <tr><td>Micrite</td><td>13</td><td>65</td></tr> </table>	1,29	CC,19	D	D	Foraminifers	5	-	Nannofossils	2	5	Skeletal Fragments	50	10	Clasts (cemented aggregates)	30	20	Micrite	13	65
1,29	CC,19																															
D	D																															
Foraminifers	5	-																														
Nannofossils	2	5																														
Skeletal Fragments	50	10																														
Clasts (cemented aggregates)	30	20																														
Micrite	13	65																														
	B	?			102K		CC																									

SITE 632		HOLE A		CORE 16X		CORED INTERVAL 2127.4-2137.1 mbsl; 131.3-141.0 mbsf																	
TIME ROCK UNIT	BIOSTRAT. ZONE / FOSSIL CHARACTER			PALEOMAGNETICS	PHYSICAL PROPERTIES	CHEMISTRY	SECTION	METERS	GRAPHIC LITHOLOGY	DRILLING DISTURB.	SED. STRUCTURES	SAMPLES	LITHOLOGIC DESCRIPTION										
	FORAMINIFERS	NANNOFOSSILS	RADIOLARIANS											DIATOMS									
?	R/P	?					1						<p>LIMESTONE</p> <p>LIMESTONE, white (10YR 8/1), throughout core, highly fragmented, may be drilling breccia.</p> <p>SMEAR SLIDE SUMMARY (%):</p> <p style="text-align: center;">1,18 D</p> <p>COMPOSITION:</p> <table border="0"> <tr><td>Foraminifers</td><td>Tr</td></tr> <tr><td>Nannofossils</td><td>Tr</td></tr> <tr><td>Skeletal Fragments</td><td>15</td></tr> <tr><td>Clasts (cemented aggregates)</td><td>20</td></tr> <tr><td>Micrite</td><td>65</td></tr> </table>	Foraminifers	Tr	Nannofossils	Tr	Skeletal Fragments	15	Clasts (cemented aggregates)	20	Micrite	65
Foraminifers	Tr																						
Nannofossils	Tr																						
Skeletal Fragments	15																						
Clasts (cemented aggregates)	20																						
Micrite	65																						
	R/P	?			0-MA83		CC	0.5															
					7-2.08																		

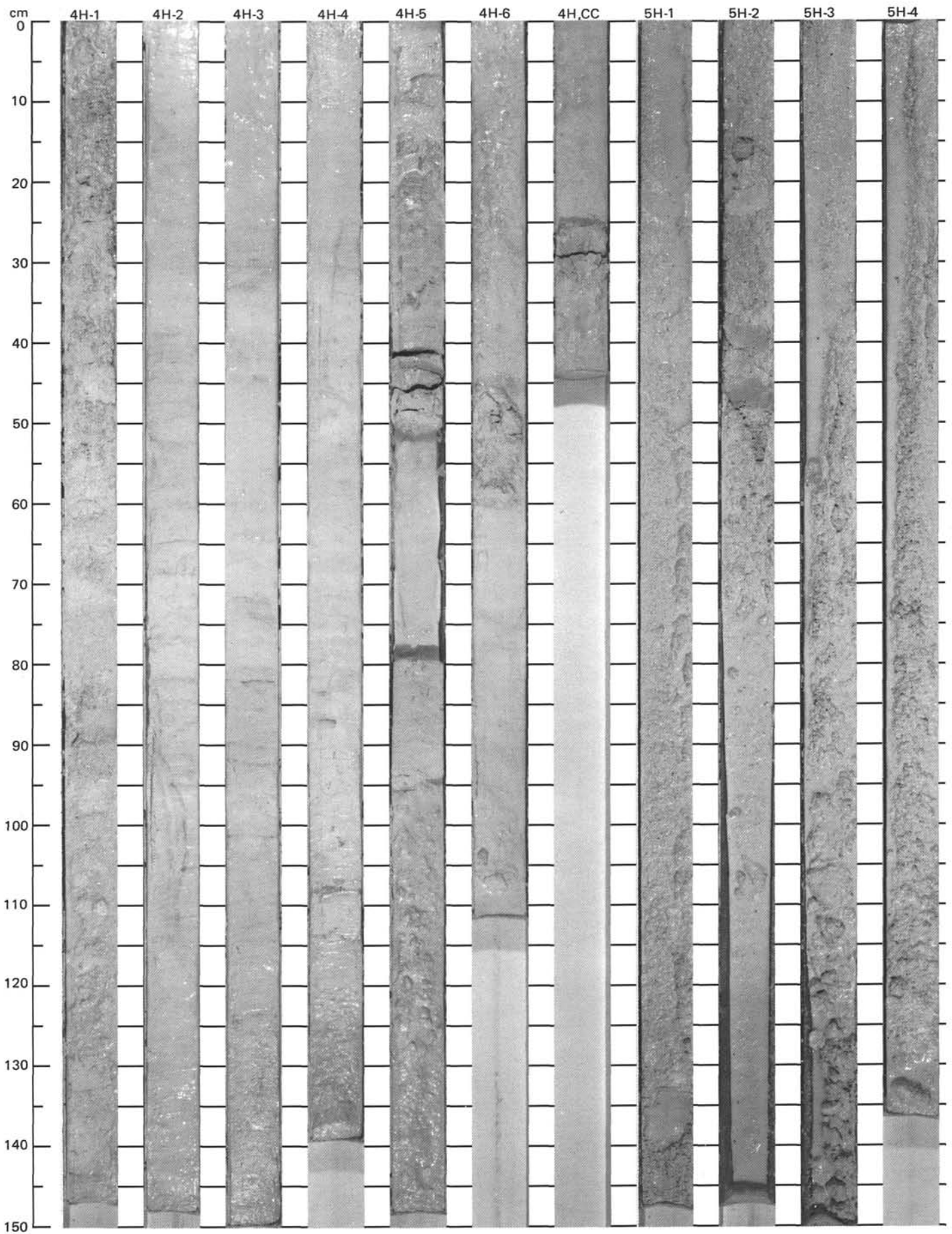
SITE 632		HOLE B		CORE 1R		CORED INTERVAL 2116.8-2126.4 mbsl; 120.7-130.3 mbsf	
TIME-ROCK UNIT	BIOSTRAT. ZONE / FOSSIL CHARACTER	FORAMINIFERS	NANNOFOSSILS	RADIOLARIANS	DIATOMS	PALEOMAGNETICS	PHYSICAL PROPERTIES
LATE MIOCENE	Indeterminate		NN11				V=2400
							7=2.13
							98%
							V=2980
							0=20.32
							7=2.30
							97%
							V=3080
							0=20.32
							7=2.30
							97%
							V=3080
							0=20.32
							7=2.30
							97%
							V=3080
							0=20.32
							7=2.30
							97%
							V=3080
							0=20.32
							7=2.30
							97%
							V=3080
							0=20.32
							7=2.30
							97%
							V=3080
							0=20.32
							7=2.30
							97%
							V=3080
							0=20.32
							7=2.30
							97%
							V=3080
							0=20.32
							7=2.30
							97%
							V=3080
							0=20.32
							7=2.30
							97%
							V=3080
							0=20.32
							7=2.30
							97%
							V=3080
							0=20.32
							7=2.30
							97%
							V=3080
							0=20.32
							7=2.30
							97%
							V=3080
							0=20.32
							7=2.30
							97%
							V=3080
							0=20.32
							7=2.30
							97%
							V=3080
							0=20.32
							7=2.30
							97%
							V=3080
							0=20.32
							7=2.30
							97%
							V=3080
							0=20.32
							7=2.30
							97%
							V=3080
							0=20.32
							7=2.30
							97%
							V=3080
							0=20.32
							7=2.30
							97%
							V=3080
							0=20.32
							7=2.30
							97%
							V=3080
							0=20.32
							7=2.30
							97%
							V=3080
							0=20.32
							7=2.30
							97%
							V=3080
							0=20.32
							7=2.30
							97%
							V=3080
							0=20.32
							7=2.30
							97%
							V=3080
							0=20.32
							7=2.30
							97%
							V=3080
							0=20.32
							7=2.30
							97%
							V=3080
							0=20.32
							7=2.30
							97%
							V=3080
							0=20.32
							7=2.30
							97%
							V=3080
							0=20.32
							7=2.30
							97%
							V=3080
							0=20.32
							7=2.30
							97%
							V=3080
							0=20.32
							7=2.30
							97%
							V=3080
							0=20.32
							7=2.30
							97%
							V=3080
							0=20.32
							7=2.30
							97%
							V=3080
							0=20.32
							7=2.30
							97%
							V=3080
							0=20.32
							7=2.30
							97%
							V=3080
							0=20.32
							7=2.30
							97%
							V=3080
							0=20.32
							7=2.30
							97%
							V=3080
							0=20.32
							7=2.30
							97%
							V=3080
							0=20.32
							7=2.30
							97%
							V=3080
							0=20.32
							7=2.30
							97%
							V=3080
							0=20.32
							7=2.30
							97%
							V=3080
							0=20.32
							7=2.30
							97%
							V=3080
							0=20.32
							7=2.30
							97%
							V=3080
							0=20.32
							7=2.30
							97%
							V=3080
							0=20.32
							7=2.30
							97%
							V=3080
							0=20.32
							7=2.30
							97%
							V=3080
							0=20.32
							7=2.30
							97%
							V=3080
							0=20.32
							7=2.30
							97%
							V=3080
							0=20.32
							7=2.30
							97%
							V=3080
							0=20.32
							7=2.30
							97%
							V=3080
							0=20.32
							7=2.30
							97%
							V=3080
							0=20.32
							7=2.30
							97%
							V=3080
							0=20.32
							7=2.30
							97%
							V=3080
							0=20.32
							7=2.30
							97%
							V=3080
							0=20.32
							7=2.30
							97%
							V=3080

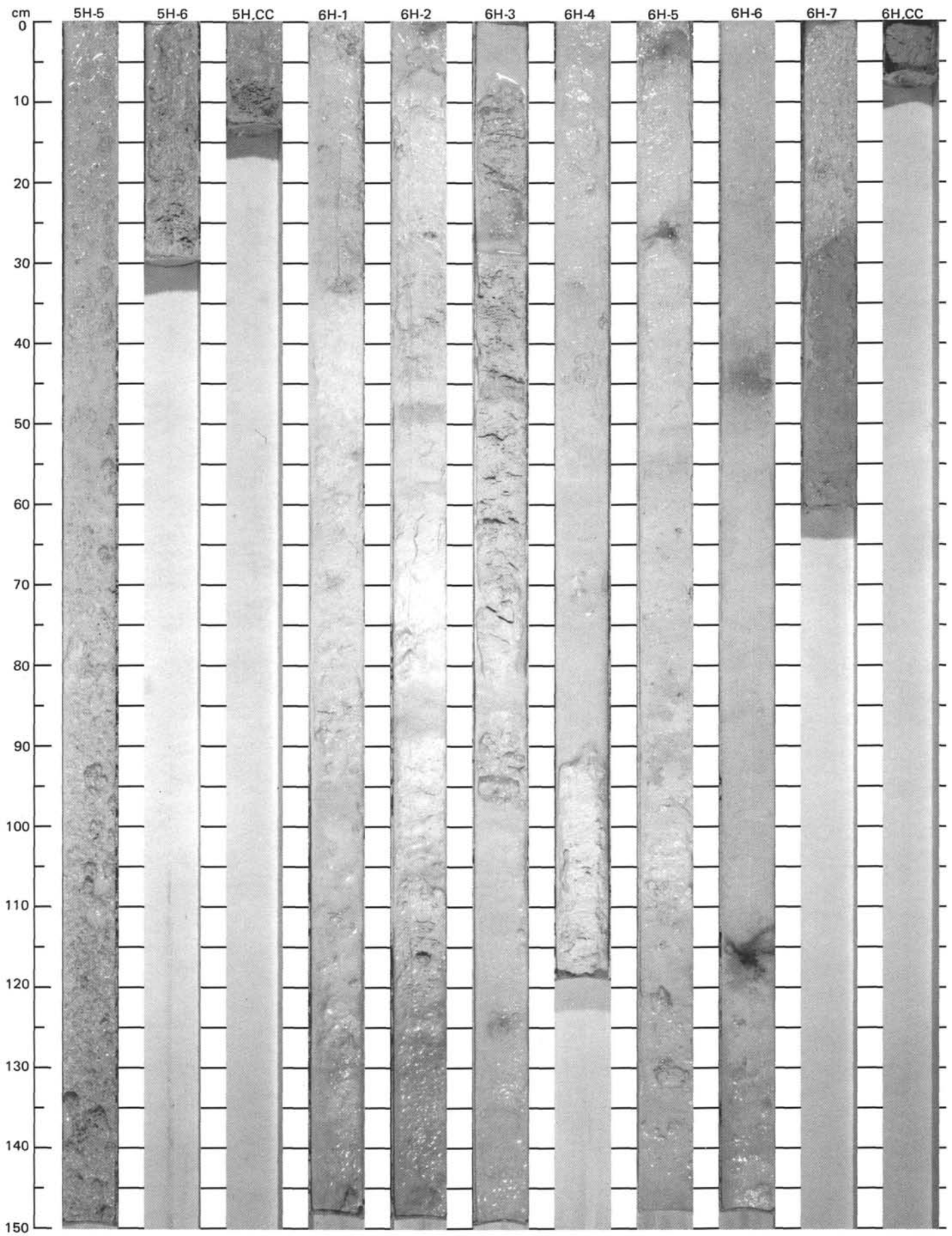
SITE 632 (HOLE A)



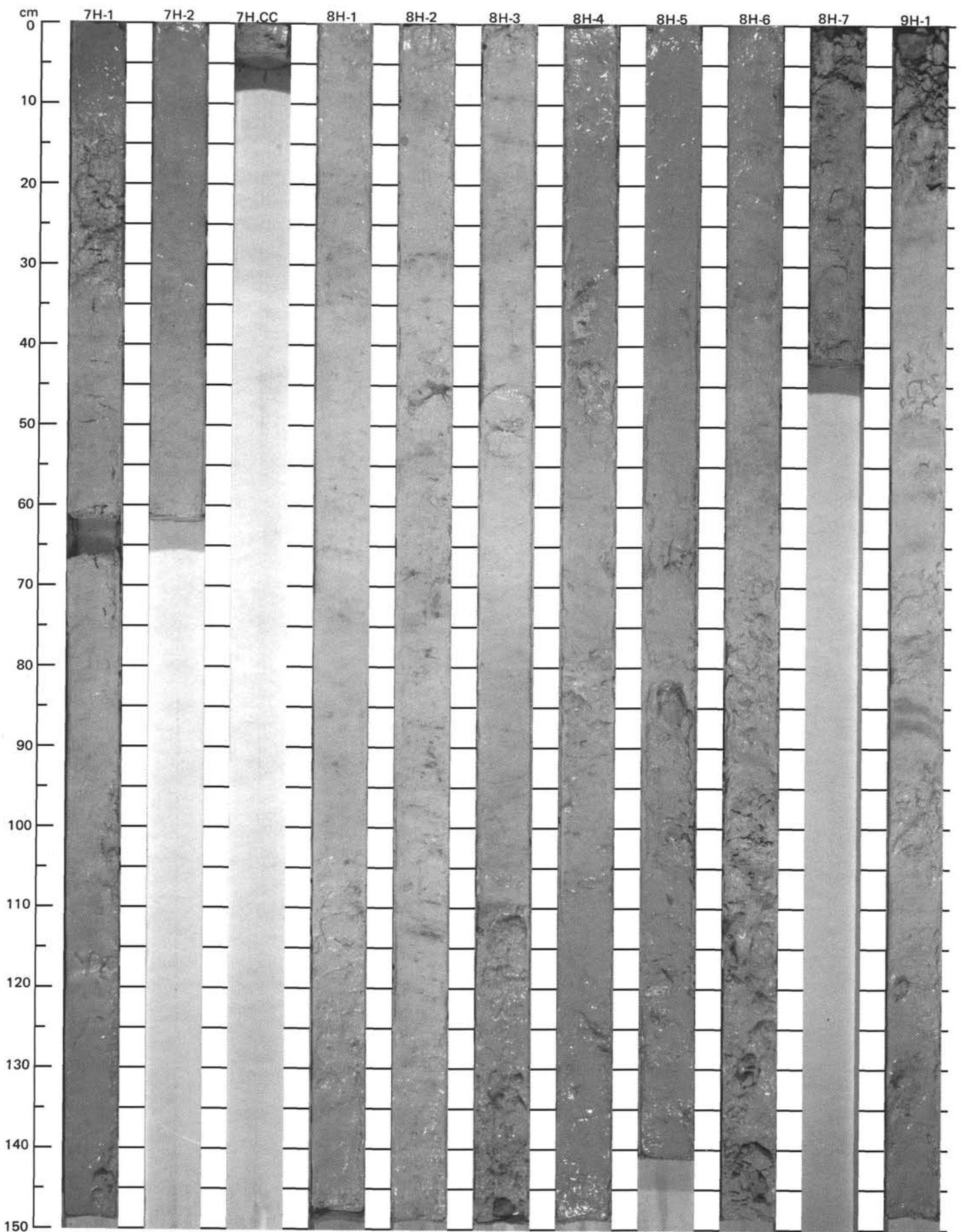


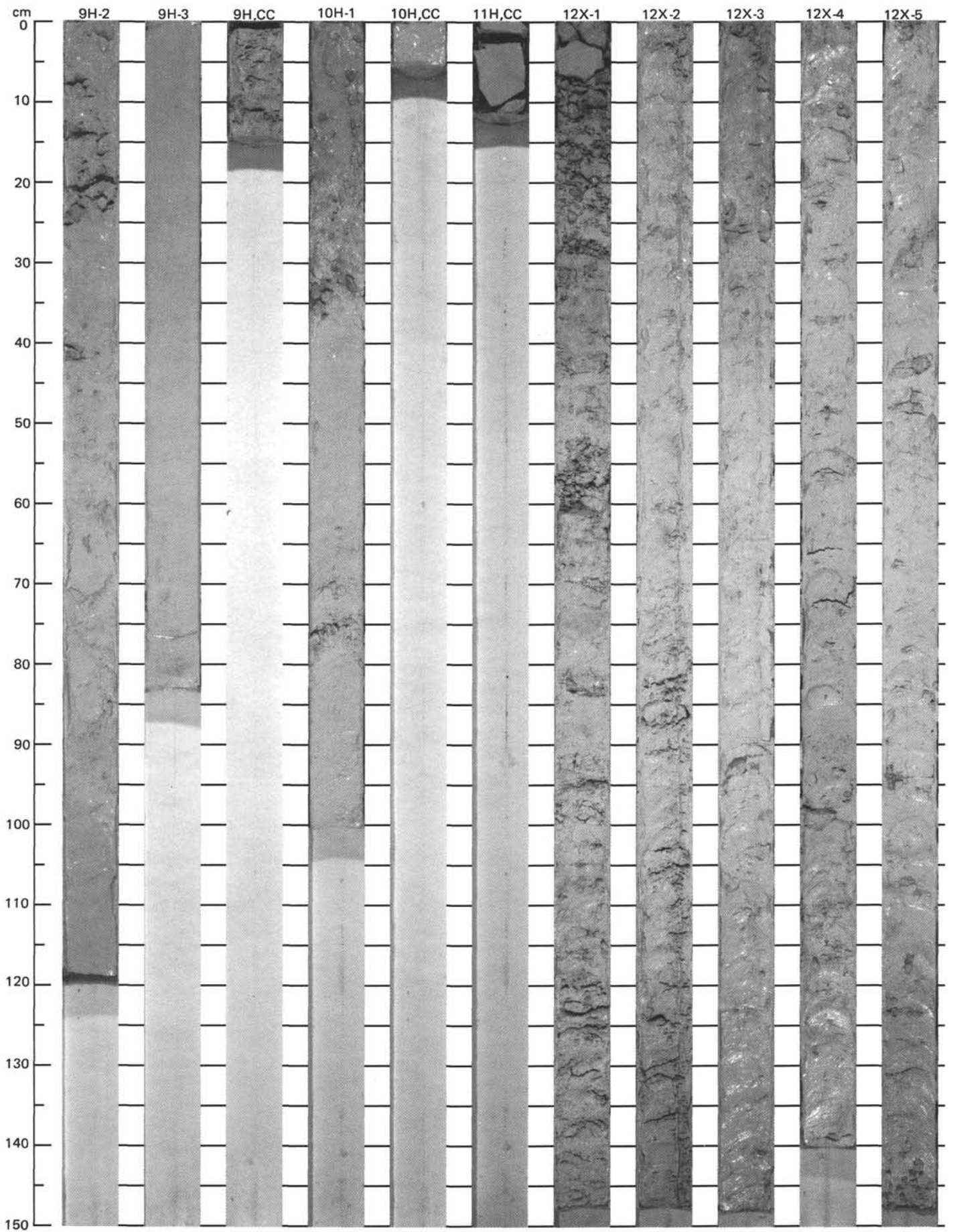
SITE 632 (HOLE A)



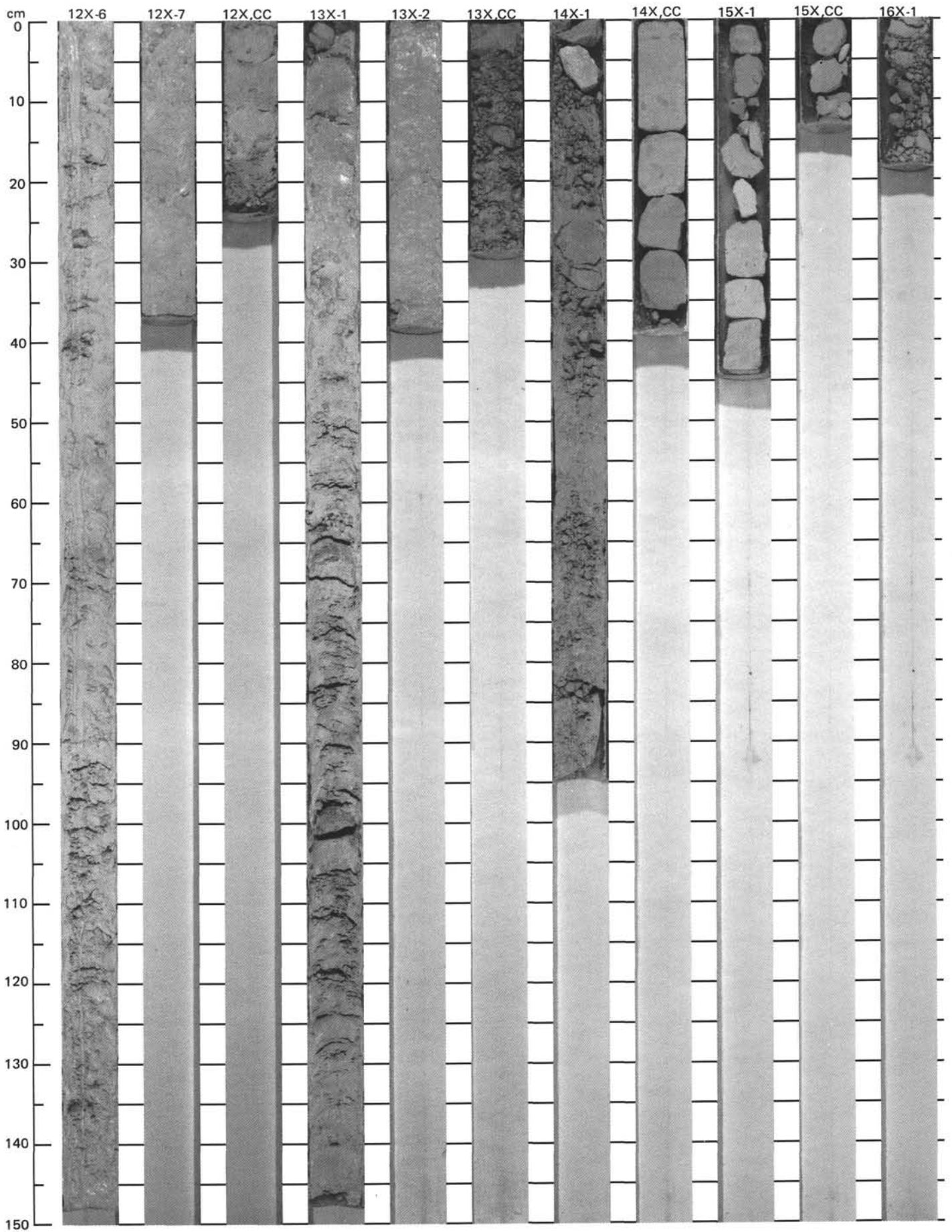


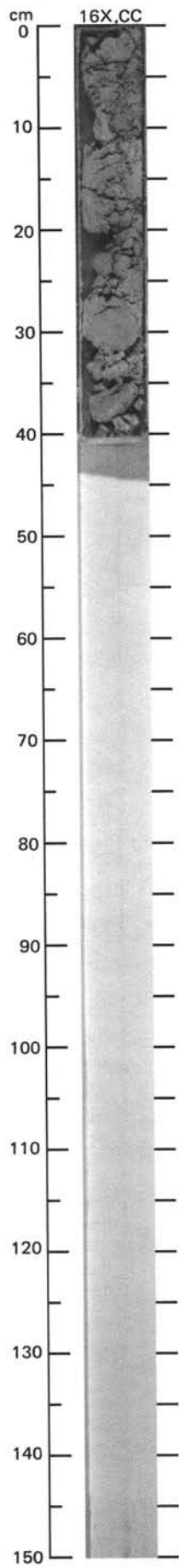
SITE 632 (HOLE A)



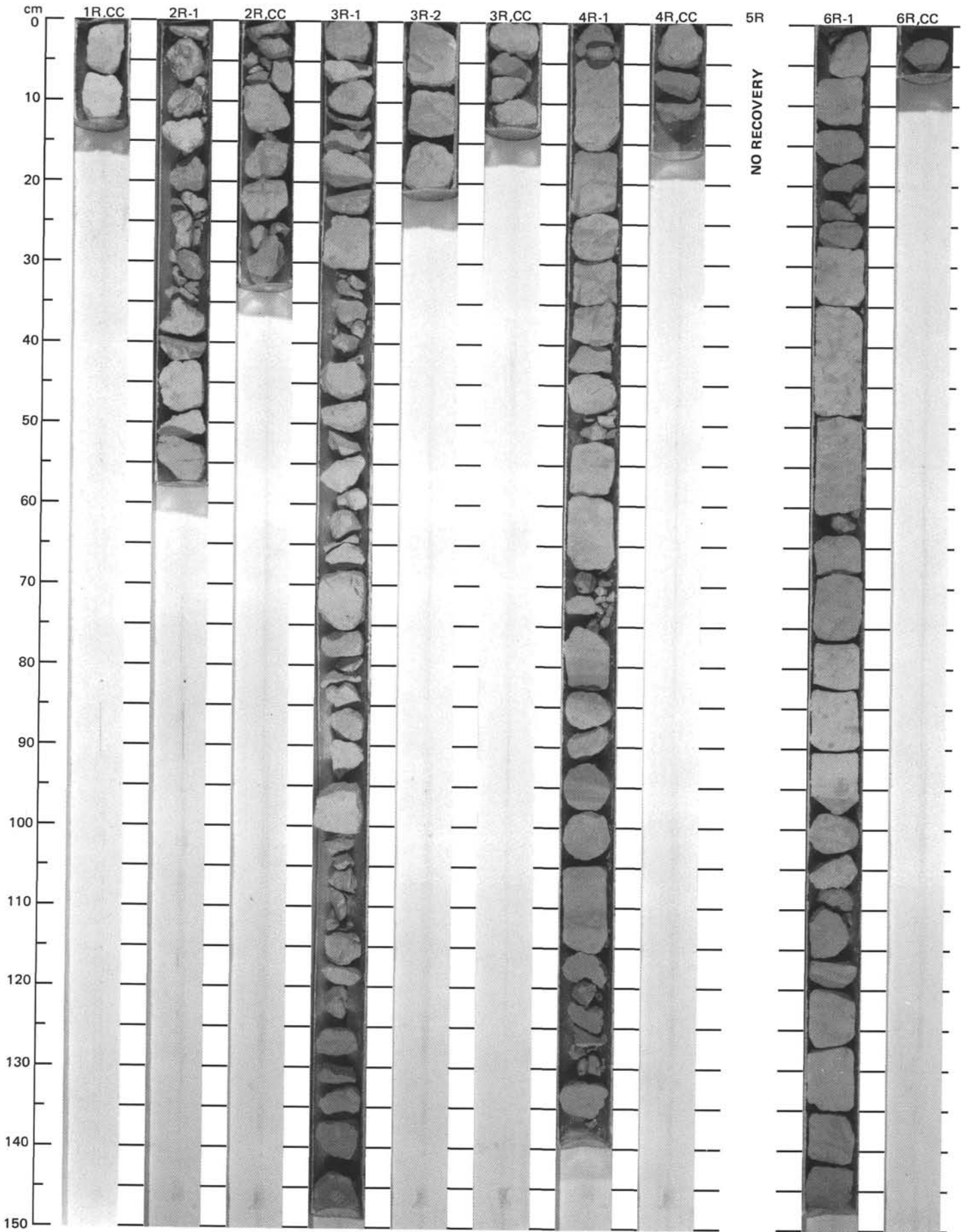


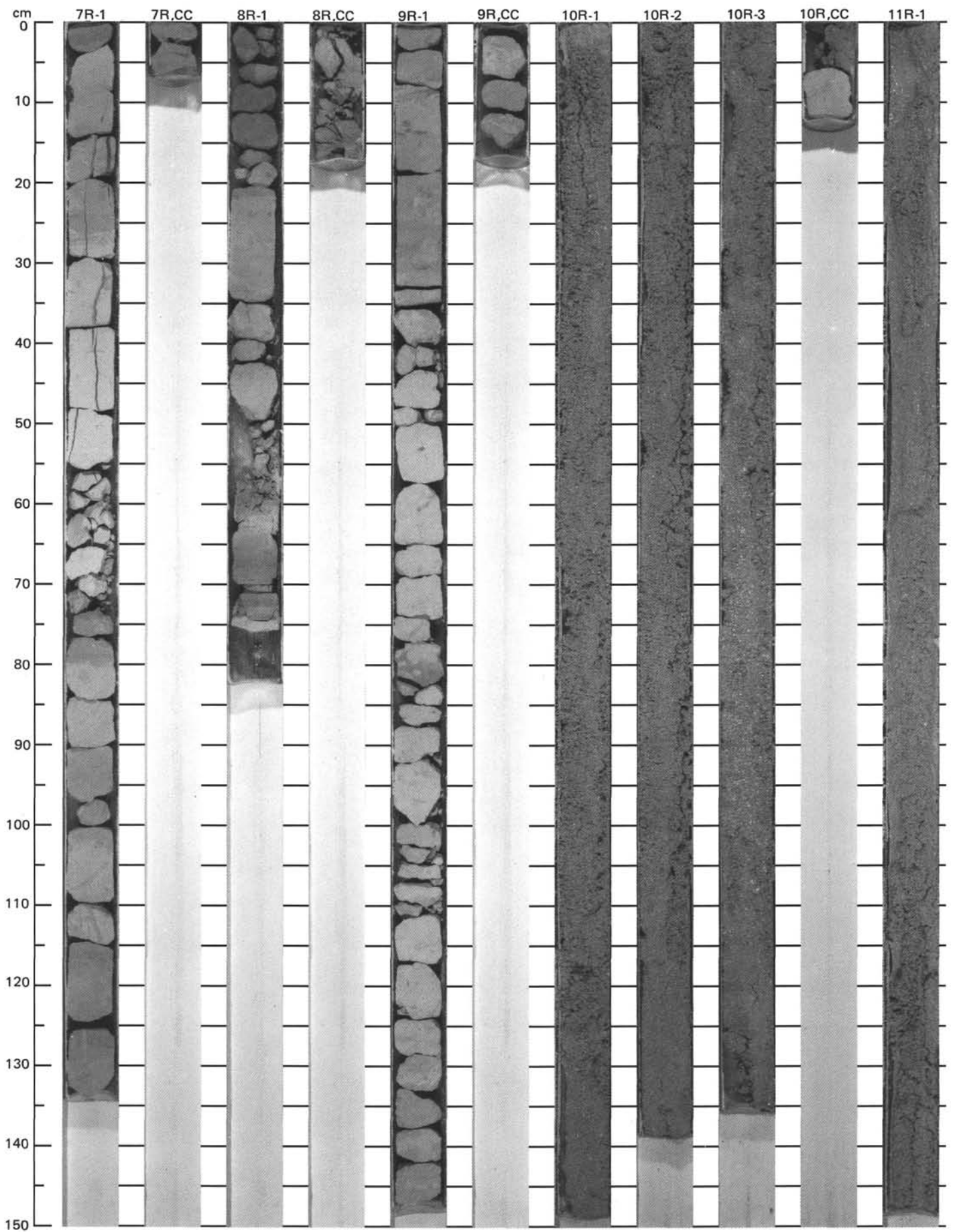
SITE 632 (HOLE A)





SITE 632 (HOLE B)





SITE 632 (HOLE B)

